2013•2014
FACULTEIT INDUSTRIËLE INGENIEURSWETENSCHAPPEN
master in de industriële wetenschappen: biochemie

Masterproef

Characteristics and effect of US parameters and surface stabilizer on the sonocrystallization process of paracetamol

Promotor :
Prof. dr. ir. Leen BRAEKEN

Promotor :
ing. JEROEN JORDENS
Prof. dr. ir. THOMAS VAN GERVEN

Gezamenlijke opleiding Universiteit Hasselt en KU Leuven

Mathijs Paredis

Proefschrift ingediend tot het behalen van de graad van master in de industriële wetenschappen: biochemie

2013•2014

Faculteit Industriële ingenieurswetenschappen

master in de industriële wetenschappen: biochemie

Masterproef

Characteristics and effect of US parameters and surface stabilizer on the sonocrystallization process of paracetamol

Promotor :
Prof. dr. ir. Leen BRAEKEN

Promotor :
ing. JEROEN JORDENS
Prof. dr. ir. THOMAS VAN GERVEN

Mathijs Paredis

Proefschrift ingediend tot het behalen van de graad van master in de industriële wetenschappen: biochemie

universiteit hasselt | KU LEUVEN

1. FOREWORD

Ultrasound can positively influence the crystallization process. Many studies already investigated the effect of different parameters such as the frequency, intensity and concentration on the MZW and the CSD. However the cavitations and ultrasound waves and the effect on the crystallization process is not yet widely studied. Little is known about the effect of these parameters on the wave types and on the cavitations. With better knowledge of the effect of these parameters, the size and shape of the crystals can be controlled and optimized, and the knowledge of the effect of ultrasound waves on crystallization will increase.

I have chosen this subject, because it was a subject, which had not yet been studied. Ultrasound waves seemed an interesting topic, and I was curious how this would affect the paracetamol crystals. Also, working with paracetamol and knowing that the purpose was to enhance the paracetamol crystal but even more to gain insight in the sonocrystallization process, and knowing these results could be of great interest in the sonocrystallization, motivated me. I had chosen to perform this thesis in a research center at a university, instead of in a company. I believed that a research company at school already knew more about the subject and the master thesis.

I would like to thank my intern promoter *dr. ing.* Leen Braeken, and my extern promoters *ing.* Jeroen Jordens and *Prof. Dr. ir.* Tom Van Gerven. They helped me with the analysis of the experiments and often discussed the results. They also helped me gaining the materials and products, needed to perform the test. A weekly meeting with *ing.* Jordens, to discuss the results which were obtained in that week, and to see which tests would be interesting to perform next. I also want to thank the KHLim and KULeuven for the provision of materials and working space. The lab assistants also helped with finding and working with the materials and computer programs.

2. CONTENT

TABLE LIST

FIGURE LIST

GRAPH LIST

EQUATION LIST

ABSTRACT

In the pharmaceutical industry, one of the most interesting applications of ultrasound is its use during crystallization processes, where ultrasound has a large influence on the quality of the products, the reproducibility, the metastable zone width (MZW) and the crystal size distribution (CSD).

In this thesis, the ultrasound wave field is characterized at standing or traveling waves using sonoluminescence. Different surface stabilizers (PUR, copper and glass) were used to alternate the wave form. The effect of cavitations (stable or transient) on the crystals and the process was investigated at different frequencies (41-1140kHz), surface stabilizers and calorimetric input power (4-15W). The cavitations were examined as noise using a hydrophone. The obtained data was combined with crystallization data e.g. MZW and CSD. Also, the effect of the stirrer was studied.

Results showed that the amount of transient cavitations increase at low frequencies, open systems and high intensities. Transient cavitations gave a low MZW and small CSD. Standing waves exist even when using an absorption material, but the standing wave ratio is lower in this case. The bands were less broad when using absorption material. Standing waves are beneficial for a low MZW, however the effect of wave pattern is not as efficient as the effect of the frequency and cavitations. No influence of the parameters was shown on the crystal shape. Overhead stirring is necessary to become a band structure, thus standing waves.

ABSTRACT IN DUTCH

Er word veel onderzoek gedaan naar ultrageluid als alternatieve energiebron in de chemische industrie. In de farmaceutische industrie wordt ultrasoon geluid vooral toegepast tijdens de kristallisatie, waar ultrageluid een grote invloed heeft op de kwaliteit van de producten, de reproduceerbaarheid, de metastabiele zone breedte (MZW) en de kristalgrootteverdeling (CSD).

In deze thesis, het ultrasoon veld zal gekarakteriseerd worden bij staande en lopende golven met behulp van sonoluminescentie. Verschillende oppervlaktematerialen, voor reflectie (Koper, Glas) of absorptie (PUR) materialen worden gebruikt voor het verkrijgen van het gewenste golftye. Het effect van de transiënte en stabiele cavitaties op de kristallen en het kristallizatieproces wordt onderzocht. van golven worden gebruikt bij de verschillende oppervlaktematerialen en verschillende frequenties tussen 41 en 1140kHz. Het calorimetrisch vermogen wordt gevarieerd tussen 4-15W. De cavitaties worden bestudeerd als ruis aan de hand van hydrofoonmetingen. Deze resultaten wordt vergeleken met de kristallisatiedata (MZW, CSD). Ook wordt de invloed van de roerder op het golfpatroon onderzocht.

Transiente cavitaties nemen toe bij lage frequenties, open systemen en hoge intensiteiten. Transiente cavitaties zorgden voor een lage MZW, en CSD. Staande golven worden altijd gedetecteerd, ook wanneer absorptiemateriaal gebruikt wordt, maar in dit geval is de hoeveelheid staande golf lager. De banden waren minder breed bij absorptiemateriaal. Staande golven verkleinen de MZW, maar minder fel als een bij een lage frequentie en transiente cavitaties. Geen invloed van de US parameters op de kristalvorm was gedetecteerd. Roeren is nodig voor een bandenstructuur, en dus staande golven te bekomen.

3. INTRODUCTION

This research is situated in the field of process intensification aiming to develop new processes which are smaller, safer, easier, environment friendly and more cost effective. [1, 2, 3]. The main goal is to gain more insight in the mechanism behind sonocrystallization by investigating the effect of a surface stabilizer and crystallization parameters on the type of ultrasound waves and cavitation bubbles produced. This thesis will investigate which cavitation bubbles and wave types will form at different, frequencies, intensities, stirring rate and surface stabilizers. Furthermore, the effect of these parameters on the CSD, crystal shape and MZW will be investigated. This will result in an opportunity to improve the reactor design and gain more insight in the sonocrystallization mechanism. First, the background of sonocrystallization and crystallization processes will be investigated. Also, earlier investigations will be discussed.

3.1 SONOCHEMISTRY

3.1.1. Principles of ultrasound

A sound wave will produce vibrations which change the density and pressure of the particles along the direction of motion of the wave. Sound propagates as a mechanical wave of pressure and displacement. Ultrasound is an oscillating sound pressure wave with a frequency range higher than 20 kHz. In this thesis high power, low frequency ultrasound with frequencies between 41 kHz and 1140 kHz, and intensities above 10 W/cm^2 will be studied. These ultrasound waves can produce cavitation bubbles. [4, 5] Ultrasound is a longitudinal pressure wave, and consist of compressions and rarefactions, as shown in figure 1. The compressions are regions of high pressure while the rarefactions are regions of low pressure. [6, 7]

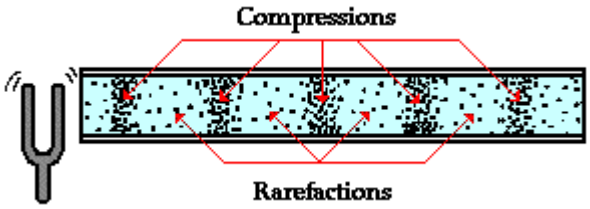

FIGURE 1: A PROPAGATING ULTRASOUND WAVE [8]

Ultrasound waves can be applied in various fields, the most important are the mechanical industry, the medical industry, the chemical industry and the pharmaceutical industry. In the mechanical industry, ultrasound can be used for nondestructive testing of products to detect objects and measure distances and invisible flaws. [9] [10] Next, in the medical industry, ultrasonic sound (sonography) is used as a medical imaging technique. [11] [12] Third, in the chemical industry ultrasound is used for cleaning, mixing and sonochemical reactions. [13, 14] Finally, in the pharmaceutical industry, one of the most interesting applications of ultrasound is the use in the crystallization process. Crystallization in the pharmaceutical industry serves mostly as a purification and separation process for the isolation of pharmaceutical ingredients. [15] The mechanical and medical industry use the ultrasound waves solely to collect information by sending high frequency sound waves, which will be reflected by the material to be examined. The reflected waves will be collected. In the chemical and pharmaceutical industry, in contrast, the waves will not have any impact, but the cavitation bubbles produced by the ultrasound waves will drive chemical reactions and interact with the crystallization process.

3.1.1. Acoustic cavitation

Cavitations are the formation of bubbles in a liquid. It usually occurs due to rapid changes of pressure. The application of ultrasound on a liquid medium will produce compression and rarefaction of the liquid molecules. If the pressure during the rarefaction is low enough, cavitation bubbles will be created. Due to the oscillating ultrasound field, the bubbles will grow when subjected to the pressure reduction, as seen in figure 2. When the bubbles attain a volume at which they can no longer absorb energy, they collapse violently during a high-pressure cycle, the voids can implode and generate a shockwave. [16] These cavitations can be stable or transient. [16] [17, 18] Stable cavitations will oscillate nonlinearly during many cycles of the acoustic wave, the bubble size will oscillate around one equilibrium size for many acoustic cycles. Transient cavitations will grow rapidly in a few acoustic cycles to more than twice the initial radius, before collapsing violently from compression. [19] The change in bubble size during a single cycle of oscillation can become so large that the bubble undergoes a cycle of explosive cavitation growth and collapses violently. [20] [17, 18]

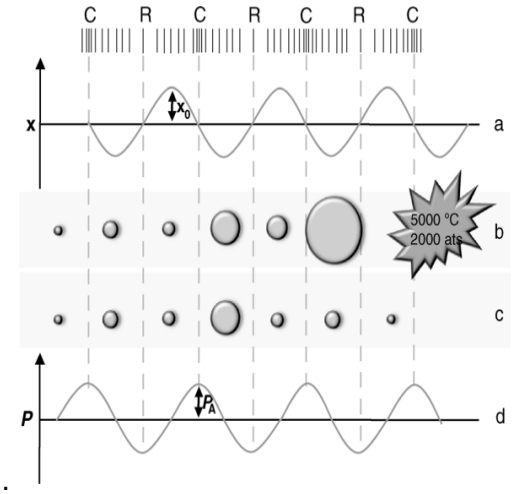

FIGURE 2: TRANSIENT (B) AND STABLE (C) CAVITATIONS [19]

3.1.2. Acoustic streaming

Lee *et al.* studied the cavitations using sonoluminescence and observed that the cavitation bubbles were moving towards the liquid surface. [1] This is caused by acoustic streaming. Due to the attenuation of the acoustic energy, cavitation bubbles will be pushed towards the liquid surface. Acoustic attenuation describes the energy loss of sound propagation. When sound propagates in a media, there is always thermal consumption of energy caused by the viscosity of the fluid. The attenuation results in the growth of an energy gradient. This causes the fluid to move in the direction of the propagating acoustic wave. Acoustic streaming depends on the wave frequency and nonlinear property of the fluid. Higher frequencies (MHz range) will enhance the acoustic streaming, attenuating more. Acoustic streaming will also increase, when the viscosity increases. A larger bubble will cause more distortion and thus more attenuation of the acoustic wave. [21, 1, 22]

Higher frequencies (MHz), cavitations are considered to have the biggest amount of attenuation caused by the acoustic wave. At higher frequencies (kHz-MHz), coalescence of the cavitations can form larger bubbles. These bubbles will show no resonance and will distort the high frequency acoustic waves, by scattering.

3.2. STANDING AND TRAVELLING WAVES

3.2.1. WAVE TYPES

Two type of waves will be discussed. A traveling and a standing wave. A traveling wave occurs when there are no reflection or interfering waves. The energy propagates in one direction. A traveling wave will periodically move at a constant speed. A standing wave, in contrast, occurs with interference of 2 propagating waves in different directions and is the sum of the amplitude of these waves. The wave nodes will remain at the same place. Between two nodes, the antinodes will oscillate between two maximums, as seen in figure 3. [16] [17, 18]

Due to the reflectivity at the boundary, the wave field can be partially standing and partially traveling when using ultrasound. The proportion of standing and traveling waves can be altered by changing the reflectivity of the boundary. [1, 23, 24] Leighton *et al.* reported an increase in standing waves at higher reflectivity of the boundary. Traveling waves occur when using an absorber at the liquid surface and standing waves occur when using a reflector. [25] [26]

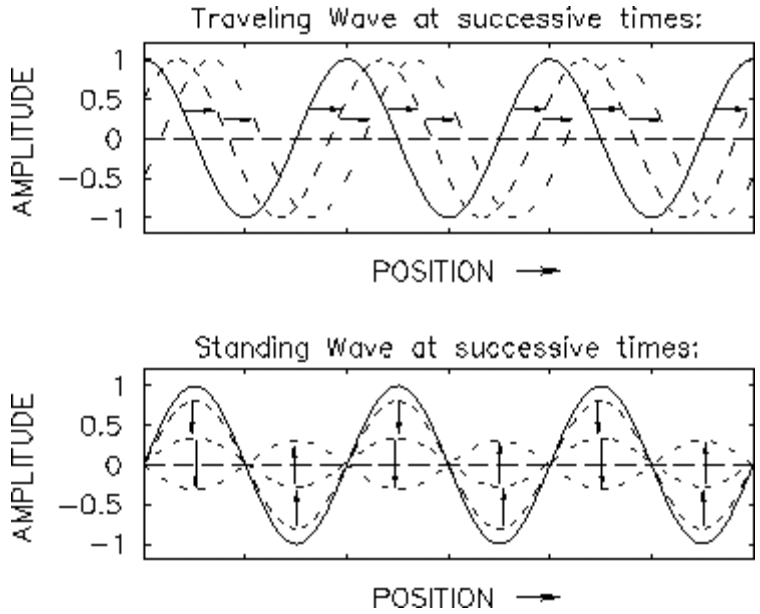

FIGURE 3: PROPAGATION OF STANDING AND TRAVELING WAVES [27]

The type of wave also seemed to have an influence on the cavitations. The acoustic radiation force is the force, exerted by the ultrasound wave on a obstacle in the path of the wave. In a standing wave field, the ultrasound radiation force drives bubbles at resonance towards the antinodes, this is the point where the amplitude of the standing wave is maximum. In a traveling wave field this force drives bubbles at resonance in the direction of the propagating wave. The radiation force from a traveling wave field can drive the bubbles toward the liquid surface.

3.2.2. PARAMETERS INFLUENCING WAVE TYPE AND SONOCHEMICAL ACTIVITY

Several parameters were said to have influence on the wave type, and thus the sonochemical activity. In this paragraph, the effect of the frequency, flow and reflection material will be discussed.

3.2.2.1. *Effect of Frequency*

Several studies investigated the effect of the frequency on the wave type and the cavitations. They stated that a lower frequency was beneficial for achieving a standing wave structure. Also at high frequency, acoustic streaming was present. At low frequencies, mainly transient cavitations were present.

Lee *et al.* studied the cavitation bubble structures using sodium dodecylsulfate. [1] They monitored the cavitation bubbles with sonoluminescence (SL), using a high speed digital camera to monitor the bubble structures at 210 frames per second. The SL images were shown in figure 4 and showed at 168 kHz a standing wave pattern and had an increased SL intensity further from the plate transducer. The standing wave structure was shown when bubbles will coalescent. At 448 kHz, they observed bubbles along the vertical axis of the propagating acoustic wave between the liquid surface and the transducer. At 726 kHz, bubbles will first emerge towards the transducer. They will increase in number and size. After 0.16 s, the bubbles were visible emerging towards the surface. This was also observed at 448 kHz. The emerging towards the surface at higher frequencies is due to acoustic streaming.

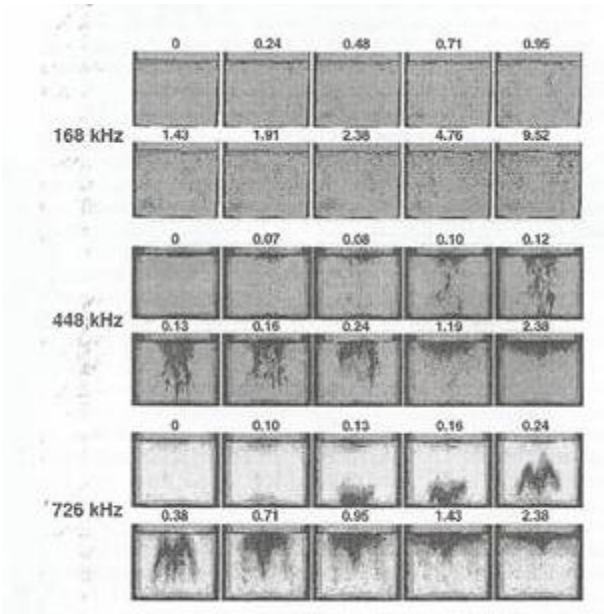

FIGURE 4: SONOLUMINESCENCE IMAGES AT 168, 448 AND 726 KHZ, MEASURED IN FUNCTION OF TIME (S) [1]

Using sonoluminescence, they also found a strong standing wave at 168 kHz. At 448 kHz, weakening of the standing wave field was observed due to large coalesced bubbles which significantly attenuate the acoustic amplitude. Consequently, the traveling wave proportion was increased. At 726 kHz, it was noted that the generated acoustic streaming disrupts the standing wave structure. [23] According to these studies, there can be stated that at higher frequencies, traveling waves will dominate, and at lower frequencies, the standing wave proportion was higher.

The frequency has, besides the wave type, also an influence on the type of cavitation bubbles formed and the sonochemical activity. Ashokkumar et al studied the multibubble sonoluminescence at different frequencies on a plate transducer. They studied water at 20 °C and an acoustic power of 20W. The authors found stable cavitations at low frequencies of 25 and 37 kHz, and transient cavitations at higher frequencies of 440kHz. [28] Bussemaker *et al.* summarized studies on the effect of the frequency on the cavitations. They stated that at lower frequencies (100 kHz and lower), the bubble has more time to grow with an increased intensity of the collapse. [29]

Lower frequencies result in larger bubbles, which in a standing wave will be pushed towards the antinodes and coalesce and attenuate the standing waves. At higher frequencies, more bubbles are formed, which will collapse and produce radicals. At even higher frequencies (MHz) the rarefaction of the waves will become too short for sonochemistry effects. The maximum frequency for cavitations to occur is dependent on the geometry, temperature, ambient pressure, viscosity and the gas composition of the reactor solution. Bussemaker *et al.* declared that radically driven processes will be maximized at high frequencies, and mechanical effects are maximized at low frequencies. [29]

3.2.2.2. Flow

The impact of the flow was investigated. The sonochemical activity increases when introducing stirring at all frequencies. However, at stirring speed higher than 900 rpm, no extra benefit was shown. Also the region of the sonochemical activity depends on the frequency.

Bussemaker *et al.* studied the effect of overhead stirring on the ultrasound field. They also compared previous studies regarding the flow effect on the sonochemical activity. [29] At both low and high frequencies, the introduction of flow in an ultrasonic reactor provides an increase in sonochemical activity. The authors, however, noted that these studies were done in different reactors and that the reactor geometry has an influence on the sonochemical activity. [29] They studied the effect of the stirring speed at different frequencies using a 2.5 mM luminol and 2.5 M sodium carbonate stock solution. When the stirring speed increases, the sonochemiluminescence images varied at each frequency. Figure 5 shows the dependency of the sonochemical yield (H_2O_2 yield) on the stirring speed at different frequencies. At 40 kHz, the overhead stirring increases the sonochemical activity with an increase in the speed of stirring up to 900 rpm. At stirring speeds above this 900 rpm, no additional benefit in activity was observed. It was assumed that at 40 kHz, the increase in sonochemical activity was a result of the reduction of coalescence of bubbles with overhead stirring, increasing the active bubble population. Bubbles which merge, will become too big for sonochemical activity and will become degas bubbles. When working at a higher frequency of 376 kHz, the standing wave structure was reduced and the intensity at the bottom of the reactor was increased. At even higher frequencies (995 kHz; 1179 kHz) sonochemiluminescence was limited to the central region. This result shows that at high frequencies, stirring can decrease the sonochemical activity.

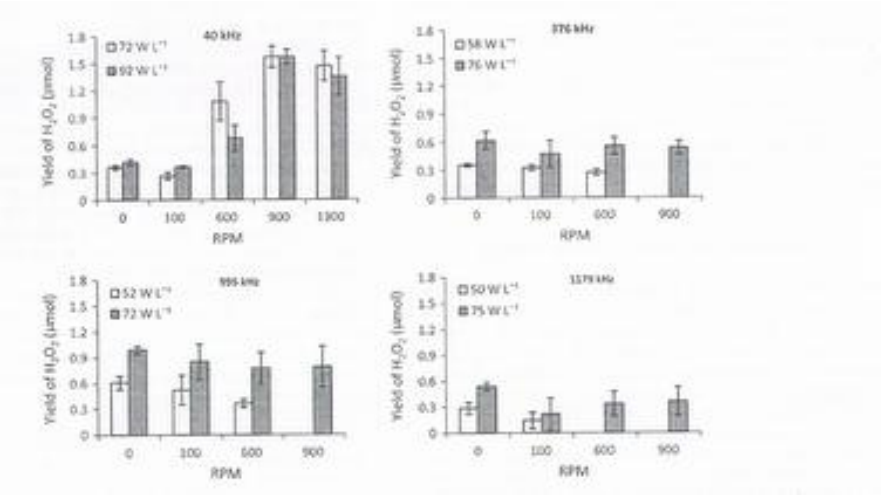

FIGURE 5: H_2O_2 YIELD IN FUNCTION OF STIRRING RATE (RPM) AT DIFFERENT FREQUENCIES (40, 376, 995 AND 1179 KHZ) [29]

Bussemaker *et al.* enumerated several possible factors which can affect the sonochemical activity in a travelling wave field, namely the reduction of the sonochemical area, the influence of stirring on the propagation of the ultrasonic wave and the reduction of the standing wave field. They stated that a stirrer can disturb the reflection of the standing wave in a solution, improve the diffusion to increase the bubble size, disturb the propagation of the US field, affect the collapse of the bubble and prevent the bubbles reaching antinodes in the standing wave, where they coalesce. [29] Rectified diffusion has been shown to enhance the presence of acoustic streaming. Rectified diffusion is entering of gas into the bubble, due to a pressure gradient at the expansion phase of the cavitation. [30]. However the authors found that acoustic streaming is present at high and low frequencies, but still more present at high frequencies. As possible explanation the authors put forward is that stirring at low frequencies enhances the rectified diffusion. However, the acoustic streaming velocity is in the order of ten times slower than the stirring speed. So they do not consider that the stirrer has no influence on the bubble growth via rectified diffusion.

3.2.2.3. Reflection material

The ratio of standing and traveling waves can be changed by altering the surface stabilizer. The surface stabilizer serves for reflecting or absorbing the ultrasound waves. If the acoustic impedance of the surface stabilizer is close to the acoustic impedance of the solution, the waves will be absorbed. The attenuation or dB-loss per distance the wave travelled through the material must be high, to ensure that most of the wave is absorbed before it reaches the other end of the surface stabilizer. At the other side of the surface stabilizer, there will be a material - air interface which will reflect a part of the wave back into the surface stabilizer and finally back into the solution in the opposite direction of the source wave. Therefore a large attenuation will ensure that only a small wave fraction will be reflected. Using a surface stabilizer with a significant different acoustic impedance than the one from the solution, will cause reflection of the wave. [31, 32]

The acoustic impedance can be calculated using following formula based on the density and the speed of sound.

$$Z = pV \qquad \text{EQUATION 1}$$

(Z = impedance ($N{\cdot}s/m^3$); V= acoustic wave speed (m/s); p = density (kg/m^3))

Bussemaker *et al.* used a lid made of foam and coated in parafilm as surface stabilizer. From sonochemiluminescence images, they found that when a standing wave is responsible for the sonochemical activity, a surface stabilizer will enhance the sonochemical activity . When a traveling wave will be responsible for the sonochemical activity, surface stabilization will decrease the sonochemical activity. [29]

Brems *et al.* has studied the effect of the ultrasound wave, varying the traveling wave component. [24] The authors used an Aptflex F28 anechoic material as surface stabilizer, and measured the bubble activity with a needle hydrophone with an aperture of 500 µm. They stated that the physical forces generated by the cavitation bubbles were maximized when the standing wave component was minimized, by introducing the anechoic material at all the vertical walls in the reactor. [28]

3.3. SONOCRYSTALLIZATION

3.3.1. PRINCIPLES OF CRYSTALLIZATION

Crystallization is the formation of crystals from a solution and consists of two phases. In the first step, the nucleation, molecules will move into clusters which will eventually form nuclei. This happens after supersaturation, the molecules will rearrange themselves in the energetically more beneficent position. In the second step, the growth step, the crystals will grow to their final size.

Several types of crystallization processes are known, namely cooling, evaporative, anti-solvent, reactive and melt crystallization.

First cooling crystallization will be discussed. This process is based on the principle that the solubility increases with the temperature, thus crystals will form simply by cooling the solution. Cooling crystallization is the result of falling temperature, leading to supersaturation, nucleation and finally crystallization. [33] [3] When the temperature reaches the solubility temperature, the solution metastable zone is reached. The metastable zone width (MZW) is defined as the difference between the solubility temperature and the nucleation temperature, as shown in figure 6. This nucleation temperature is the temperature at which crystals are formed.

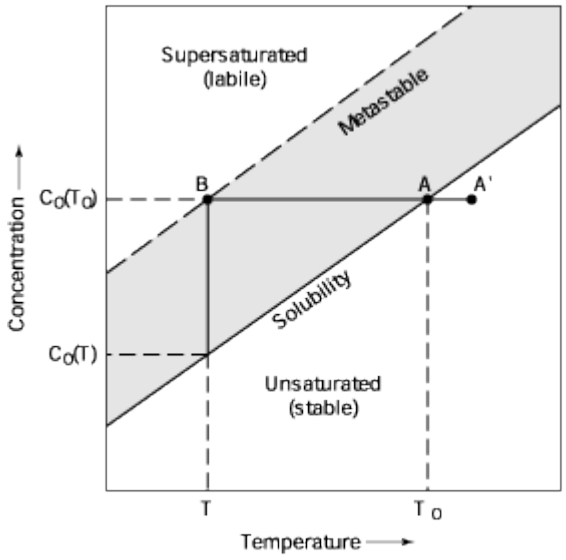

FIGUUR 6: METASTABLE ZONE WIDTH [34]

The second technique of evaporative crystallization will form nuclei by increasing the solute concentration by evaporation of the solvent. The temperature will be constant. [2]

Another technique is anti-solvent crystallization. In this process a second solvent, an anti-solvent, is added to the solution to reduce the solubility of the solute. Anti-solvent crystallization can be carried out at temperatures near the ambient temperature. [35]

Next, reactive crystallization involves the simultaneous reaction and solid-liquid phase separation. An in situ product separation takes place to enhance the conversion of equilibrium limited reactions. In the pharmaceutical industry, this process is often used by reacting the product with a specific optically active resolving agent producing two derivatives easily separated by crystallization. [36, 37, 38]

Finally melt crystallization generally removes heat and cools the liquid melt to create a driving force for the formation and growth of crystals [39]. Melt crystallization is a technique used for purification and separation of mixtures of chemicals and metals, due to solid-liquid separation.

Crystallization in the pharmaceutical industry serves mostly as a purification and separation process for the isolation of pharmaceutical ingredients. Here, the exact crystal size, shape, appearance and homogenous crystals are important for the purity of the crystallized pharmaceutical products. The crystal size distribution (CSD) [40] defines the size of the crystals. The volume% in function of the particle diameter (μm) are be examined. The size of the crystals will be examined, this is important for the pharmaceutical industry. Homogeneous and smaller crystals will be beneficial for the purity of the paracetamol crystals.

3.3.2. SONOCRYSTALLIZATION

Sonication can have a significant effect on the crystal size distribution. Most articles report a reduction in particle size and narrowing of the span. Ultrasonic parameters such as the frequency, intensity and sonication time are observed to influence the MZW and CSD.

Several papers report a decrease in reduction time by application of ultrasound. Higher ultrasonic intensities resulted in smaller induction times. Luque de Castro *et al.* investigated the effect of the US time on the crystal size during the antisolvent crystallization of K_2SO_4 in water (0.0156 g/g water). The induction time is the time elapsed between the creation of supersaturation and the appearance of crystals, and is dramatically reduced when using US. The induction time in the absence of US was found to be 9000 s. When US was applied, this induction time was reduced to 1000 s. Also, shorter US times are not capable of giving a uniform mixture of the solution and precipitant, will burst nucleates at a lower supersaturation and allows them to grow large crystals. [2] The production of smaller crystals can be obtained using longer US treatment. [41]. Harzali *et al.* also investigated the induction time, using $ZnSO_4 \cdot 7H_2O$ in water at 0.16 and 30 W and found that the overall induction time decreases when applying a higher ultrasonic intensity. [3]Without US, an induction time above 6000 s was found. At 16 W, this induction time decreases below 2000 s and at 30 W, the induction time is below 1000 s. Virone *et al.* studied the pressure in the cavitation bubbles and the effect on the nucleation rate. For insonated batches a strong reduction in induction times with high reproducibility was found. [42]

The ultrasonic intensity has also an influence on the metastable zone width (MZW). Lecis *et al.* examined the effect of the ultrasonic intensity on the MZW during the cooling crystallization of paracetamol. The calorimetric power was varied between 3-7 W, the frequency was kept constant at 97.97 kHz and the paracetamol concentration was 18 g/l. The largest MZW reduction was achieved at a power of 7 W. [2]

Luque de Castro *et al.* investigated the effect of US power on crystallization of calcium carbonate at 0.10 and 100 W. Via electron scanning microscopy there was also stated that the crystal size decreases with increasing US power. [41] Increasing the *US* intensity increases the crystallization rate and decreases the particle size. When the US power and intensity become, however, too high (above 40 W), abrasion of the particles was observed. [41]

Low-frequency waves cause less cavitation but these cavitation bubbles will, however, be more intense. At higher frequencies, the MZW reduction will decrease and low frequencies allow faster nucleation. [43, 33] Li *et al.* studied the sonocrystallization of spectinomycin hydrochloride (SH) with a concentration of 0.17 kg SH/kg H_2O. [44]The frequency was varied between 15, 20, 25 and 30 kHz. The power output was kept at 400 W. Results gave no significant difference in the crystal size distribution and shape. These results were explained by the hypothesis that different low frequency wavelengths have the same influence on nucleation and growth of the crystal. [44] Wohlgemuth *et al.* observed the crystallization of adipic acid. Ultrasound waves at 204 kHz; 355.5 kHz and 610 kHz were used and the influence on the MZW and crystal size distribution during the crystallization was investigated. The insonation period was set at 10 seconds. The power was held at 200 W and the experiments were executed in a 1.2 l reaction vessel. The results show almost no dependence of the frequency on the MZW. [45] Kordylla *et al.* investigated the crystallization of dodecandioic acid and the effect of the ultrasonic frequency and power on the cooling process. Ultrasound waves at 355.5 kHz and 1046 kHz were tested in the same reactor setup as Wohlgemuth *et al.* Kordylla *et al.* stated that the best performance was reached at a frequency of 355.5 kHz, achieving an efficiency of 0.36. The power was varied between 100 and 200 W for both frequencies. They stated that a constant power is important when measuring different frequencies. [46]

These papers investigated the effect of the frequency on a limited frequency range. It could be expected that the effect on crystallization is limited in this range. Also, different powers, products and reactor geometries were used, which makes it hard to compare. Jordens *et al.* therefore investigated the effect of a wide range of ultrasonic frequencies on the MZW during the cooling crystallization of paracetamol. . The experiment was performed at 41, 98, 165, 570, 850 and 1140 kHz, without surface stabilizer, thus liquid-air as interface. The calorimetric power was kept constant at 8 W and the concentration of the paracetamol solution was 20 g/l. The results stated that the maximum reduction in MZW of 17 °C was achieved at a frequency of 41 kHz. [33]

Meifang *et al.* compared the sonochemical activity in a closed and a open system and investigated the changes to acoustic cavitation bubbles at various frequencies and power levels. They considered an open system as the liquid interface was open to the atmosphere. The system was considered closed when the liquid surface was covered with a glass lid. [47] They varied the power between 10 W and 60 W at a frequency of 213kHz, and found that for open and closed systems, the intensity increases significantly with an increase in the applied power up to 40 W. At very high power levels, the cavitation activity may not increase with of power because several events such as coalescence between bubbles, degassing and bubble clustering may dominate. They also varied the frequency between 213, 315, 647 and 1056 kHz for open and closed systems. At 213 and 315 kHz the cavitation activity was slightly higher in a closed system. At 647 and 1056 kHz the closed system looks more homogeneous, and the cavitation activity seems to move away from the transducer end of the open system. They studied the difference between a closed and an open system and stated that an open system creates more active cavitation bubbles. The reason for a lower activity in the closed system compared to the open system might be related to the existence of standing waves where bubbles are "pushed" into antinodes and the resultant clustering of bubbles may lead to a decrease in the number of active cavitation bubbles. A closed system generates a relatively higher number of stable cavitation bubbles.

3.3.3. HYPOTHESIS BEHIND SONOCRYSTALLIZATION

Cavitation bubbles, produced by the ultrasound waves, are said to cause a faster nucleation. [43] [41] [2] [48] Literature describes five crystallization mechanisms caused by cavitations namely, the hypothesis of cooling, pressure, evaporation, segregation and heterogeneous nucleation.

The first hypothesis states that crystallization occurs because of the cooling effect. With the expansion of the cavitation bubble, the surrounding fluid cools down which results in a brief increase of supersaturation, followed by nucleation and crystallization. However, Hunt and Jackson calculated the cooling effect for cavitation bubbles is less than 1°C for bubbles up to 0,1 mm in diameter. [49] [50] This temperature change is too small to produce nucleation. [2]

A second hypothesis states that localized high pressure areas were caused by the collapse of the cavitation bubble. This can result in an increase of the melting point and a decrease in solubility, causing supersaturation and nucleation [51]. However, studies revealed that ultrasound also enhances nucleation of products which solubility increases with pressure. This can cast the pressure hypothesis into question. Harzali *et al.* investigated the pressure effect using a pressure independent crystal, namely Zinc sulphate heptahydrate. [3] They found a drastically reduction of the induction time using ultrasound.

The third hypothesis states that during the growth of the cavitation bubble, evaporation of the solvent from the surface of the cavity into the bubble occurs. The cavity will fill with vapor and thus cooling the surface, causing supersaturation on the surface due to expansion. [2] Duan *et al.* studied cavitations, due to evaporation-induced negative pressure in transparent nanofluidic channels, and found that local expansions at the nanochannel entrances could result in entrapped bubbles that act as nuclei for cavitation. The growth rate of vapor bubbles during this confined cavitation process only depends on the water evaporation at the nanochannel entrance. The resulting water evaporation is not diffusion limited and can thus occur at a much faster rate than evaporation without cavitation. [52] The evaporation effect, however, is not significant enough to produce a temperature change large enough to produce nucleation. [53] [3]

The fourth theory of the segregation states that after implosion, the crystal precursors and the solvent molecules are separated shortly. At the end of the bubble collapse, a gas recompression in the cavitation will stop the inward motion of the mixture. In crystallization processes, the clusters will be more dense than the surrounding liquid and undergo an inward drift motion due to these difference in density, become overconcentrated near the bubble wall for about 1 ns. Harzali *et al.* evaluated the concentration of the clusters as they become segregated from the liquid by the bubble motion, using Zinc sulphate heptahydrate in water. They found that segregation can enhance the nucleation process. [3] An oversaturation occurs, which can increase the nucleation effect. [2]

Finally, literature describes a fifth theory which states that ultrasonic crystallization occurs as a result from heterogeneous nucleation. Brown states that cavitations offer nucleation centers for the crystals to initially form around. [54] Later, Mazhul states that "the cavitational rupture themselves can become crystallization centers." [55] The result is a decrease of the energy barrier for nucleation, giving a significant increase in crystallization. In industry seed crystals are frequently used as a nucleation centre from which crystals can grow. They allow recrystallization by eliminating the need for a random molecular interaction. [56]

The segregation and heterogeneous nucleation hypothesizes are believed to have the most effect on crystallization. [49] [33] The segregation theory will require a larger amount of transient cavitations. More transient cavitations will collapse and produce a larger amount of pressure, enhancing the segregation. The heterogeneous hypothesis, in contrast, just requires cavitation bubbles of any sort.

Little is known about the effect of the crystallization parameters, surface stabilizer and stirrer, on the wave types ,the cavitations and the crystallization process. With better knowledge of the effect of these parameters, the size and shape of the crystals can be controlled and optimized, and the knowledge of the effect of ultrasound waves on crystallization will increase.

4. MATERIAL & METHODS

Tests are performed to investigate the effect of the ultrasonic frequency, intensity and applied surface stabilizer on the cavitation type, CSD and MZW during the cooling crystallization of paracetamol. In this section first, the experimental setup will be described, next, the procedure followed during the crystallization process and finally the analytical techniques to measure the MZW, CSD, crystal shape, wave and cavitation type.

4.1. EXPERIMENTAL SETUP

A 180 ml batch reactor was used for this experiment, as shown in figure 7. The reactor has a double jacketed glass wall, and a Lauda ECO RE45 water bath was used to control the temperature in the reactor. A plate transducer is used at the bottom of the reactor. One transducer was used for frequencies of 41 kHz and 98 kHz (Ultrasonics world MPI 7850D_20_40_60 H transducer), another transducer was used for frequencies of 570 kHz and 1140 kHz (Meinhardt E/805/T/M) At the top of the reactor, a surface stabilizer (copper, glass, PUR) was placed to adjust the standing/travelling wave ratio. The solution was stirred using a Cole Palmer mixer at 400 rpm. The waves were generated by a G5100 A 50 MHz waveform generator, and amplified by a E&I 1020L RF power amplifier. The temperature in the reactor was measured with a Pico Tv08 type K thermocouple. The caloric input power was varied between 4 W and 15 W.

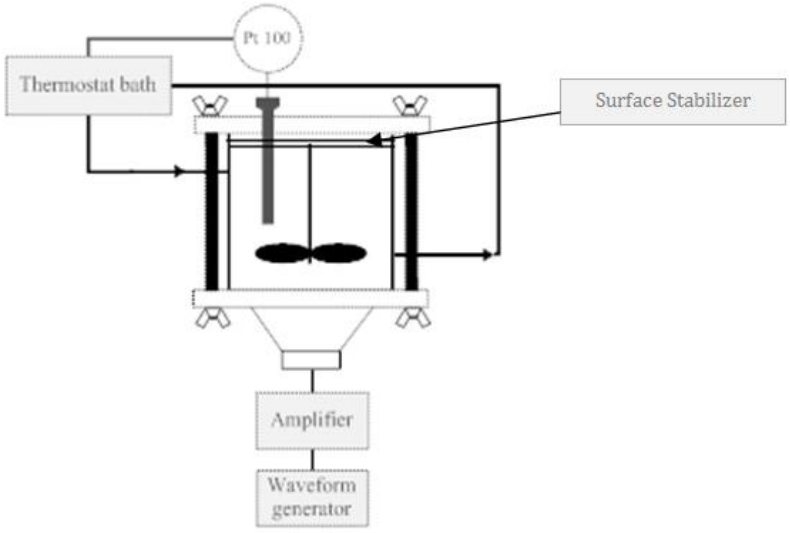

FIGUUR 7:: EXPERIMENTAL SETUP [33]

Although it is simple to measure the consumable electric energy, it does not characterize the power of cavitation processes. In order to transfer the exact power to the solution, calorimetric tests need to be performed. [57] The reactor vessel was filled with 180 mL of ultra-pure water, the liquid was stirred at 400 rpm, and kept at a temperature of 20 °C. The wave generator was used to generate a peak to peak voltage which was amplified and sent to the ultrasound transducer. Next, the temperature increase was recorded for 2 min at different input powers and the calorimetric power was calculated using equation 2 over these 2 min while applying ultrasound.

Using the temperature change over the examined time, the caloric power to the solution can be calculated with:

$$P_{CAL} = C_p . M . (\frac{DT}{DT}) \qquad \text{EQUATION 2}$$

(P_{cal} = power transferred to the solution (W); Heat capacity: c_p=4186 J/kg.K; mass: m=0.180 kg) [33] [58]

4.2. SURFACE STABILIZERS

Different surface stabilizers were used to vary the standing/traveling wave ratio (equation 3). The reflection coefficient determines the fraction of the wave that is reflected. When the impedance of the liquid differs more from the impedance of the surface stabilizer, a larger reflection was obtained.

$$R = (\frac{Z_2 - Z_1}{Z_2 + Z_1})^2 \qquad \text{EQUATION 3}$$

(R = the reflection coefficient (-), Z_1 = the acoustic impedance of the liquid (MRayl = 10^6 $\frac{Pa}{m/s}$) and Z_2 = the acoustic impedance of the reflection material (MRayl)) [59]

Copper, Glass and PUR (Polyurethane) were chosen as surface stabilizers because of their differences in reflection coefficient. In table 1, the impedances and reflection coefficients were calculated. Copper has the highest reflection coefficient (0.88) and is expected to produce a higher ratio of standing waves. PUR has a low reflection coefficient, and is expected to produce mostly traveling waves. [60] [61] [62] Two values for attenuation of PUR were found: 46,1 dB/cm at 4 MHz [63] and 73,0 dB/cm at 5 MHz [64] [26]. At lower frequencies, no attenuation values were found, but these values can give a good indication for the attenuation loss.

Table 1: Impedance and reflection coefficient for reflection materials

Material	Impedance (MRayls)	Reflection coefficient (compared to water)	Reflection % (compared to water)
Water	1.48		
PUR (Apltile SF5048)	1.89	5.10^{-4}	1.5
Copper	44.60	0.88	88.0
Glass	13.00	0.63	63.0

4.3. CRYSTALLIZATION

A paracetamol solution of 20 g/l in ultra-pure water was made. The solution was heated to 50°C and stirred until all the crystals were dissolved. Next, the solution was filtered over a 0.45 µm Millipore filter to remove solid impurities. 180 mL of the solution was brought into the reactor and kept on 40°C (6°C above solubility temperature). Next, this solution was cooled at a rate of circa 0.7 °C/min until nucleation was detected visually. Literature stated that the solubility temperature of a 20 g/L paracetamol solution is 34.05°C [33]. The calorimetric power was kept constant at 8 W to obtain a stable intensity for different frequencies. Parameters that were varied are:

- The frequency: 41 kHz, 98kHz and 1140kHz
- The reflection material: PUR, Glass, Copper

4.3.1. *MZW MEASUREMENTS*

The MZW was measured as the difference between the solubility temperature of 34.05°C and the nucleation temperature. This nucleation temperature was defined as the temperature at which crystals are first detected visually. [65] Every crystallization test was repeated at least 3 times, to ensure reproducibility.

4.3.2. *CSD MEASUREMENTS*

The crystal solution of 180 ml was filtered over a 0.45 µm Millipore filter and the residue was dried in an oven at 50°C for minimum 5 hours. The Crystal Size Distribution (CSD) was measured with a Mastersizer 3000 laser diffraction meter, who can measure particles from 0.01 to 3500 µm. The crystals were added in n-hexane. This is a cheap solvent wherein paracetamol does not dissolve. 1% Lecithin was added to prevent adhesion to the cell window (2,64 g dissolved in 400 ml n-hexane). [66] The stirrer of the dispersion unit was rotated at 2400 rpm. A laser diffractometer measures particle size distributions by measuring the angular variation in intensity of light scattered as a laser beam passes through a dispersed particulate sample. Large particles scatter light at small angles relative to the laser beam and small particles scatter light at large angles, as illustrated in figure 8. A red light source (Max. 4 mW He-Ne, 632.8 nm) and a blue light source (Max. 10 mW LED, 470 nm) were used. [67] Light of smaller wavelengths (blue laser) is more sensitive to sub-micron particles, larger wavelengths (red laser) are used to measure larger particles. The angular scattering intensity data is then analyzed using the Mastersizer V2,20 program to calculate the size of the particles responsible for creating the scattering pattern. After initializing, the background was measured. Hereafter, the sample was added and measured. The diffractometer was washed two times with 99% acetone and two times with n-hexane before measuring the next sample.

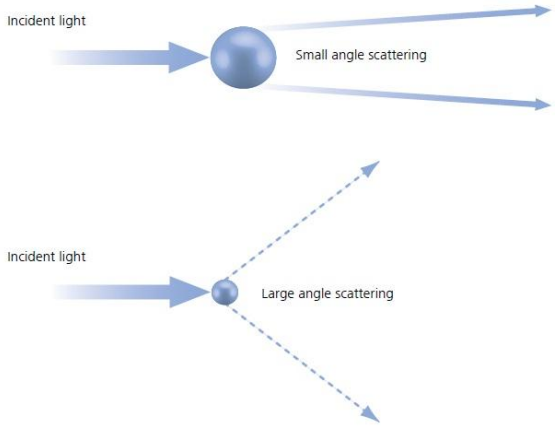

FIGURE 8: LIGHT SCATTER IN A LASER DIFRACTOMETER AT DIFFERENT SAMPLE SIZES [68]

The D50; D4,3; D3,2 and span value will be measured.

The D50 or Dx(50) value characterizes the size of the grains. The D50 is the size in microns that splits the distribution with half above and half below this diameter. So half the amount of crystals is smaller than this value. This value represents the median value of the crystal size. A higher D50 value means that more large crystals are present. The D10 and D90 values were also detected. The D90 value characterizes the largest crystals. 10% of the crystals are larger than the D90 value. The D10 value characterizes the smaller crystals, where 10% of the crystals are smaller than the D10 value. [69, 70, 71]

The D4,3 value stands for the volume mean, and the results represent the volume contribution. A larger D4,3-value means that a larger volume contribution was measured. The D3,2 value stands for the surface mean, and the results represents the surface contribution. A larger D3,2-value means that a larger surface contribution was measured [69, 71].

The span calculation is the most common format to express distribution width. [69, 71] The span will be calculated with equation 7.

$$Span = \frac{D_{v\,0,9} - D_{v\,0,1}}{D_{v\,0,5}} \qquad \text{EQUATION 4}$$

The span includes two points which describe the coarsest and finest parts of the distribution. These are typically the D90 and D10. The span is not the same as the peak width, because the span works with D90, D10, the tail also has an influence. Also when dividing by the D50, the position of the peak also plays roll

4.3.3. CRYSTAL SHAPE MEASUREMENTS

The crystal shape was measured using a SEM (scanning electron microscope). A sample of the filtered crystals was added on carbon tabs. The tabs were be sputtered with a 7 nm layer of carbon, to make them conductive. These samples were be measured in the SEM (Siemens Philips XL30 FEG). The SEM scans the crystals with a beam of electrons. These electrons interact with the atoms in the sample, producing signals that describes the surface topography and composition to obtain a two-dimensional scanning image showing a shape, a composition of a sample. The SEM has a resolution better than 1 nm [72].

4.4. STANDING OR TRAVELING WAVES

Tests were performed to check whether standing or travelling waves were formed at different surface stabilizers. Also, the effect of the frequency and power on the wave type is investigated. The waves were measured using sonochemiluminescence (SLC) with luminol.

Pressure variations due to the propagation of ultrasound waves result in the growth and collapse of cavitation bubbles filled with gas and/or vapor [2][40]. Furthermore, it has been shown that extremely high local temperatures and pressures may be generated during the collapse or implosion of such bubbles. Within the cavitation bubble, or the layer of solution immediately contacting the cavitation bubble, the sonochemical effects take place. The method for detecting US waves using luminol was applied to the determination of trace amounts of H_2O_2 in purified water without any special pre-treatments [73]. Ultrasound will break the hydrogen peroxide bond and form hydroxyl radicals (reaction 1), however these radicals have a short lifespan and will form hydrogen peroxide or superoxides (reaction 2,3) .

$$H_2O_2 \rightarrow 2\,HO^{\bullet} \qquad \text{reaction (1)}$$

$$2HO^{\bullet} \rightarrow H_2O_2 \qquad \text{reaction (2)}$$

$$HO^{\bullet} + H_2O_2 \rightarrow O_2^{\bullet} + H_3O^{+} \qquad \text{reaction (3)}$$

Chemiluminescent reactions of luminol are oxidations occurring under basic conditions. When luminol reacts with the hydroxide, a dianion is formed. The oxygen then reacts with the luminol dianion. The product of this reaction, an organic peroxide, is very unstable and immediately decomposes , losing nitrogen to produce 3-aminophthalic acid with electrons in an excited state. As the excited state relaxes to the ground state, the excess energy is liberated as a photon, visible as blue light (λ≈ 425nm). The global reaction is described in reaction 4 [74, 75, 76].

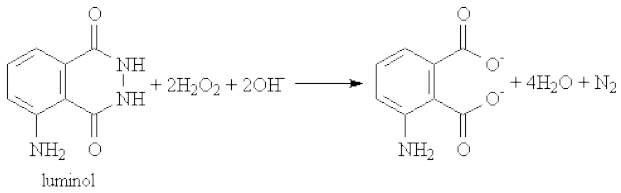

luminol

reaction (4)

A stock solution of 100 mM NaOH and 10 mM luminol in 200 ml was made (0.84 g NaOH; 0.35g luminol). Next, 180 ml solution was added to the reaction vessel. Ultrasound was applied on the solution in a dark room. The frequency was varied between 41 kHz, 570 kHz and 1140 kHz,the power between 4 W, 8 W and 15 W and copper, glass, PUR and air (open system) were used as surface stabilizers. The temperature was held at the nucleation temperature depending on the frequency and surface stabilizer (annex 4). SCL images were captured for 30 seconds using a long-exposure camera (canon 600DS). Each experiment was repeated 2 to 3 times to ensure the reproducibility of the results. [28]

The number and type of bands, as well as the distance between these bands were investigated at different frequencies. The band shape was compared between different surface stabilizers. Also the influence of the stirrer was investigated. Measurements were performed at 0 and 400 rpm and without a stirrer. Finally a comparison was made between a horn and a plate transducer.

4.5. STABLE OR TRANSIENT CAVITATIONS

The type of bubbles will be measured using a hydrophone (Picoscoop 5242A oscilloscoop 2CH 60 MHz). The hydrophone is based on a piezoelectric transducer which means that a voltage will be generated when subjected to a pressure change. The hydrophone measures the average pressure. A piezoelectric material can convert an ultrasound signal into an electrical signal, because sound is a pressure wave. When a mechanical effect like pressure is applied to a piezoelectric material, the polarization of the material will change and cause a output voltage which is proportional to acoustic pressure input. This results in the desired frequency response [77, 78]. The acoustic level (dBV) will be displayed in function of the frequency at different power levels. The spectrum is obtained by FFT (Fast Fourier Transformation) using hamming windowing. One spectrum is shown in figure 9.

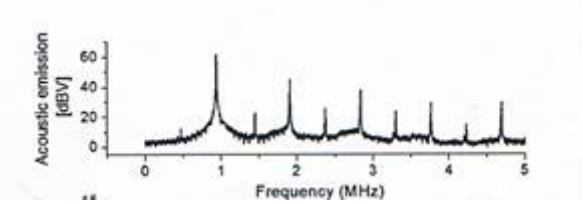

Figure 9: Cavitation spectrum at forward power of 450 mW/cm². integer and half integer harmonic peaks *[24]*

Frohly *et al.* found that the bubble type can be monitored based on the cavitation noise. [16] The cavitation noise was measured with a broadband hydrophone DAPCO NP 10-3, and the signal is digitalized and displayed, in a logarithmic scale. The cavitations were measured in water at 20°C. The transducer consists of a 6x6 cm piezoelectric transducer, driven at 1.075 MHz. The intensity was varied between 12 and 300 mW/cm^2. Absorbing rubber was used as surface stabilizer. The influence of the acoustic intensity on the cavitation noise was investigated.

The hydrophone measures the dBV in function of the frequency. They used the cavitation noise, which they obtained by numerical integration, as a reference to represent whether stable or transient cavitation bubbles are present. At higher intensities (60 mW/cm^2, or 1.67 mW), they found a broadband on the line spectrum, called “white noise” (figure 10). Each bubble in a cavitation field can behave as a secondary source of acoustic emission. The cause can be the emission of a shock wave by the bubble during its collapse. This shockwave can cause a contribution to the noise in the spectrum. The noise is visible as a increase in surface under the spectrum, due to extra shockwaves. The surface under the peaks will be considered as peak contribution, while the other peaks are considered as noise contribution. Transient cavitations will collapse faster and thus they produce more noise. Transient cavitations are related to a high value of acoustic noise. [16] [3, 16]

Not only transient cavitations can be the cause of the noise. Also stable cavitations are able to produce a pressure wave after collapsing inducing more noise. A stable cavitation bubble, however, does not explodes as fast and violent as a transient cavitation bubble, resulting in a much larger contribution in the noise.

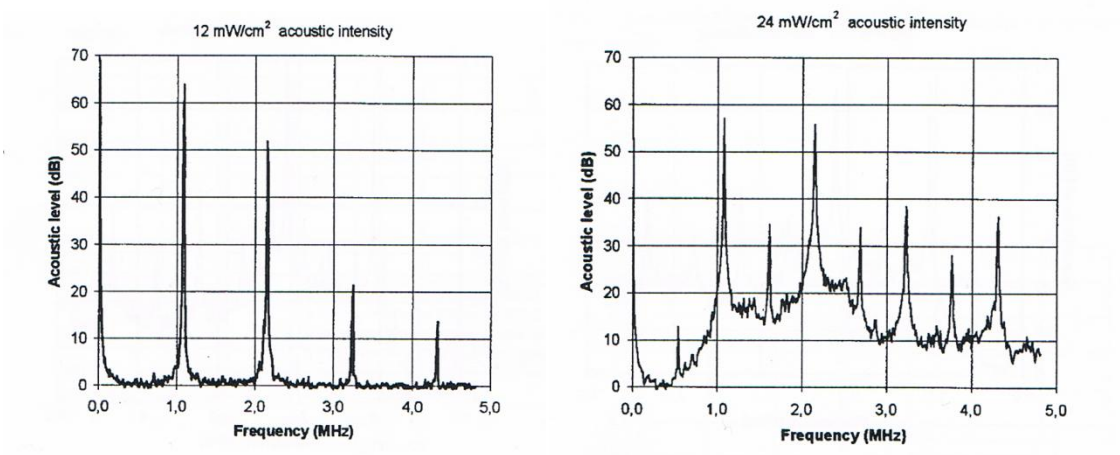

FIGURE 10: CAVITATION NOISE SPECTRUM AS A DIFFERENT ACOUSTIC INTENSITIES AT 1,075 MHZ [16]

In this thesis, the reaction vessel was filled with 180 ml MilliQ water and ultrasound was applied. The frequency (41 kHz, 570 kHz and 1140 kHz) the power (4 W, 8 W and 15 W) and the reflection material (copper, glass, PUR and air (open system)) were varied. Qualitative study will result in a visual detection of the spectrum to see whether or not cavitation noise is present. The surface of the noise distribution will be measured, and compared in a peak/noise ratio for a quantitative study. [16] [79] The surface beneath the chart will be measured using the trapezium rule.

$$\int_a^b f(x)\,dx \approx (b-a)\left[\frac{f(a)+f(b)}{2}\right] \qquad \text{EQUATION 5}$$

The surface beneath the peaks will be considered peak contribution under the first five peaks, the surface beneath the areas between the first five peaks will be considered noise contribution as shown in figure 11. The ratio peak/noise will be compared between different frequencies, surface stabilizers and intensities.

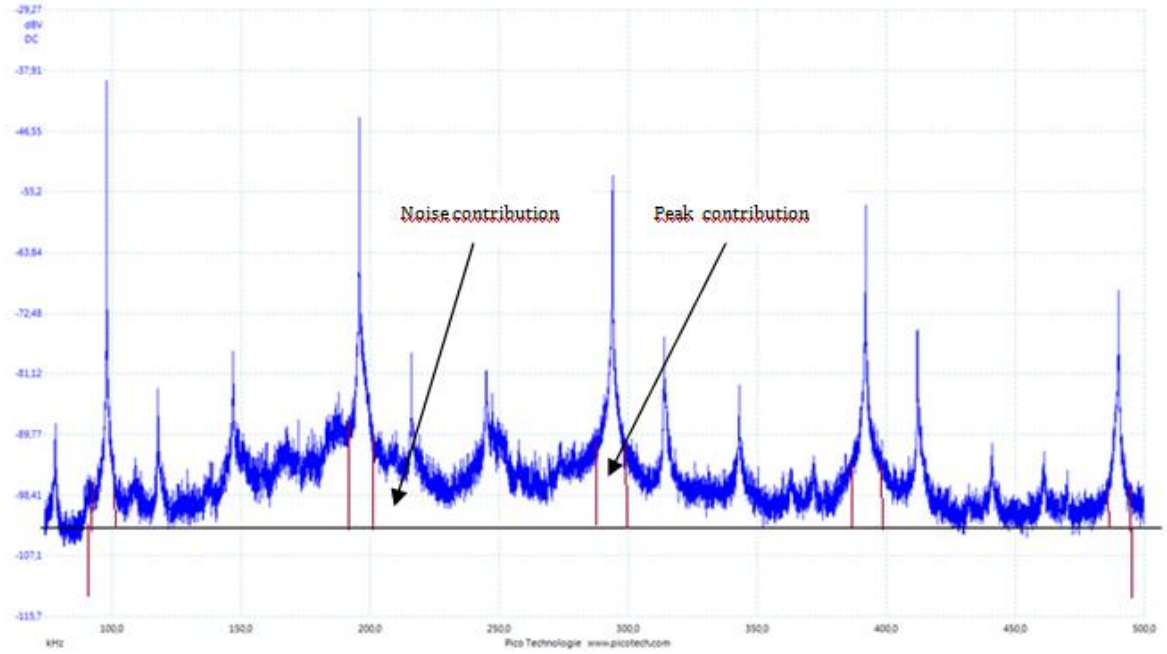

FIGURE 11: MEASURING METHOD FOR PEAK AND NOISE CONTRIBUTION

The effect of the frequency and surface stabilizer on the noise was studied. Also the effect of the hydrophone position in the reactor on the cavitations was investigated. Finally, the impact of a stirrer on the cavitations will be examined.

5. RESULTS & DISCUSSION

The effect of the frequency was investigated on the wave type, cavitations, the MZW, CSD and crystal shape. The effect of the surface stabilizer on the wave type, cavitations and MZW was investigated. Finally, the effect of the stirrer on the wave type and cavitations were investigated.

5.1. CALORIMETRIC MEASUREMENTS

First, calorimetric tests were performed for copper, glass, air and PUR at 41 kHz, 98 kHz and 1140 kHz. De temperature increase was measured when using ultrasound. [80] As an example, the calorimetric study with Copper at 1140 kHz with 300 mV peak to peak is shown in graph 1. The input power was 42 W (53 W forward; 11 W reverse).

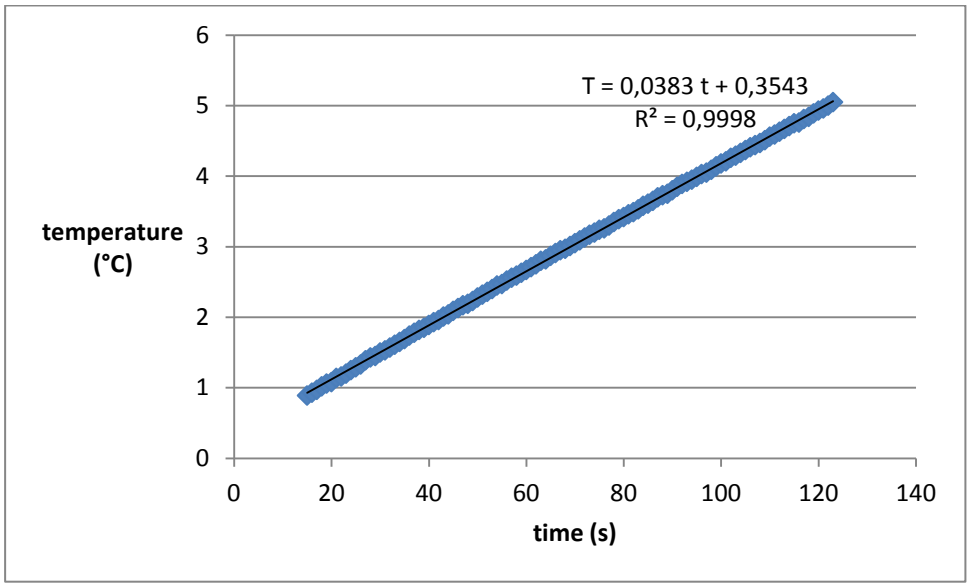

GRAPH 1: CALORIMETRIC STUDY (COPPER, 1140KHZ, 300MVPP)

With the slope $(\frac{dT}{dt})$, the calorimetric power can be calculated using equation 2.

The calorimetric power of copper at 1140 kHz and 300 mVpp is:

$$P_{cal} = 26{,}58\ W$$

This experiment was repeated at varying peak to peak voltages. The relation between the calorimetric power and input power for copper at 1140 kHz was shown in graph 2.

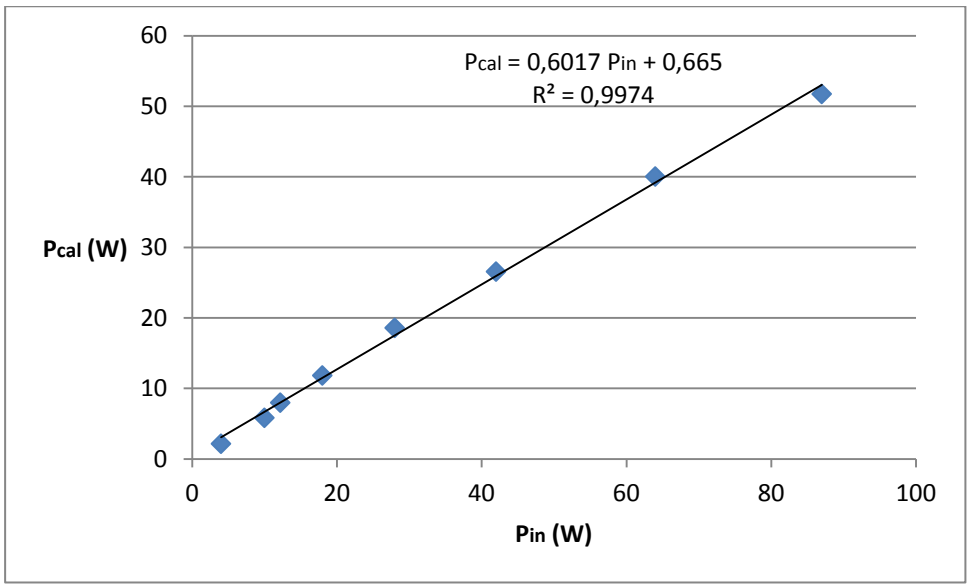

GRAPH 2: CALORIMETRIC POWER – ELECTRICAL POWER RELATION (COPPER AT 1140 KHZ)

This was repeated for all P_{cal} and P_{in} relation the surface stabilizers and frequencies. The results were shown in table 2.

TABLE 2:P_{CAL} AND P_{IN} RELATION

Frequency	**Pcal**	**Pin**			
		Surface stabilizer			
		Copper	Glass	PUR	Air
1140 kHz	4 W	6 W	5 W	7 W	8 W
	8 W	12 W	11 W	12 W	14 W
	15 W	24 W	22 W	24 W	25 W
570 kHz	4 W	5 W	5 W	5 W	9 W
	8 W	13 W	13 W	13 W	16 W
	15 W	26 W	26 W	26 W	28 W
98 kHz	4 W	5 W	5 W	7 W	9 W
	8 W	9 W	14 W	13 W	16 W
	15 W	17 W	26 W	24 W	19 W
41 kHz	4 W	5 W	8 W	6 W	7 W
	8 W	9 W	14 W	13 W	14 W
	15 W	17 W	23 W	26 W	25 W

The calorimetric tests were performed until a forward power of 50 W, and no flattening of the $P_{cal}(P_{in})$ graph was detected. So the relation between P_{cal} and P_{in} is a linear relation under an electric input power of 50W.

When using copper or glass as surface stabilizer, the input power was less stable compared to PUR, where the input power was more stable.

At higher frequencies, a lower peak to peak voltage must be applied to become the same calorimetric power. Higher frequencies are said to produce more energy, and thus a lower peak to peak voltage needed to be applied. This probably indicates that the high frequency transducer is more efficient than the low frequency transducer.

Using copper at low frequencies, a significantly lower input power was necessary compared to PUR and glass. A reason could be the higher thermal conductivity of copper as shown in table 3, however this would result in a higher input power necessary, because of the heat loss trough the copper surface. [81] So the results were not as expected. A other reason could be that the power transferred is very dependent on the position of the copper stabilizer [82]. A small change in the position of the surface stabilizer could double or halve the transferred power. The position of the surface stabilizer is very important. The copper could have be slightly oblique when using calorimetric measurements at 41 kHz.

TABLE 3: SURFACE STABILIZERS: THERMAL CONDUCTIVITY

Material	Thermal conductivity
copper	401 W/m K
glass	1,05 W/m K
PUR	0,03 W/m K
air	0,024 W/m K

5.2. Impact of the Frequency

5.2.1. Crystallization

5.2.1.1. MZW

The effect of the frequency was studied on the MZW for copper, PUR and glass as surface stabilizer. Each test was performed at least 3 times. Results from previous studies were added to increase the precision of the tests. Annex 1 shows the average MZW, the standard deviation, and the reduction in MZW. The MZW was shown in graph 3.

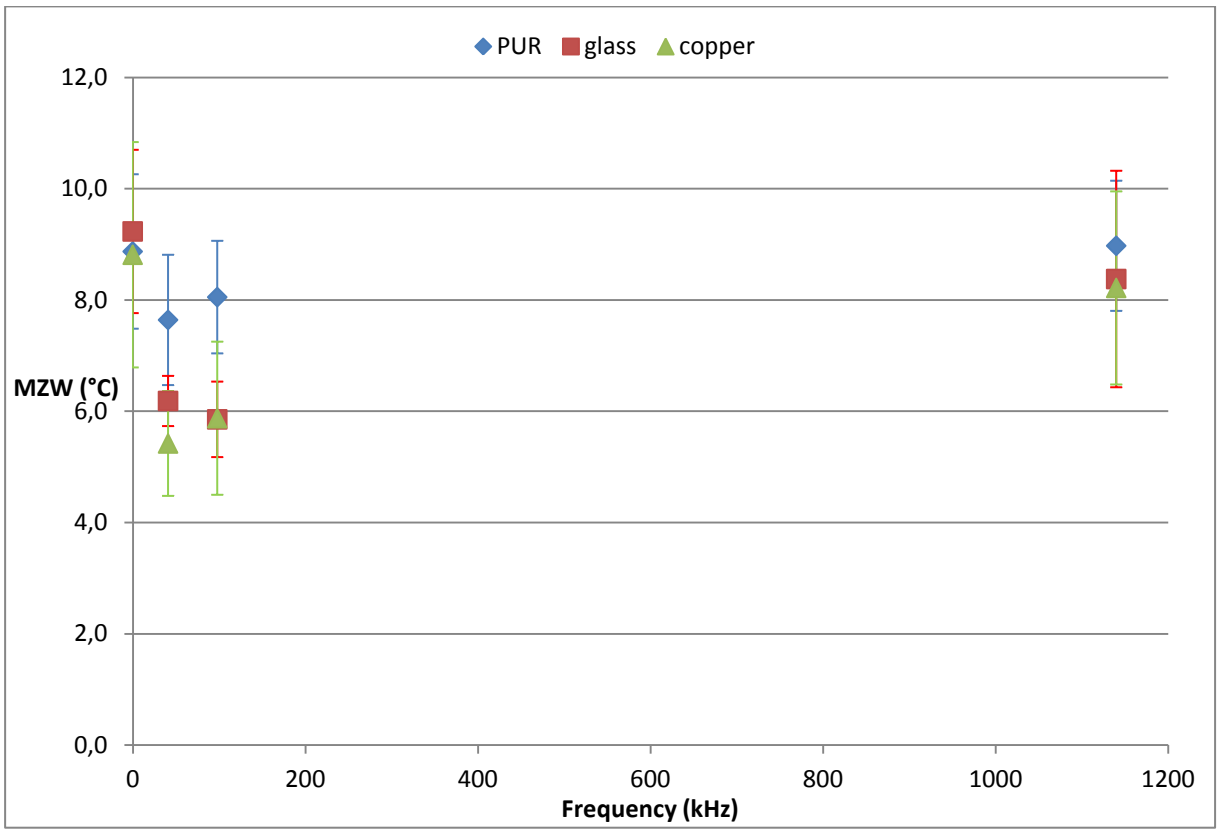

GRAPH 3: MZW WITH STANDARD DEVIATION AT DIFFERENT FREQUENCIES AND SURFACE STABILIZERS (GLASS, COPPER, PUR)

The MZW reduction was clearly larger at low frequencies for all surface stabilizers. At 1140 kHz, no significant reduction in MZW was detected. At 41 kHz and 98 kHz, a larger reduction in MZW was detected. The reduction reaches a maximum of 3.4°C when using copper as a surface stabilizer at a frequency of 41 kHz. Also notable is a larger standard deviation in the MZW at high frequencies. Using a constant power is important. The tests at higher frequencies showed a less stable input power compared to using lower frequencies. Kordylla *et al.* varied the power between 100 W and 200 W. They stated that a constant power is important when measuring different frequencies. [46]In this experiment, a maximum power of 50W was applied. This could be a reason for the higher standard deviation at high frequencies.

Between 41 kHz and 98 kHz, no significant differences in MZW reduction can be observed. This corresponds with the results of Wohlemuth *et al.* [45] who studied the dependence of the frequency at 204 kHz, 355.5 kHz and 610 kHz and showed almost no dependency of the frequency on the MZW. When using a larger frequency range, a clear difference in MZW reduction, however, is detected. The measurements of MZW were shown to have quite a large standard deviation in the crystallization process. This can be a result of a large volume (180 ml) where the crystallization takes place. So measuring at small differences in frequency will not be able to produce significant differences in the MZW. When comparing the MZW reduction over a broad frequency range of 1140 kHz and 41 kHz, a larger reduction in MZW was detected. This result is in agreement with the ones observed in literature. Kordylla *et al.* studied the MZW reduction at 355.5 kHz and 1046 kHz and found a larger reduction at the lowest frequency [46]. Jordens *et al.* studied the crystallization at 41, 98, 165, 570, 850 and 1140 kHz and also found that a lower frequency gives the largest MZW reduction. [33]

5.2.1.2. CSD

The crystal size distributions are displayed in annex 2 giving the volume % as a function of the particle diameter (µm).

At higher frequencies, a larger tail is observed with all surface stabilizers. This can be due to non-ideal mixing [83]. Non homogeneous mixing results in the formation and growth of crystals at different periods. Earlier coalescence will result in larger crystal clusters, leading to a tail. Crystals which coalesce later, will result in smaller clusters. Larger frequencies will cause less ideal mixing and less uniform crystallization.

Copper shows variation in crystal size at different frequencies. Using copper at high frequencies, the peak shifts slightly to the left compared to the blanco peak, meaning crystals will be smaller when using ultrasound with copper as reflector. At lower frequencies, the peak moves even further towards the smaller crystals. At 98 kHz and 41 kHz, the crystal size will be significantly smaller than when using no ultrasound. Glass did not show much variation to the blanco. At 41 kHz, almost no variation was shown. At 98 kHz and 1140 kHz, the peak is located slightly to the left, meaning smaller crystals were present. PUR showed almost no variation to the blanco. At all frequencies, the peaks of the US treated samples and those of the blanco, overlap.

The width of the peak will also be examined. Copper showed smaller peaks at low frequency, meaning that low frequencies result in a more homogeneous crystal size. High frequencies also gave smaller peaks than when using no US, but wider peaks than when working at low frequencies. A smaller peak describes more homogeneous crystals. Glass showed a small peak at 1140 kHz, but with a large tail. At 98 kHz the peak width was wider and at 41 kHz no reduction in width was noticed compared to the blanco. The peak width when using PUR showed no dependency of the frequency.

The crystal size distribution at different frequencies will be further examined using the D50-, D3,4-, D2,3- and span-value. However, these results cannot give a significant conclusion, because of the tail. The results were mentioned below, but were not discussed. The results were displayed in annex 3.

The D50 values at different frequencies for PUR, glass and copper are shown in table 4.

TABLE 4: DX (50) VALUE AT DIFFERENT FREQUENCIES (COPPER, GLASS, PUR)

Surface Stabilizer	Frequency	Dx (50) – value (µm)
PUR	Blanco	64.60
PUR	41 kHz	49.62
PUR	98 kHz	68.50
PUR	1140 kHz	79.72
Glass	Blanco	72.86
Glass	41 kHz	80.07
Glass	98 kHz	56.90
Glass	1140 kHz	44.46
Copper	Blanco	102.00
Copper	41 kHz	51.42
Copper	98 kHz	54.34
Copper	1140 kHz	77.38

The D4,3- and D3,2- values are shown in table 5.

TABLE 5: D3,4 AND D3,2 VALUE AT DIFFERENT FREQUENCIES (COPPER, GLASS, PUR)

Surface Stabilizer	Frequency	D 4,3 – value (µm)	D 3,2 – value (µm)
PUR	Blanco	73.98	51.53
PUR	41 kHz	61.18	36.26
PUR	98 kHz	83.88	54.82
PUR	1140 kHz	128.40	63.72
Glass	Blanco	80.74	57.66
Glass	41 kHz	86.53	62.02
Glass	98 kHz	74.26	41.72
Glass	1140 kHz	64.74	33.28
Copper	Blanco	113.00	80.94
Copper	41 kHz	64.14	37.76
Copper	98 kHz	66.04	42.84
Copper	1140 kHz	95.62	63.26

The span is displayed in table 6.

TABLE 6: SPAN VALUE AT DIFFERENT FREQUENCIES (COPPER, GLASS, PUR)

Surface Stabilizer	Frequency	Span
PUR	Blanco	1.60
PUR	41 kHz	1.85
PUR	98 kHz	1.55
PUR	1140 kHz	1.84
Glass	Blanco	1.49
Glass	41 kHz	1.40
Glass	98 kHz	1.86
Glass	1140 kHz	2.35
Copper	Blanco	1.44
Copper	41 kHz	1.67
Copper	98 kHz	1.76
Copper	1140 kHz	1.78

Copper showed smaller crystals when applying ultrasound. The smallest crystals were obtained at low frequencies. PUR did not show much difference in crystal size when using ultrasound. The results when using glass showed a small difference in crystal size. The tail was observed to be larger at high frequencies, indicating a less homogeneous crystal growth.

Bonné *et al.* studied the effect of the frequency on the crystal size distribution with copper as surface stabilizer. They stated that sonocrystallization can produce smaller particles. They also found a lower crystal size distribution and D50 value at lower frequencies, confirming that low frequency crystallization is beneficial for smaller crystals. [82]

5.2.1.3. CRYSTAL SHAPE

The crystal shape was measured using SEM. The results were shown in annex 4. The scale of the images is shown at the bottom of each picture. Images were taken at scale of 100 µm and 200µm. Measurements were performed at 0 kHz, 41 kHz and 1140 kHz, using PUR, copper and glass as surface stabilizer. Results did not show any differences in crystal shape. The frequency does not have an influence on the crystal shape. Also a different surface stabilizer does not affect the shape.

Luque de Castro *et al.* found that between low-frequency US waves (15 - 30 kHz) no substantial differences in shape, mean size or size distribution in the resulting crystals was observed. Therefore, these wavelengths seem to have the same influence on nucleation and crystal growth. The authors stated as a possible explanation that they the wavelengths are much larger than the size of the nuclei and crystals. [41]

5.2.2. *ULTRASOUND WAVES*

The impact of the frequency on the ultrasound waves were investigated, to detect the position of the cavitation bubbles in the reactor. Luminol measurements at 8W calorimetric power were done with 3 different stabilizers and air. Results were shown in figure 12.

With copper as surface stabilizer 4 bands were detected at 41 kHz, equally divided between the surface and the level of the stirrer. The distance between the bands was 1.60 cm. At 98 kHz, the test results showed 7 bands with a distance of 0.80 cm between the bands, but the band under the copper surface and at the level of the stirrer had a significantly larger diameter than the other bands. At 570 kHz and 1140 kHz, the area around the stirrer was slightly illuminated. When the power was increased, the solution illuminated throughout and no bands were distinguishable.

With glass as surface stabilizer, also 4 bands were detected, equally divided between the surface and the level of the stirrer. The distance between the bands was 1.65 cm. At 98 kHz, results gave 6 to 7 bands, the bands were wider than when using copper, but not as wide as at 41 kHz. The distance between the bands was 0.65 cm. At 570 kHz and 1140 kHz, the same result was obtained than at copper. However using glass, the band was slightly more visible, and also the area around the stirring bar illuminated.

Using PUR , at 41 kHz, 3 bands were detected, with a distance of 1,9 cm between the bands. However, the bands were less illuminated than when copper or glass was used. PUR at 98 kHz gave 6 bands with a distance of 1.10 cm. At 570 kHz and 1140 kHz, the same result was obtained using glass and copper. PUR gave an increase in illumination at the level of the stirrer and around the bar.

Using air, at 41 kHz, 3 bands were detected with a distance of 2.3 cm between the bands. At 98 kHz, air gave 7 bands with a distance of 0.9 cm. At 570 kHz, the results were the same as at PUR. At high frequencies, illumination at the height of the stirrer was barely visible. When the power was increased, the solution illuminated throughout. But still no bands were distinguishable.

Annex 6 shows the wavelengths at different frequencies. Results show that the distance between the bands is approximately half the wave length. This could indicate that the illuminated bands were at the antinodes of the standing waves. The transducers used in these experiments provide a sinusoidal wave. The waves are pushed into the antinodes. Theoretically, the first visible band should be at the first antinode, which is located at ¼ the wavelength. However, the first illuminated band is always located at the level of the stirrer. This indicates that the stirrer has a large impact on the position illuminated bands and on the position of the cavitation bubbles.

Bands were always visible, at all surface stabilizers, and frequency. The bands were located at $\lambda/2$. At lower frequencies, less bands were visible. A band structure indicates standing waves. According to these studies, there can be stated that at higher frequencies, traveling waves will dominate, and at lower frequencies, the standing wave proportion was higher.

These results confirm the results found in literature, which stated that a lower frequency was beneficial for achieving a standing wave structure. Also at high frequency, acoustic streaming was present. At low frequencies, mainly transient cavitations were present. Lee *et al.* stated that at high frequencies the standing wave structure will disrupt, due to acoustic streaming. At low frequencies, the standing wave ratio will be the highest. The images however did not show a band structure. No stirrer was used in the experiments by Lee *et al.* [1]A stirrer can have a large influence on the band pattern.

Ashokkumar *et al.* stated that at lower frequency, the bubble collapse will be more intense. They declared that at lower frequencies (100 kHz and lower), the bubble has more time to grow with an increased intensity of the collapse. At higher frequencies, more bubbles are formed, which will collapse and produce radicals. At even higher frequencies (MHz) the rarefaction of the waves will become too short for sonochemistry effects. This could be a reason why, at high frequencies no band structure is shown in the measurements with luminol, and a larger intensity is needed to create a visible band structure.

Copper (Z=44,6 MRayl; Rcoef= 0,88)

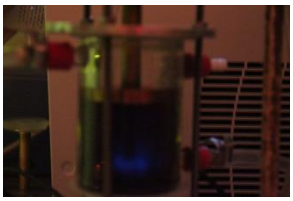
1140 kHz
Distance = not detectable
No bands visible

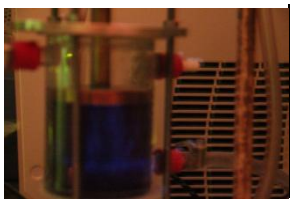
570 kHz
Distance < 1mm
+ 50 bands (at high P)

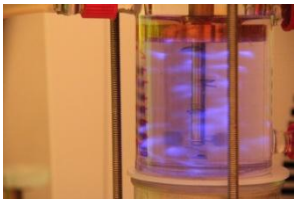
98 kHz
Distance = 0.80cm
7 bands

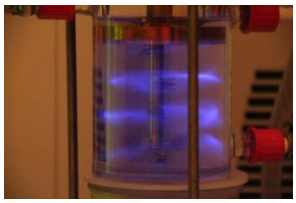
41 kHz
Distance = 1.60 cm
4 bands

Glass (Z= 12,1 MRayl; Rcoef = 0,63)

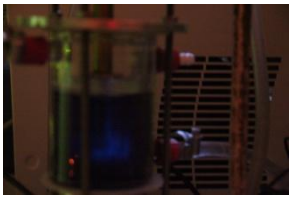
1140 kHz
Distance = not detectable
No bands visible

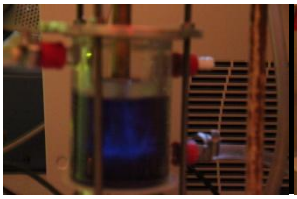
570 kHz
Distance < 1mm
+ 50 bands (at high P)

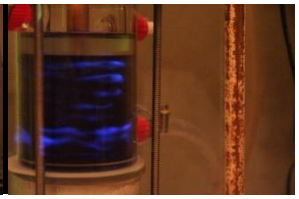
98 kHz
Distance = 0.90cm
6/ 7 bands

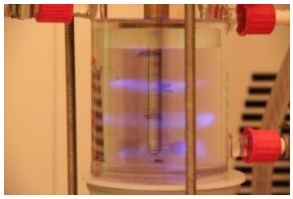
41 kHz
Distance = 1.65 cm
4 bands

PUR (Z= 2 MRayl; Rcoef= 5 10^{-4})

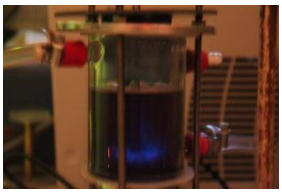
1140 kHz
Distance = not detectable
No bands visible

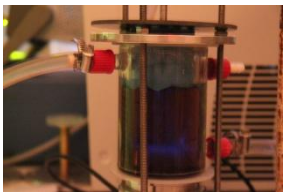
570 kHz
Distance < 1mm
+ 50 bands (at high P)

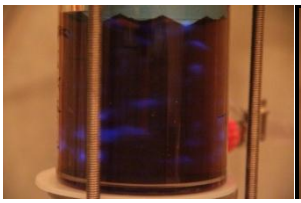
98 kHz
Distance = 1.10 cm
6 bands

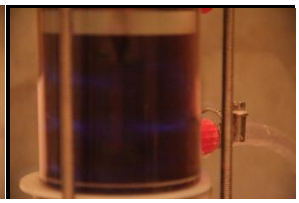
41 kHz
Distance = 1.90 cm
3 bands

Air (Z= MRayl; Rcoef=)

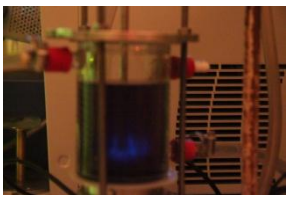
1140 kHz
Distance = not detectable
No bands visible

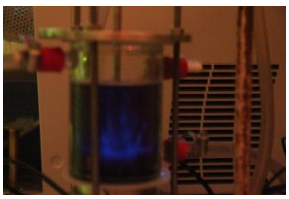
570 kHz
Distance < 1mm
+ 50 bands (at high P)

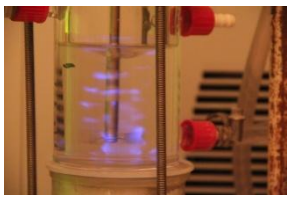
98 kHz
Distance = 0.90 cm
7 bands

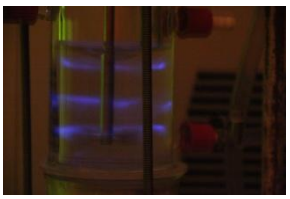
41 kHz
Distance = 2.30 cm
3 bands

FIGURE 12: IMPACT OF FREQUENCY AND SURFACE STABILIZER AT 8W ON US WAVES

5.2.3. CAVITATIONS

The frequency dependency was measured using air and PUR as surface stabilizer when no stirrer was present. At first the acoustic noise is compared, based on the graphs, shown in annex 7.

Using PUR, little noise was detected at high frequencies (570 kHz-1140 kHz). At the lower frequencies (41 kHz-98 kHz), significantly more noise was detected. This indicates more transient cavitations. [3, 16]

When using air as interface, at high frequencies, still little noise was detected. At low frequencies the noise also increases. At all frequencies, the noise seemed to be larger with air than with PUR, however quantitative studies can give unambiguous results.

Next, quantitative test were done, calculating the peak/noise ratio. The peak/noise ratio was calculated and shown in table 7.

TABLE 7: PEAK/NOISE RATIO: FREQUENCY DEPENDENCY

	air	PUR
Frequency	peak/noise	peak/noise
41 kHz	0.1863	0.1783
98 kHz	0.3790	0.6143
570 kHz	0.3978	0.5983
1140 kHz	0.3874	0.8028

At 41 kHz, the peak/noise is significantly lower, compared to higher frequencies, resulting in a larger noise contribution, indicating more transient cavitation bubbles. This confirms the quantitative findings.

At higher frequencies, PUR shows a peak/noise ratio of approximately 60%, and at even higher frequencies 80%. At 41 kHz, the ratio decreases to 18%. Air has a ratio of almost 40% at high frequencies. At 41kHz, the ratio decreases to 18,5%. At 41 kHz, no significant difference in noise contribution is noticed. At high frequencies (98 kHz-1140 kHz), air has a significantly higher noise contribution compared to PUR. This can be a result of air being a open system. This will be further discussed when the influence of surface stabilizers were discussed.

Notable is that the graphs in annex 7 with visibly more noise, has also a wider peak. When almost no noise is detected, the peaks will be smaller. This can be slightly confounding in the calculations of the contributions. These results cannot be taken absolute, however they give a quantitative indication of the present noise. These results match with the qualitative results.

At high frequencies, PUR did not show much illuminated images using luminol. This can be the result of a reduced number of transient cavitations present, shown by a small noise contribution. However air did also not show many illuminations at 8 W, and here, the noise contribution is significantly higher. Nevertheless, a hypothesis can be that the illumination increases when more transient cavitations are present. These results also confirm the findings of Ashokkumar *et al.*, who declared that at lower frequency, the bubble collapse will be more intense. [28] A more violent collapse produces more noise, giving a decrease in the peak/noise ratio. More, and violent collapses can be an indication for transient cavitation bubbles.

5.3. IMPACT OF THE SURFACE STABILIZER

The impact of the surface stabilizer on the MZW, wave type and cavitations will also be discussed.

5.3.1. CRYSTALLIZATION

The impact of the surface stabilizer on the MZW was investigated. The results were shown in annex 1, and graph 3, where the impact of the frequency on the MZW was discussed.

At high frequencies (1140 kHz – 570 kHz), no significantly difference was detected in MZW reduction between the surface stabilizers. At lower frequencies (98 kHz – 41 kHz), using PUR at surface stabilizer, the reduction in MZW is significantly lower than when using glass or copper. Copper and glass are reflective materials, and produce a larger ratio of standing waves. PUR is an absorptive material, and produces a smaller ratio of standing waves. This results in the conclusion that standing waves have a positive effect on the MZW reduction.

Jordens *et al.* showed a reduction in MZW of 10.3°C at 41 kHz. [33] They used no surface stabilizer, thus an open system containing 150 ml instead of 180 ml solution. All other parameters were the same as in this experiment. They obtained a much larger reduction in MZW. At 41kHz, a mean reduction of 17°C was detected. Using copper, the mean reduction was 3.4°C. The MZW under silent conditions is much larger without surface stabilizer. This can be because a surface stabilizer can have irregularities in the surface, decreasing the MZW. Impurities can serve as a nucleation centre, where crystals will start to grow. A larger amount of impurities can result in a faster primary nucleation. [84]

Meifang *et al.* studied the difference between a closed and open system and stated that an open system created more active cavitation bubbles. [47] The reason for a lower activity in the closed system compared to the open system might be related to the existence of standing waves where bubbles are “pushed” into antinodes and the resultant clustering of bubbles may lead to a decrease in the number of active cavitation bubbles. A closed system generates a relatively higher number of stable cavitation bubbles. An open system showed a larger MZW reduction. A higher amount of active cavitations can be a reason for a higher MZW reduction when using an open system.

Notable was that the copper and PUR surface was often damaged by the ultrasound waves after using, especially at high frequencies. Both materials were damaged because of the cavitation collapse, resulting in a local high temperature and pressure. Also, copper gained a black layer of copper oxide.

5.3.2. ULTRASOUND WAVES

The effect of the surface stabilizer on the ultrasound waves was investigated. The results were shown in figure 12. Copper and Glass gave almost the same results at low frequency. Four bands will form, equally divided between the stirrer and the surface material. At low frequencies, copper gave the narrowest bands. Glass gave slightly but visually distinguishable wider bands than copper. PUR showed the widest bands. These bands were less visible, but clearly wider than at copper or glass. Using air, also 3 small bands were detected.

At higher frequencies one clear band was formed at the level of the stirrer, and multiple, but turbulent bands slightly illuminated around the stirring bar. Here, PUR and air will show the same results as copper and glass. At high frequency, not enough pressure, due to cavitations collapsing, was present to make the luminol illuminate. Increasing the intensity resulted in a band spectrum. Because of the uncountable bands, no significantly conclusion about the band width can be stated at 570 and 1140 kHz. All bands were equally divided between the surface stabilizer and the level of the stirrer. There could be stated that at all surface stabilizers, standing waves were detected. When the reflection coefficient of the surface stabilizer increases, the bands become smaller. This could indicate that when smaller bands were detected, the ratio of standing waves/ traveling waves is larger.

The results confirmed the results from Bussemaker *et al.*, who stated that surface stabilizers is predominantly responsible for the sonochemical activity. [29]They also stated that when using a surface stabilizer, the sonochemical activity will decrease. In this thesis, only PUR gave a less clear image.

5.3.3. CAVITATIONS

Dependency of the surface stabilizer on the cavitation type was investigated. The results were shown in annex 8. No stirrer was present. At high frequencies (1140 kHz- 570 kHz), Copper, Glass, Air and PUR were compared. PUR did not show much noise, so very little transient cavitations were detected. However, glass, copper and air showed significantly more cavitation noise. To detect a difference in open and closed systems at high frequencies, quantitative studies were necessary, to measure the difference in noise/peak contribution.

At lower frequencies, Air and PUR as surface stabilizers were investigated. Air gave slightly more noise, thus the amount of transient cavitations were larger when using air. Air is an open system, PUR a closed system.

Meifang *et al.* studied the difference between a closed and open system and stated that an open system created more active cavitation bubbles. [47]And that a closed system can produce more stable cavitation bubbles. This can also be the reason why the reduction in MZW when using air is much larger.

Quantitative measurements were studied . The peak/noise ratio was calculated and shown in table 8. The influence of surface stabilizers was investigated at high (1140 kHz) and low (41 kHz) frequencies. No stirrer was present.

TABLE 8: PEAK/NOISE RATIO: SURFACE STABILIZER DEPENDENCY

	41 kHz	**1140 kHz**
surface stabilizer	peak/noise	peak/noise
Copper		0.9266
Glass		0.8473
PUR	0.1357	0.7413
Air	0.1208	0.4379

At 41kHz, no difference between PUR and Air was noticed. The peak/noise ratio lies around 13%. At high frequencies, copper gave the highest peak/noise ratio, resulting in the lowest amount of transient cavitation bubbles. Glass and also PUR gave slightly higher noise contribution. However air gave a significantly higher contribution. Air is an open system and is said to produce more active cavitation bubbles. [48] Copper and glass at low frequencies were not measured, because of limitations in the material. The hydrophone was not able to reach the solution trough the glass and copper surface. Glass and copper are believed to give a slightly higher amount of noise and transient cavitations, because of the smaller MZW, however this cannot be proved.

Here, the peak noise ratio using PUR and air was again calculated. These results vary from the results in table 7. A comparison was made and shown in table 9.

TABEL 9: REPEATABILITY OF THE PEAK/ NOISE RATIO MEASUREMENTS

	Air	**PUR**
Frequency	peak/noise	peak/noise
41 kHz	0.1863	0.1783
41 kHz	0.1208	0.1357
1140 kHz	0.3874	0.8028
1140 kHz	0.4379	0.7413

A large error was shown on the peak noise ratio. The graph with visibly more noise, has a wider peak. When almost no noise is detected, the peaks will be smaller. So these results can best not be taken absolute, however they give a quantitative indication of the present noise.

Comparing the noise contribution with the illuminated bands, copper, glass and PUR did not show much illumination. Only illumination around the stirrer was detected. This indicates that at high frequencies, the peak/noise ratio is too high, giving less transient cavitations illuminating the luminol.

Brems *et al.* stated that the physical forces generated by the cavitation bubbles were maximized when the standing wave component was minimized, by introducing the anechoic material at all the vertical walls in the reactor. [28] This was not found in these experiments. When PUR was used to decrease the standing wave component, the physical (pressure) force decreases at high frequencies. At low frequencies, no difference was shown in physical force. However, air and PUR were compared, where air is an open system and PUR a closed system. Meifang *et al.* stated that an open system created more active cavitation bubbles. [47] This could also affect the cavitations. To prove the statement of Brems *et al.*, comparison must be made between a reflection and a absorption material in closed systems.

5.4. IMPACT OF THE POWER/INTENSITY

5.4.1. ULTRASOUND WAVES

The power was also varied between 4, 8 and 15 W. The results were shown in annex 9. At higher input power, the bands become more illuminated, but also more turbulent. At lower power, the intensity clearly decreases. Also, at high frequencies, when a higher power was applied, a wide band will form between the stirrer and the surface stabilizer or air. Table 10 describes the minimum input power to visually detect multiple bands at higher frequencies.

TABLE 10: ELECTRIC POWER NECESSARY TO ESTABLISH VISIBLE BANDS AT HIGH FREQUENCIES

Material	Frequency	Power input necessary to become one broad band
Copper	570 kHz	26.90 W
Copper	1140 kHz	35.50 W
Glass	570 kHz	22.50 W
Glass	1140 kHz	29.30 W
PUR	570 kHz	37.65 W
PUR	1140 kHz	44.40 W

At low frequencies (41 kHz, 98 kHz) a band spectrum of multiple small bands was formed. The bands become less illuminated when the power was decreased to 4 W. When the power increases to 15 W, the bands become more intense en turbulent. At higher frequencies (570 kHz, 1140 kHz), only one vague band at the height of the stirrer was shown, sometimes also a vague small band around the stirring bar was visible. Using a high enough power input, many small bands were clearly visible between the stirrer and the surface stabilizer. At lower power, hardly any illumination was detected. Here, not enough transient cavitations will be present, to enhance the illumination process. Figure 13 describes the impact of the intensity on the wave structure using copper at different frequencies.

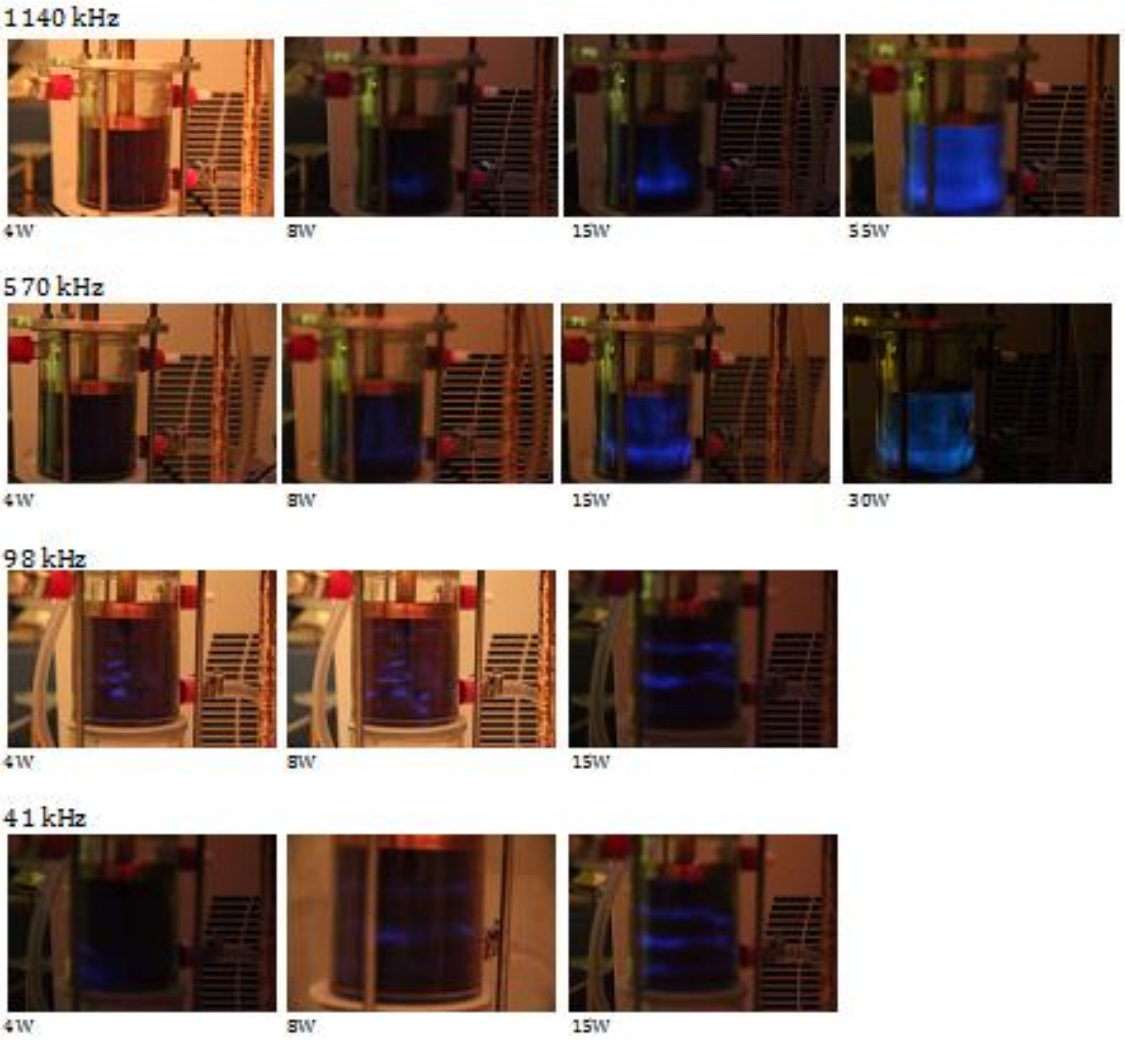

FIGURE 13: IMPACT OF THE INTENSITY ON THE WAVE STRUCTURE USING COPPER AT DIFFERENT FREQUENCIES

5.4.2. CAVITATIONS

At all frequencies, the noise increases at a higher intensity. A higher acoustic intensity can produce a larger amount of transient cavitations at all frequencies and surface stabilizers. However, to prove this and become a uniform conclusion, quantitative measurements are performed, using no surface stabilizer thus air as boundary, at 4, 8 and 15 W calorimetric power. The results were shown in table 11. The graphs were added in annex 10.

TABLE 11: PEAK/NOISE RATIO: (CALORIMETRIC) POWER DEPENDENCY WITHOUT SURFACE STABILIZER (AIR)

	41 kHz	**1140 kHz**
power	peak/noise	peak/noise
4 W	0.2596	0.6678
8 W	0.1863	0.3874
15W	0.1182	0.3478

The results confirms the statement of Frohly *et al.* [16], where the effect of the intensity on the acoustic noise was investigated on a absorptive rubber material. Frohly *et al.* studied the acoustic intensities between 12 $\frac{mW}{cm^2}$ and 300 $\frac{mW}{cm^2}$. In these studies the power was varied between 62.5 $\frac{mW}{cm^2}$ and 234.4 $\frac{mW}{cm^2}$. However, Frohly *et al.* did not performed quantitative studies, they only visually detected the noise present, and concluded that at higher calorimetric power, the cavitation noise increases. At 4 W, luminol studies did not show a bright image of the illuminations. The noise contribution is smaller, so not much transient cavitations were present. At high frequencies, measurements at 4 W did not show any image. The peak/noise contribution of 0.67 results in too little cavitations present to light up the luminol. At 41 kHz, however, bands were visible. The peak/noise ratio of 0.26 is small enough to produce visible light. Also measuring at 1140 kHz at 8 W, resulting in a peak/noise ratio of 0.39, illumination was visible. When the noise ratio increases, the illumination also increases. This confirms that at high noise more transient bubbles are present, lighting up the luminol.

5.5. Impact of the Stirrer

5.5.1. Ultrasound waves

The effect of the stirrer on the ultrasound waves was investigated at low frequencies (41 kHz – 98 kHz). The results were shown in annex 11. The use of a stirrer seems to have a great influence on the ultrasound waves. At 98 kHz, a band pattern was shown when using a stirrer at 400 rpm. When no stirrer was used all surface stabilizers gave no band pattern, but a rather random spectrum. No clear patterns were detected. At 41 kHz, Copper, glass and Air did not show much illuminated spots at 8 W, when the intensity was increased, the illuminated spots became more visible at the level of the stirrer. A possible explanation can be that without a stirrer, coalescence of the bubbles occurs, resulting in a decrease of the illumination. Using PUR however, broad illuminated areas were detected in the reactor (figure 14). However these were not bands. The illuminated spots formed multiple small lines in a vertical direction. A possible explanation here can be that when no stirrer was used, the bubbles were not pushed towards the bands, resulting in a traveling wave pattern. If this is the case, the stirrer has a great influence on the creation of standing waves.

FIGURE 14: LUMINOL TESTS AT 41 KHZ WITHOUT A STIRRER (LEFT: USING PUR; RIGHT: USING GLASS)

When using a stirrer at 0 rpm, at low frequencies, no clear illumination was shown, only small hardly visible random illuminations at the height of the stirrer. At some images, hardly visible random illuminations were shown. At low frequencies, still random waves were present, but the illumination is not strong enough to produce visible images. This can be because of the reflection of the stirrer, which reflects the waves towards the reactor wall.

At high frequencies, the effect of the stirrer was also investigated. At 1140 kHz, using a stirrer at 400 rpm, the area around the stirrer was illuminated. At 570 kHz, the area around the stirrer and the stirring bar was illuminated. When testing at 0 rpm, more or less the same results were shown. At 1140 kHz the area around the stirrer was illuminated, and at 570 kHz the area around the stirring bar was also illuminated. When removing the stirrer, however, a clear illuminated cone shape was detected at all surface stabilizers.

The cone shape can be explained with the Bjerknes force or the acoustic radiation forces on cavitation bubbles. This is also referred to as Bjerknes forces. [85]. "The primary forces cause bubbles to migrate in an acoustic field or to gather in certain areas, such as pressure nodes or antinodes of standing sound waves. The secondary forces make them attract or repel each other, and can also lead to stable bubble structures under certain conditions." [85]

High pressure zones which usually attract small bubbles (with a radius smaller than the resonance radius, around 120 μm at 20 kHz) become repulsive zones. Due to the repulsive primary Bjerknes force, bubbles cannot enter this zone and pass round it. The radial diameter of this repulsive zone decreases when bubbles go further away from the radiating surface, leading to the formation of the cone. At larger distances, the repulsive zone disappears and the symmetry axis becomes an attractive zone. A narrow channel is created, carrying the bubbles from the "top" of the cone to the bottom of the tank. The secondary Bjerknes forces play a major role within the channels by assembling the tiny streamers into larger ones. [86] [87]

The cone shape was only visible when not using a stirrer at high frequencies. The stirrer, whether or not rotating affects the cone structure and the acoustic radiation force. The waves can be pushed away by the stirrer, or reflect on the stirrer blades. At low frequencies, the acoustic radiation force is smaller, this can be a reason for not showing clear images at low frequencies without a stirrer.

Using no stirrer did not show a band structure. Trying to create a standing wave pattern without a stirrer, the distance of the surface stabilizer from the transducer will be varied, to see if any band patterns will be detected. When the distance is varied, reflection will occur at a different part in the wave, possibly creating non-moving nodes due to the propagating waves in different direction. The distance was varied using copper at 41, 98, 570 and 1140 kHz. The results were shown in annex 12. No standing wave pattern was shown, no bands were distinguishable. So changing the distance of the surface stabilizer did not create standing waves, when a stirrer is absent. The conclusion is that a stirrer is necessary to produce a band pattern. The impact of the stirrer using copper is displayed in figure 15 and 16.

With stirrer 400RPM

98kHz

41kHz

No stirrer

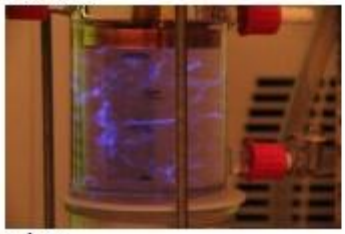

98kHz

41kHz

With stirrer 0RPM

98kHz

41kHz

FIGURE 15: IMPACT OF STIRRER AT LOW FREQUENCIES USING COPPER

With stirrer 400RPM

1140 kHz

570 kHz

No stirrer

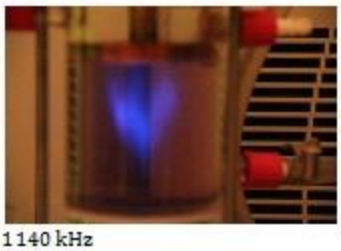

1140 kHz

570 kHz

With stirrer 0RPM

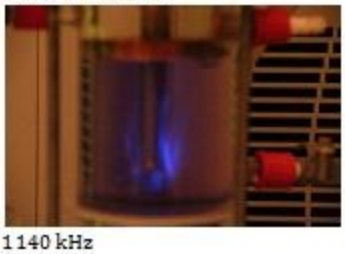

1140 kHz

570 kHz

FIGURE 16: IMPACT OF STIRRER AT HIGH FREQUENCIES USING COPPER

5.5.2. CAVITATIONS

The effect of the stirrer on the cavitations will be also investigated. Using the hydrophone the cavitation noise was measured using no surface stabilizer. Measurements were done at 400rpm, 0 rpm and no stirrer. Annex 13 shows the cavitation noise at 41 kHz. Also at 98, 570 and 1140 kHz, no differences were detected in cavitational noise at all frequencies. This results in the conclusion that the amount of transient cavitations remains the same, independent of the stirring rate. The stirrer causes a band structure, indicating standing waves. This could mean that the cavitations are also independent of the type of wave.

Hereafter, the effect of the height of the hydrophone was measured. In previous measurements, the hydrophone was held at a constant height of 2,5 cm above the reaction bottom. Results, showed in annex 14 showed variation at different heights without using a stirrer. At some levels, slightly more noise was detected, however, no unambiguous trend was shown. The peak height of the first harmonic peak was measured. Here, the height slightly decreases when the distance from the transducer increases. Close to the wall of the reactor, the peak was the smallest.

Results show the pressure, caused by the cavitations doesn't vary, the peaks and surface beneath the peaks were the same whether or not a stirrer was used. The wave spectrum, however, does vary. Using a stirrer, bands were shown. The absence of a stirrer resulted in random illuminations. This means the cavitations were present, but not located at the same place than when using a stirrer. Due to the overhead stirrer, cavitation bubbles are pushed towards the antinodes, where luminol shows illuminated bands, proving the bubbles were concentrated at those bands, but the pressure produced by these cavitations remains the same, giving the same noise spectrums when measuring with a hydrophone.

Bussemaker *et al.* stated that the sonochemical activity increases when introducing stirring up to 900 rpm at all frequencies. In this thesis, the effect of the stirrer was compared between 0 rpm and 400 rpm. At 400 rpm, the sonochemical activity strongly increases, especially at low frequencies. [29] Bussemaker *et al.* assumed that at 40 kHz, the increase in sonochemical activity was a result of the reduction of coalescence of bubbles with overhead stirring, increasing the active bubble population. Bubbles which merge, will become too big for sonochemical activity and will become degas bubbles. Also, the stirrer can disturb the reflection in a standing wave field.

5.6. PLATE VS. HORN TRANSDUCER: WAVE FORM

The difference in wave form between a plate transducer and a horn transducer was also shortly studied. Up to this point only a plate transducer was used. A horn transducer is a metal bar with at the tip a piezoelectric material, as shown in figure 17. [88]

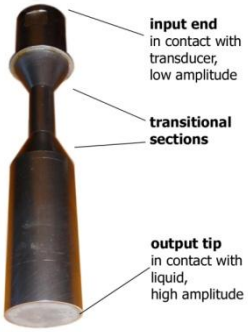

FIGURE 17: IMAGE OF A HORN TRANSDUCER [89]

A Hielscher UP50H Horn transducer (200-240 V) of 41 kHz was used. The horn was set at continuous mode, the amplitude was set at 20% and 100%. The power is thus 12.5 W and 50 W respectively. Air was used as surface stabilizer. The distance from the horn to the bottom of the reactor was varied between 1 cm and 7 cm. The results were shown in annex 15. At 20% amplitude, thus 12.5 W, only the area under the piezoelectric material is strongly illuminated. Also the whole area under the horn tip showed a less bright illumination. At 100% amplitude, or 50 W, the whole liquid showed illuminated bands, when the distance between the piezoelectric material and the bottom of the reactor is 3 cm or smaller.

However, these bands were not at one single height, but rather random, as shown in figure 18. This can be a result of the stirring caused by the ultrasonic horn transducer. When the horn is put at a higher distance of the bottom, the area under the horn was illuminated, comparable to the results at 12.5 W. This can be a result of the stirring effect which decreases when the horn is put higher in the reactor.

Hereafter the effect of the stirrer was investigated using a horn. The overhead stirrer at 400 rpm was used at the same level at the tip of the ultrasonic horn. The horn was set at 20% and 100%. At 12.5 W the area around the piezoelectric material illuminated, and the stirrer slightly dispersed the illuminated spot. At 50 W, the bands were also affected by the stirrer and gave a different but still random band pattern was shown. The use of overhead stirring did not create a stable band pattern, thus no clear standing wave pattern was visible.

The results were compared with a plate transducer. The horn transducer at 50 W provides stirring starting from the piezoelectric material, giving random illuminations, not constantly at the same place. Stirring with an overhead stirrer using a plate transducer resulted in multiple horizontal bands. The plate transducer at 8 W showed stable bands, who remained at the same position. However increasing the calorimetric power, resulted in also unstable and turbulent bands. The plate transducer however, gave multiple bands with a distance between the band half the wavelength. The horn transducer did not show multiple distinguishable bands. A plate transducer can produce standing waves using a stirrer, who pushes the cavitations into the antinodes. A horn transducer did not clearly showed a band structure, which could indicate a rather traveling wave structure.

FIGURE 18: US WAVES USING A HORN TRANSDUCER AT 50 W (LEFT) AND 12.5 W (RIGHT)

6. CONCLUSIONS

A smaller MZW was obtained when transient cavitations are present. Transient cavitation bubbles are more present at low frequencies. Also a larger ratio of standing waves, obtained when using reflection material are beneficial for the reduction in MZW. Transient cavitations and standing waves are beneficial for a small MZW and CSD.

The metastable zone width is clearly smaller when working at low frequencies (41 kHz – 98 kHz). At high frequencies (1140 kHz – 570 kHz), no significant reduction in MZW was shown. Using Glass (reflection coefficient = 63%) and copper (reflection coefficient = 88%) as surface stabilizer, the reduction in MZW was significantly larger, than when using PUR (reflection coefficient = 1,5%). Standing waves are enhancing the reduction in MZW. A maximum reduction in MZW of 3.4°C was found using copper at 41 kHz. No significant difference in MZW was shown between 41 kHz and 98 kHz, or between copper and glass proving that a large standard deviation is present on the MZW at the crystallization process of paracetamol.

The results were compared with air, measured by Jordens *et al.*, who used the same parameters, only using a volume of 150 ml instead of 180 ml. [33] Air, being an open system, showed a much larger reduction in MZW (17°C at 41 kHz). The MZW using ultrasound is the same as when using copper. The larger reduction is due to a very large MZW when using no ultrasound.

Studies of the crystal size distribution showed that at low frequencies (41 kHz – 98 kHz) smaller crystals were formed. At high frequencies (1140 kHz), the crystals were larger, but still smaller than when using no ultrasound. These results were detected using copper as surface stabilizers, The change in CSD using glass was much smaller, PUR did not show significant differences in CSD. The CSD was measured using the D50; D3,2; D4,3 and span values. The tests with the laser diffractometer were only performed once, resulting in a larger error on the results. The crystal shape did not vary at different surface stabilizers and frequencies.

Studies of the ultrasound waves using luminol showed ±3 bands at 41 kHz, ±7 bands at 98 kHz and uncountable bands at 570 kHz and 1140 kHz. The distance between the bands can be stated to be half the wavelength. Standing waves are always present using ultrasound. However, depending on the reflectivity of the surface stabilizer, the ration standing/traveling waves can be altered. PUR gave broader bands, copper and air gave the smallest bands. A smaller reflection coefficient results in a broader band and a smaller ratio of standing waves. The cavitation bubbles are pushed towards the antinodes, where illuminated bands are formed. Larger reflectivity of the surface stabilizer gave a smaller MZW, confirming that standing waves are beneficial in reducing the MZW.

The cavitation bubbles were investigated and showed more noise at low frequencies, resulting in a larger amount of transient cavitations. Air showed a peak noise ratio of 0.19 at 41 kHz and 0.39 at 1140 kHz. PUR showed a ratio of 0.18 at 41 kHz and 0.80 at 1140 kHz. At low frequencies the difference between reflection-absorption material and open-closed system is not shown. At high frequencies, no large difference is detected between reflectors and absorbers, but an open system produces a significant more amount of transient cavitations than a closed system. High frequencies did not show many illuminations at 8 W. Only the part around the stirrer was illuminated. Also, at high frequencies, not much transient cavitations were present. The intensity needed to be increased to produce visibly illuminated bands. At higher intensities, the bands become more turbulent but also more visible. Also the noise contribution increases, resulting in a larger amount of transient cavitations. Expected is that at a high calorimetric power, the MZW will decrease, because of the presence of more transient cavitation bubbles. Studying the MZW, when more noise was detected the MZW was smaller. Lower frequencies are beneficial for the crystallization process. These results confirmed the results found in literature.

The effect of the stirrer was investigated. Using an overhead stirrer at 400 rpm, stable bands were shown using luminol. Without a stirrer, random illuminated spectrums were visible. At high frequencies a cone shape was detected, due to acoustic radiation force. At low frequency, acoustic streaming is less present, the image was not strongly illuminated. Trying to create a standing wave pattern, and stable bands, the height of the surface stabilizer was varied. This did not result in a band pattern. Using a stirrer, the standing waves are present. Using no stirrer the waves were rather random. When measuring the cavitations, no difference was shown between using a stirrer or using no stirrer. This means that the pressure produced by the cavitations will remain the same, but the stirrer pushes the cavitations towards the antinodes, resulting in a band pattern.

The difference between a horn and a plate transducer was also investigated. Stirring with an overhead stirrer using a plate transducer resulted in multiple horizontal bands a distance between the band half the wavelength. Increasing the calorimetric power, resulted in also unstable and turbulent bands. The horn transducer did not show multiple distinguishable bands. A plate transducer can produce standing waves using a stirrer, who pushes the cavitations into the antinodes. A horn transducer did not clearly showed a standing wave pattern, not even when a stirrer was used.

7. BIBLIOGRAPHY

[1] J. e. a. Lee, "Spatial distribution Enhancement of Sonoliminescence Activity by Altering Sonication and Solution Conditions," *Journal of Phys. Chem,* pp. 15333-15341, 2008.

[2] D. Lecis, T. Sneyers and T. H. Leonaers, Writers, *Ultrasound-assisted crystallization of paracetamol.* [Performance]. Departement IWT, KHLim.

[3] H. Harzali and O. Louisnard, "Experimental study of sono-crystallisation of ZnSO4 . 7H2O and interpretation by the segregation theory," *Ultrasound Sonochemistry,* no. 18, pp. 1097-1106, 2011.

[4] V. J. Sanchez Morcillo, "Special issue on ultrasonic research," *open journal of acoustics,* 2013.

[5] Innovative Ultrasonics, "High Power Ultrasound Technology," Innovative Ultrasonics, 2008. [Online]. Available: http://www.innovativeultrasonics.com/applications/.

[6] T. e. al., "Ultrasonic fluid quantity measurements," *dynamic vehicular applications,* pp. 11-35, 2013.

[7] NDT resource center, "Modes of Sound Wave Propagation," NDT, 2014. [Online]. Available: http://www.ndt-ed.org/EducationResources/CommunityCollege/Ultrasonics/Physics/modepropagation.htm.

[8] "Compressions and Rarefactions," The Physics Classroom, 2014. [Online].

[9] J. Blitz and G. Simpson, Ultrasonic Methods of Non-destructive Testing, London UK: Chapman & Hall, 1996.

[10] I. Scott and C. Scala, "A review of non-destructive testing of composite materials," *NDT International,* no. 15, p. 75–86, 1982.

[11] A. Carovac, S. Fahrudin and D. Junuzovic, "Application of Ultrasound in Medicine," *Acta Informatica Medica,* no. 3, p. 168–171, 2011.

[12] A. P. e. a. Sarvazyan, "Shear wave elasticity imaging: a new ultrasonic technology of medical diagnostics," *Ultrasound in Medicine & Biology,* p. 1419–1435, 1998.

[13] M P Interconsulting, "Ultrasonic Metallurgy," M P Interconsulting, 2011. [Online]. Available: http://www.ultrasonicmetallurgy.com/.

[14] Hielscher – Ultrasound Technology, "technolo," Hielscher, 1999. [Online]. Available: http://www.hielscher.com/technolo.htm.

[15] B. Negi, "Crystallization in the Pharmaceutical Industry," 2008. [Online]. Available: http://www.pharmatutor.org/articles/crystallization-in-pharmaceutical-industry.

[16] J. Frohly, S. Labouret, C. Bruneel, I. Looten-Baquet and R. Torguet, "Ultrasonic cavitation monitoring by acoustic noise power measurement," pp. 2012-2020, 2000.

[17] E. Neppiras, "Acoustic cavitation," *Methods of experimental physics,* no. 61, pp. 159-251, 1980.

[18] R. Apfel, "Acoustic cavitation predicion," *Journal of acoustic soc.,* pp. 1624-1633, 1981.

[19] H. Santos and C. Lodeiro, "The Power of Ultrasound," [Online]. Available: http://www.wiley-vch.de/books/sample/3527319344_c01.pdf.

[20] C. Brennen, "Dynamics of Oscillating Bubbles," Oxford University Press, 1995. [Online]. Available: http://authors.library.caltech.edu/25017/4/chap4.htm.

[21] T. G. Leighton, S. D. Meers and P. R. White, "Propagation through nonlinear time-dependent bubble clouds and the estimation of bubble populations from measured acoustic characteristics," 2003.

[22] W. P. Mason, "Acoustic Streaming," in *Physical Acoustics V2B: Principles and Methods*, Elsevier, 2012, pp. 265-330.

[23] J. Lee, M. Ashokkumar, K. Yasui and T. Tuziutu, "Development and optimization of acoustic bubble structures at high frequencies," *Ultrasonics Sonochemistry,* no. 18, pp. 91-98, 2011.

[24] S. Brems, M. Hauptmann and E. Camerotto, "Physical forces exerted by microbubbles on a surface in a traveling wave field," *Ultrasonics,* no. 54, pp. 706-709, 2014.

[25] T. G. Leighton, The Acoustic Bubble, London: Elsevier, 1994.

[26] D. McClements, "Advances in theapplication of ultrasoundin food analysis andprocessing," *Trends in Food ,Science& Technology ,* pp. 293-299, 1995.

[27] J. Brewer, "Standing Waves," 2002. [Online]. Available: http://www.jick.net/~jess/hr/skept/Waves/node8.html.

[28] M. Ashokkumar, J. Lee, Y. Iida and K. Yasui, "Detection and control of stable and transient acoustic cavitation bubbles," *Phys. Chem. ,* pp. 10118-10121, 2009.

[29] M. Bussemaker and D. Zhang, "A phenomenological investigation into the opposing effects of fluid flow on sonochemical activity at different frequency and power settings; 1 overhead stirring," *Ultrasonice Sonochemistry,* no. 21, pp. 436-445, 2014.

[30] T. L. Szabo, "Cavitation and Bubble destruction," in *Diagnostic Ultrasound Imaging: Inside Out*, Oxford, Elsevier, 2004, p. 612.

[31] A. Goldstein and B. Hung, "Ultrasound pulse-echo reflection from test object cylindrical reflectors.," pp. 102-113, 1982.

[32] P. Garu, "Acoustic & Mechanical Properties of Neoprene Rubber for Encapsulation of Underwater Transducers," *International Journal of Scientific Engineering and Technology,* pp. 231-237, 2012.

[33] J. Jordens, B. Gielen, L. Braeken and T. Van Gerven, *Determination of the effect of the ultrasonic frequency on the cooling crystallization of paracetamol,* Leuven.

[34] N. Zaitseva, "Crystal Growth / Aqueous Solutions," 2002. [Online]. Available: http://chemconnections.org/crystals/KDP-solution-chem.html.

[35] M. Giulietti and A. Bernardo, "Crystallization by Antisolvent Addition and Cooling," pp. 380-396.

[36] A. P. Sinha, "Reactive Crystallization," in *Mass Transfer: Principles and Operations*, New Delhi, 2012, pp. 529-535.

[37] Kulprathipanja, "Reactive Crystallization," in *Reactive Separation Processes*, London, Taylor & Francis, 2002, pp. 209-220.

[38] K. e. a. Choong, "Optimization of semi-batch reactive crystallization process," *Chemical Engineering science,* no. 59, pp. 1529-1540, 2003.

[39] GEA Messo PT, "Melt Crystallization: The efficient Purification Alternative," GEA Messo PT, [Online]. Available: http://www.niroinc.com/pdfs/evaporation_crystallization/melt_crystallization.pdf.

[40] J. Garside, A. Mersmann and J. Nyvlt, Measurement of Crystal Growth and Nucleation Rates, UK: IChemE, 2002.

[41] M. Luque de Castro, "Ultrasound-assisted crystallization (sonocrystallization)," *Ultrasonics Sonochemistry,* p. 717–724, September 2007.

[42] C. Virone, H. Kramer, G. van Rosmalen and A. Stroop, "Primary nucleation induced by ultrasonic cavitation," *Journal of Crystal Growth,* no. 15, p. 9–15, 2006.

[43] I. Quesada-Peñate, C. Julcour-Lebigue, U.-J. Jáuregui-Haza Ulises-Javier, A.-M. Wilhelm and H. Delmas, "Sonolysis of levodopa and paracetamol in aqueous solutions," *Ultrasonics Sonochemistry,* 2009.

[44] H. Li, H. Wang, T. Bao, Z. Guo and M. Zhang, "Rapid sonocrystallization in the salting-out process," *Journal of Crystal Growth,* pp. 192-198, 2003.

[45] K. Wohlgemuth, F. Ruether and G. Schembecker, "Sonocrystallization and crystallization with gassing of adipic acid,," *Chemical Engineering Science,* pp. 1016-1027, 2010.

[46] A. Kordylla, S. Koch, F. Tumakaka and G. Schembecker, "Towards an optimized crystallization with ultrasound: Effect of solvent properties and ultrasonic process parameters,," *Journal of Crystal Growth,* pp. 4177-4184, 2008.

[47] Z. Meifang, Y. Nor Saadah Mohd and A. Muthupandian, "Correlation between sonochemistry and sonoluminescence at various frequencies," *RSC advances,* no. 3, pp. 9319-9324, 8 April 2013.

[48] Z. Meifang, Y. Nor Saadah Mohd and A. Muthupandian, "Correlation between sonochemistry and sonoluminescence at various frequencies," *RSC advances,* no. 3, pp. 9319-9324, 2013.

[49] S. L. Hem, "The effect of ultrasonic vibrations on crystallization," *Ultrasonics,* pp. 202-207.

[50] D. Hunt and K. Jackson, "Nucleation of Solid in an Undercooled Liquid by Cavitation," *Journal of Applied Physics,* pp. 254 - 257, 2009.

[51] K. Ohsaka and E. Trinh, *Dynamic Nucleation Of Ice Induced by a Single Stable Cavitation Bubble,* California.

[52] C. Duan, R. Karnik, L. Ming-Chang and A. Majumdara, "Evaporation-induced cavitation in nanofluidic channels," *Proc Natl Acad Sci U S A,* pp. 3688-3693, 2012.

[53] B. Storey and A. Szeri, "Water vapour, sonoluminescence and sonochemistry," 2000.

[54] B. Brown and I. E. Goodman, "High-intensity ultrasonics," in *High-intensity ultrasonics: industrial applications*, London, 1965.

[55] M. Mazhul, Writer, *Cavitation Phenomena and the Formation of Crystal Nuclei..* [Performance]. 1954.

[56] T. Bergfors, "Seeds to crystals," *Journal of strucural biology ,* pp. 66-76, 2003.

[57] M. Margulis and I. M. Margulis, "Calorimetric method for measurement of acoustic power absorbed in a volume of a liquid," *Ultrasonics Sonochemistry,* p. 343–345, 2003.

[58] T. Kikuchi and T. Uchida, "Calorimetric method for measuring high ultrasonic," *Journal of Physics,* pp. 1-5, 2011.

[59] "NDT Resource Center," [Online]. Available: http://www.ndt-ed.org/EducationResources/CommunityCollege/Ultrasonics/Physics/reflectiontransmission.htm.

[60] Onda Corperation, "Acoustic properties of solids," Onda, 11 April 2003. [Online]. Available: http://www.ondacorp.com/images/Solids.pdf.

[61] A. Goldstein and B. Hung, "Ultrasound pulse-echo reflection from test object cylindrical reflectors.," pp. 102-113, 1982.

[62] K. D. Garu and T. K. Chaki, "acoustic and mechanical properties of neoprene rubber for encapsulation of underwater transducers," *international journal of scientific engineering and technology,* no. 1, pp. 231-237, 2012.

[63] E. Ginzel and R. Ginzel, "Ultrasonic properties of a new low attenuation dry couplant elastomer," 15 December 2013. [Online]. Available: http://www.ndt.net/article/ginzel/ginzel.htm.

[64] Onda corporation, "Tables of Acoustic Properties of Materials (Solids and Rubbers)," [Online]. Available: http://www.ondacorp.com/.

[65] P. Barret, B. Glennon and B. O'Sullivan, *Solubility Curve and Metastable zone Width,* Dublin, 2002.

[66] K. Byung-Man, L. Ji Eun, A. Jang-Hyuk and J. Tea-Hong, "Laser Diffraction Particle Sizing By Wet Dispersion Method For Spray-dried infant formula," *Journal of Food Engineering,* pp. 324-330, 2009.

[67] Malvern Instruments, "Mastersizer 3000," Malvern Instruments, 2014. [Online]. Available: http://www.malvern.com/en/products/product-range/mastersizer-range/mastersizer-3000/default.aspx.

[68] Malvern Instruments, "Overview of Important Particle Characterisation Techniques," Malvern Instruments, 27 August 2013. [Online]. Available: http://www.azom.com/article.aspx?ArticleID=9937.

[69] Horiba, "Understanding and Interpreting Particle Size Distribution Calculations," Horiba, 2014. [Online]. Available: http://www.horiba.com/scientific/products/particle-characterization/education/general-information/data-interpretation/understanding-particle-size-distribution-calculations/.

[70] A. e. a. Lawerenz, "Preparation Methods and Survay of Optical Measurements of Slurry Abrasives," CiS Forschungsinstitut für Mikrosensorik und Photovoltaik, Germany.

[71] Z. Stojanovic and S. Marcovic, "Determination of Particle size distribution by Laser Diffractometer," pp. 11-20, 2000.

[72] H. Todokoro and M. Ezumi, "For producing a two-dimensional scan image of a sample". USA Patent US5872358 A, 16 february 1999.

[73] A. e. a. Duarte, "Luminol-Doped Nanostructured Composite Materials for Chemiluminescent Sensing of Hydrogen Peroxide," pp. 2762-2772, 2010.

[74] NCSU – Dept. of Chemistry, *Chemiluminescence with Luminol.*

[75] D. Larsen, "Luminol," University of California, [Online]. Available: http://chemwiki.ucdavis.edu/Development_Details/Approaches/VVV_Demos/Luminol.

[76] T. Freeman and W. Seitz, "Chemiluminescence fiber optic probe for hydrogen peroxide based on the luminol reaction," *Anal. Chem.,* p. 1242–1246, 1978.

[77] NDT Recource Center, "Characteristics of Piezoelectric Transducers," NDT, 2014. [Online]. Available: http://www.ndt-ed.org/EducationResources/CommunityCollege/Ultrasonics/EquipmentTrans/characteristicspt.htm.

[78] ONDA, "Theory of Operation of Hydrophones," ONDA, 2014. [Online]. Available: http://www.ondacorp.com/tecref_tutorialhydrophone_theory.shtml.

[79] Calcutta Institute of Technology , "Advantages of Blackman Window over Hamming Window Method for designing FIR Filter," *International Journal of Computer Science & Engineering Technology (IJCSET),* no. 4, pp. 1181-1189, 2013 .

[80] T. Kikuchi and T. Uchida, "Calorimetric method for measuring high ultrasonic power using water as a heating material," *Journal of Physics: Conference Series,* no. 279, pp. 1-5, 2010.

[81] "Thermal Conductivity of some common Materials and Gases," Engineering ToolBox, 2014. [Online]. Available: http://www.engineeringtoolbox.com/thermal-conductivity-d_429.html.

[82] C. Bonné, T. Claes, S. Daniels and H. Jehoel, *Effect of the wave type on sonochemical crystallisation of paracetamol,* Diepenbeek, 2014.

[83] M. e. a. Jiang, "Towards achieving a flattop crystal size distribution by continuous seeding and controlled growth," *Chemical Engineering Science,* pp. 2-9, 2012.

[84] K. Sangwal, Additives and Crystallization Processes: From Fundamentals to Applications, England: Wiley, 2007.

[85] A. Doinikov, "Bjerknes forces and translational bubble dynamics," *Bubble and Particle Dynamics in Acoustic Fields,* pp. 1-49, 2005.

[86] A. Moussatov, C. Granger and B. Dubus, "Cone-like bubble formation in ultrasonic cavitation field," *Ultrasonics Sonochemistry,* pp. 191-195, 2003.

[87] O. Louisnard, "A simple model of ultrasound propagation in a cavitating liquid. Part II: Primary Bjerknes force and bubble structures," *Ultrasonics Sonochemistry,* pp. 66-76, 2012.

[88] T. Li, J. Ma and A. Low, "Horn-Type Piezoelectric Ultrasonic Transducer: Modelling and Applications," November 2011. [Online]. Available: http://cdn.intechopen.com/pdfs-wm/24193.pdf.

[89] "Barbell Horn Ultrasonic Technology," ISM, 2014. [Online]. Available: http://sonomechanics.com/technology/barbell_horn_ultrasonic_technology/.

[90] I. Quesada-Peñate, C. Julcour-Lebigue and U.-J. Jáuregui-Haza, "Sonolysis of levodopa and paracetamol in aqueous solutions," *Ultrasonics Sonochemistry,* no. 16, p. 610–616, June 2009.

ANNEX

Annex 1. CRYSTALLIZATION RESULTS

	PUR			glass			copper			air		
frequency (kHz)	MZW (°C)	reduction (°C)	STDEV	MZW (°C)	reduction (°C)	STDEV	MZW (°C)	reduction (°C)	STDEV	MZW (°C)	reduction	STDEV
0	8,9		1,4	9,2		1,5	8,8		2,0	18,7		1,5
41	7,6	1,2	1,2	6,2	3,0	0,5	5,4	3,4	0,9	8,4	10,3	0,6
98	8,1	0,8	1,0	5,9	3,4	0,7	5,9	2,9	1,4	9,3	9,4	0,1
1140	9,0	-0,1	1,2	8,4	0,9	1,9	8,2	0,6	1,7	10,1	8,6	2,9

Annex 2. CRYSTAL SIZE DISTRIBUTIONS

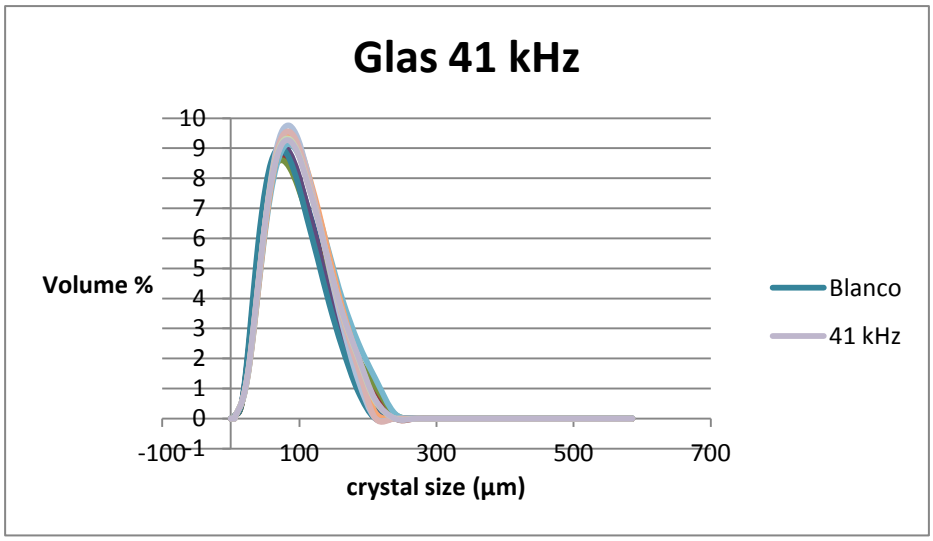

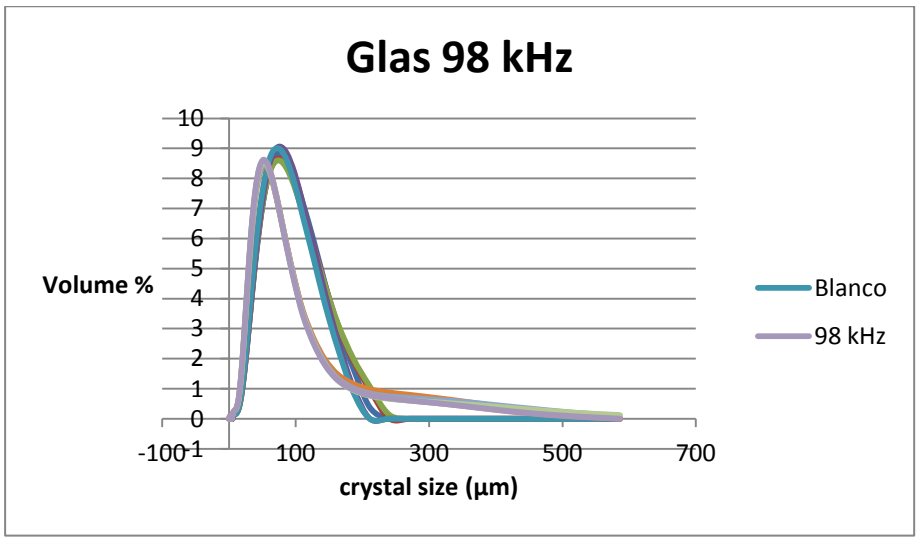

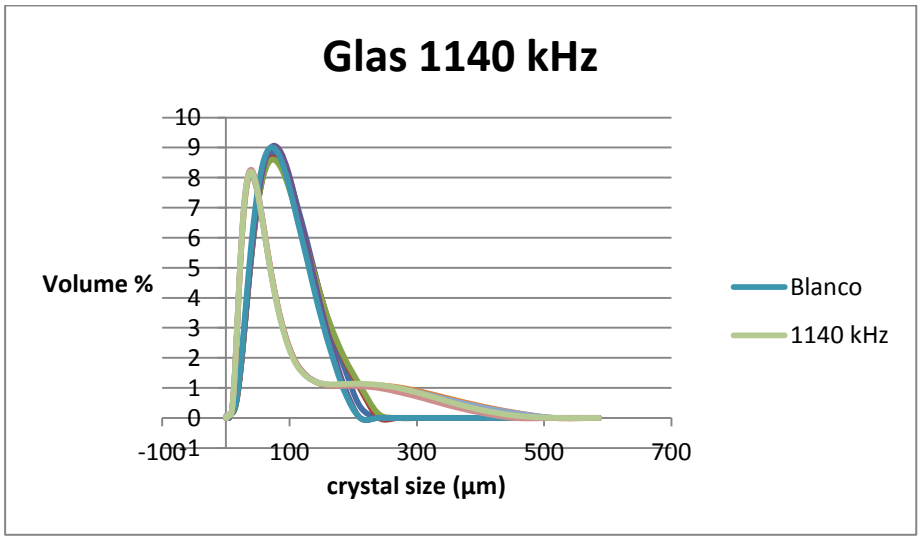

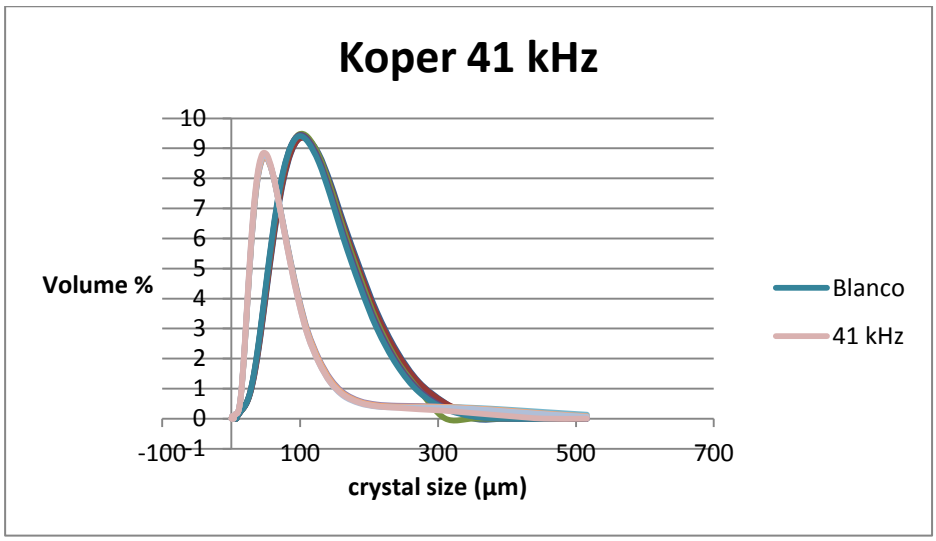
Koper 41 kHz
Volume %
10
9
8
7
6
5
4
3
2
1
0
-1
-100
100
300
500
700
crystal size (µm)
Blanco
41 kHz

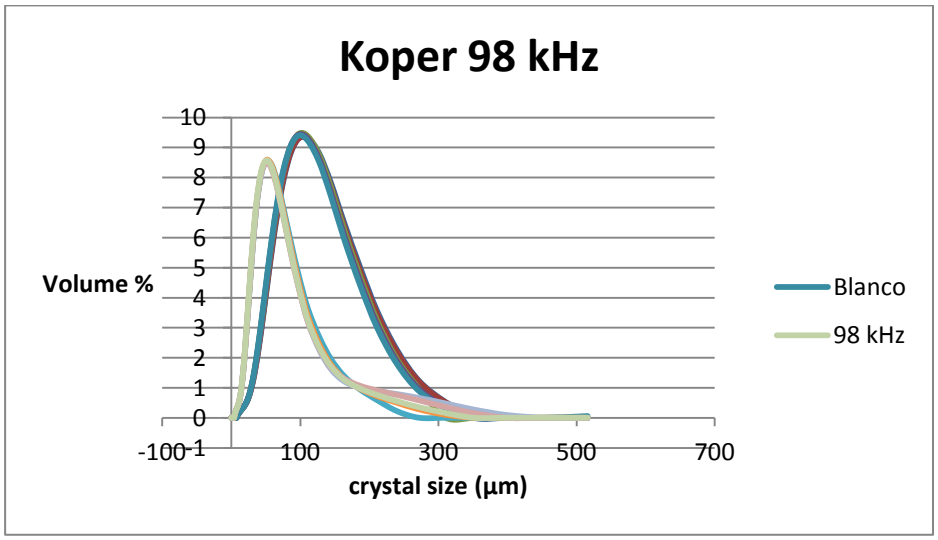
Koper 98 kHz
Volume %
10
9
8
7
6
5
4
3
2
1
0
-1
-100
100
300
500
700
crystal size (µm)
Blanco
98 kHz

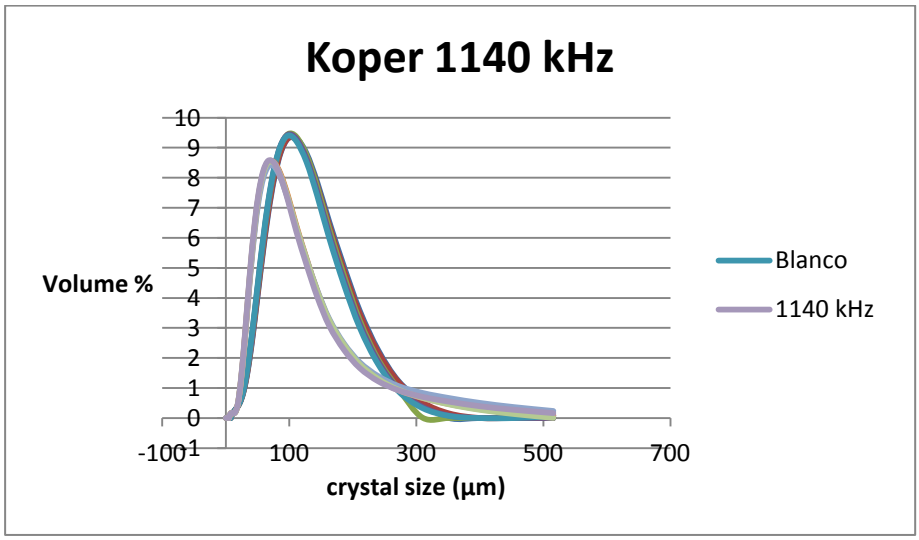
Koper 1140 kHz
Volume %
10
9
8
7
6
5
4
3
2
1
0
-1
-100
100
300
500
700
crystal size (µm)
Blanco
1140 kHz

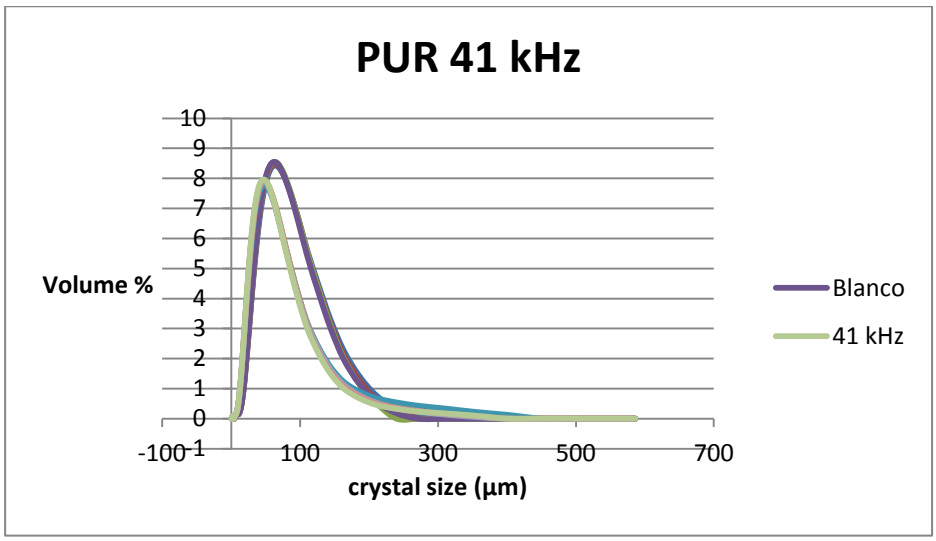
PUR 41 kHz
Volume %
10
9
8
7
6
5
4
3
2
1
0
-1
-100
100
300
500
700
crystal size (µm)
Blanco
41 kHz

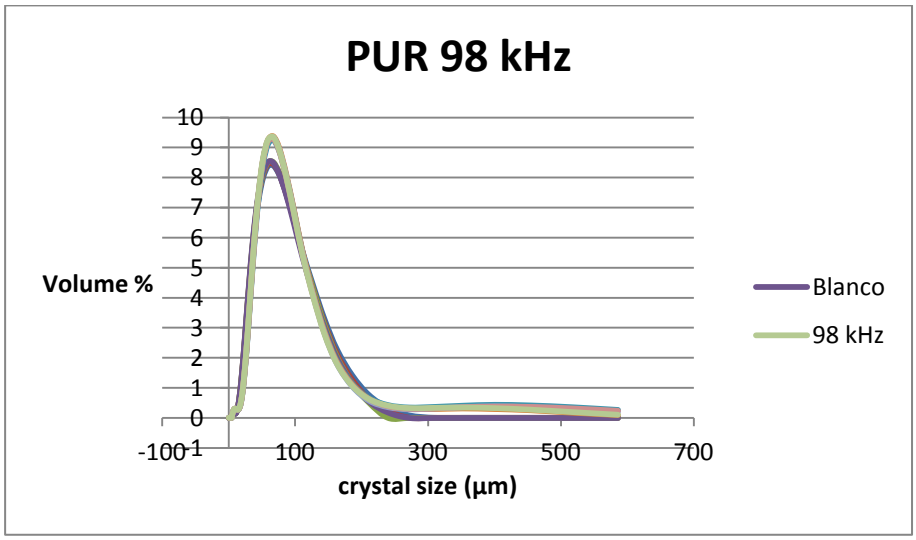
PUR 98 kHz
Volume %
10
9
8
7
6
5
4
3
2
1
0
-1
-100
100
300
500
700
crystal size (µm)
Blanco
98 kHz

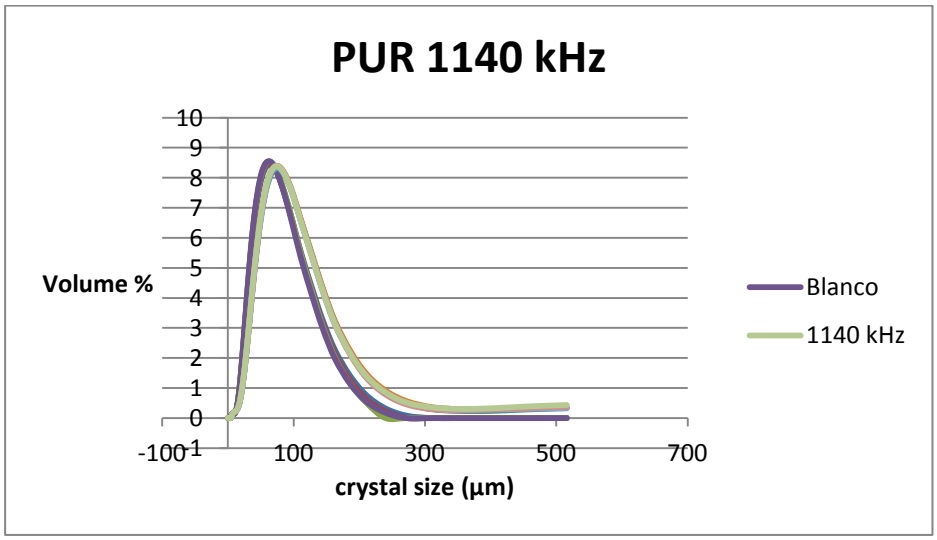
PUR 1140 kHz
Volume %
10
9
8
7
6
5
4
3
2
1
0
-1
-100
100
300
500
700
crystal size (µm)
Blanco
1140 kHz

Annex 3. CSD: D50; D4,3; D3,2 AND SPAN

D50 Value at different frequencies (copper, glass, PUR)

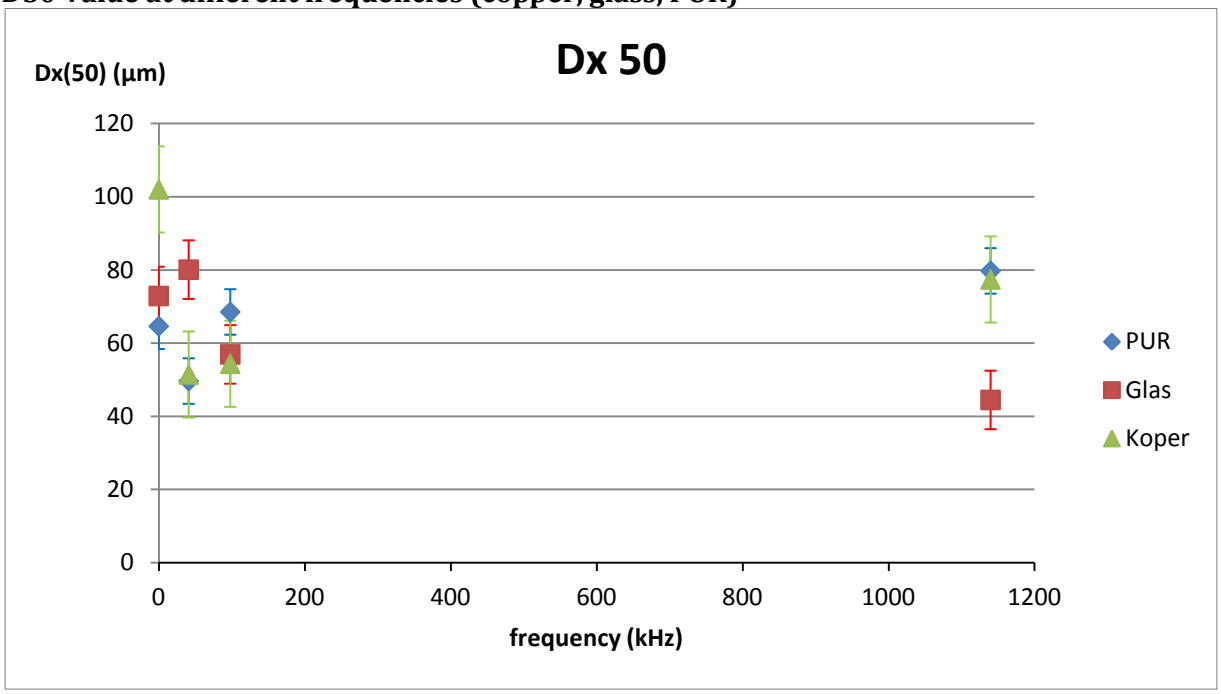

D4,3 Value at different frequencies (copper, glass, PUR)

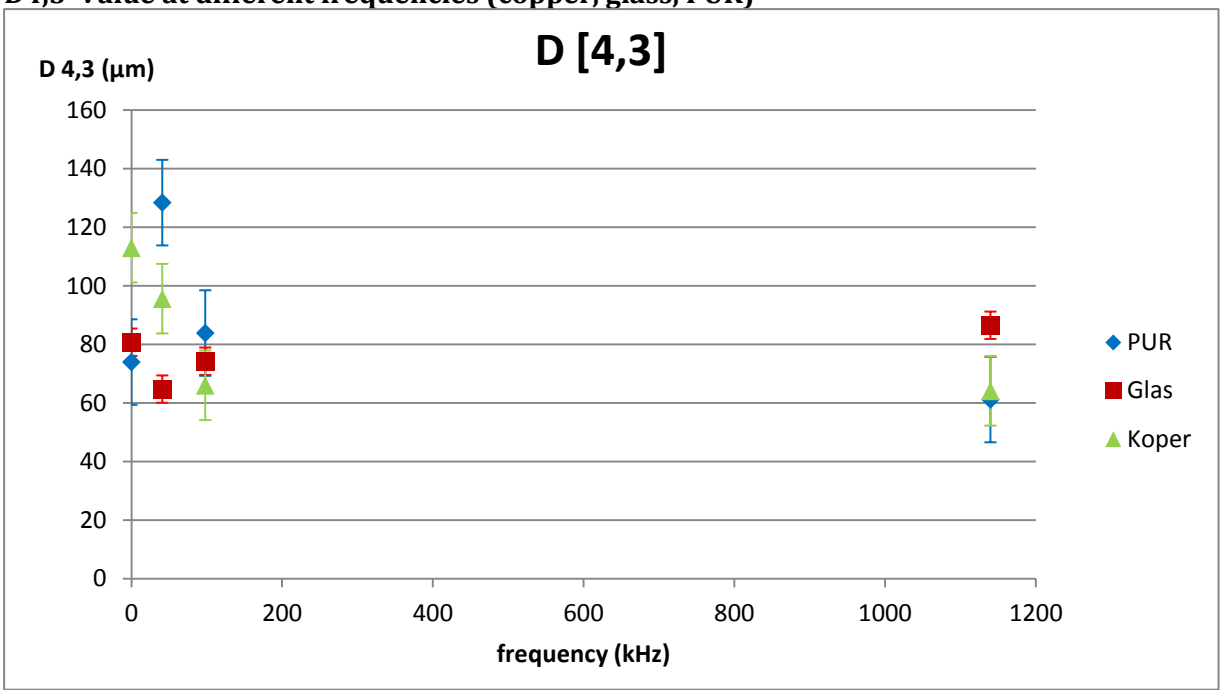

D3,2 Value at different frequencies (copper, glass, PUR)

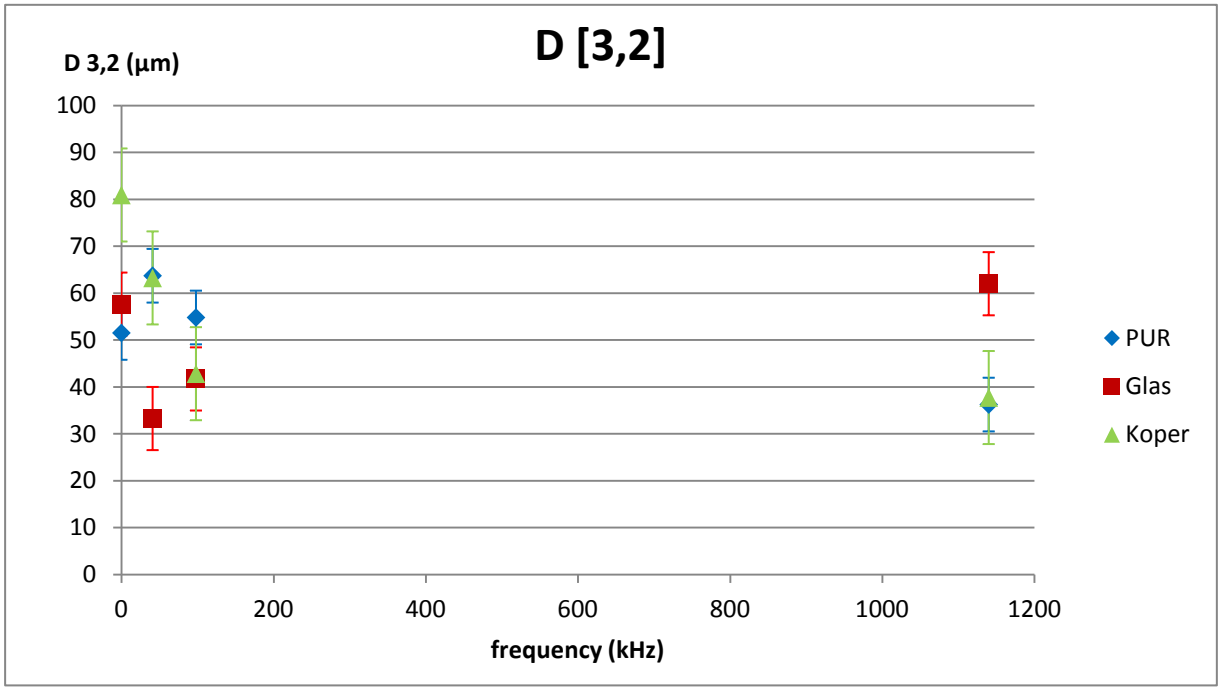

Span Value at different frequencies (copper, glass, PUR)

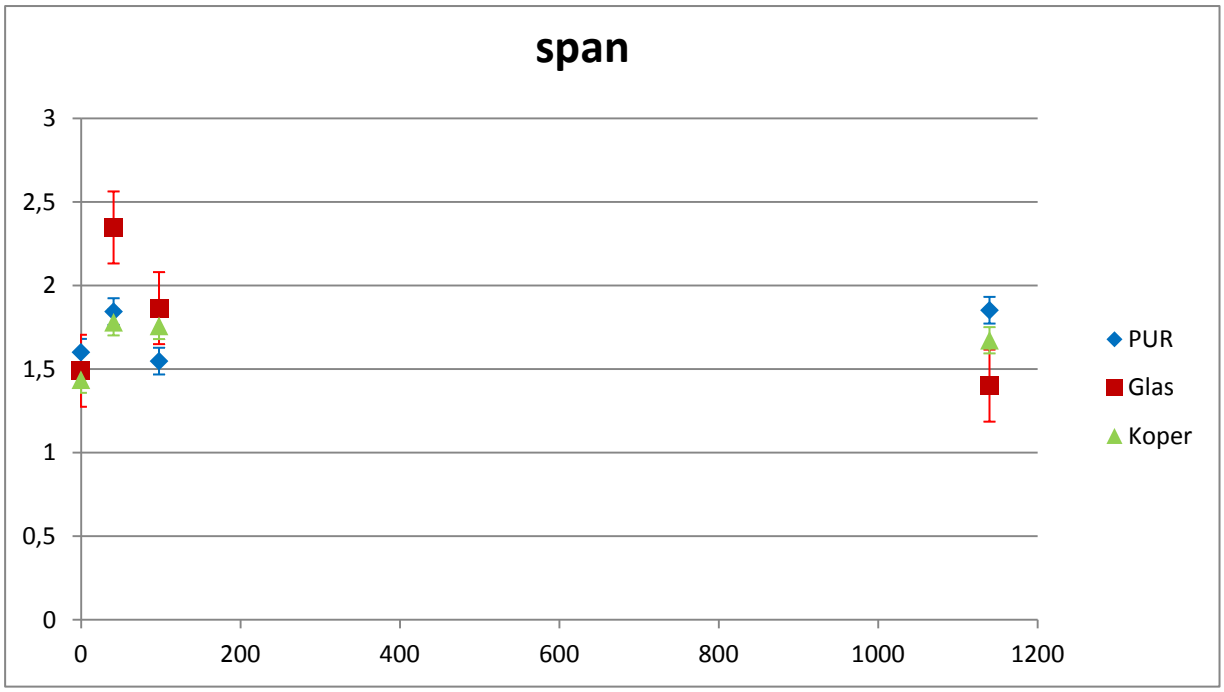

Annex 4. CRYSTAL SHAPE

4.1. COPPER

Blanco

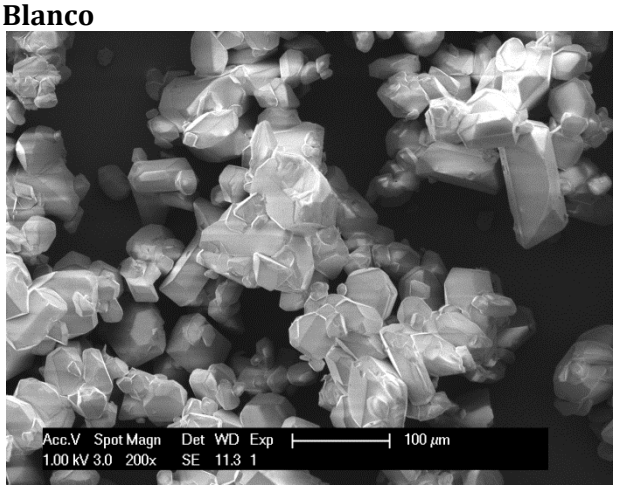

1140 kHz

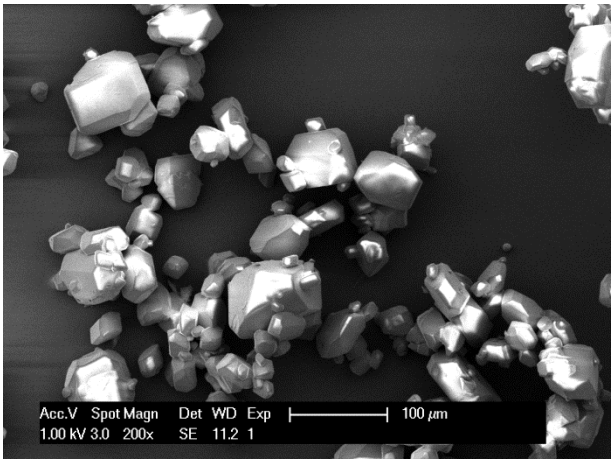

41 kHz

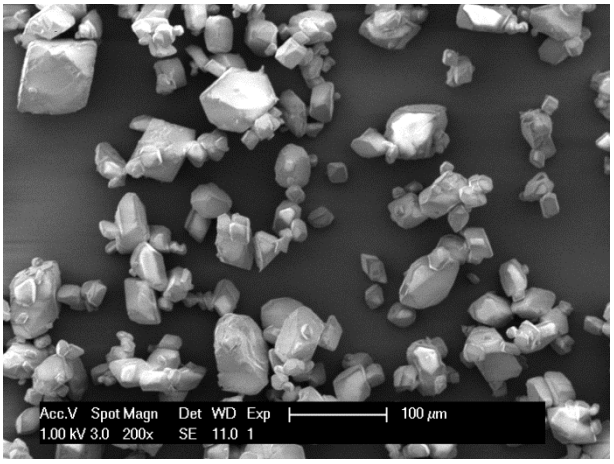

4.2. GLASS

Blanco

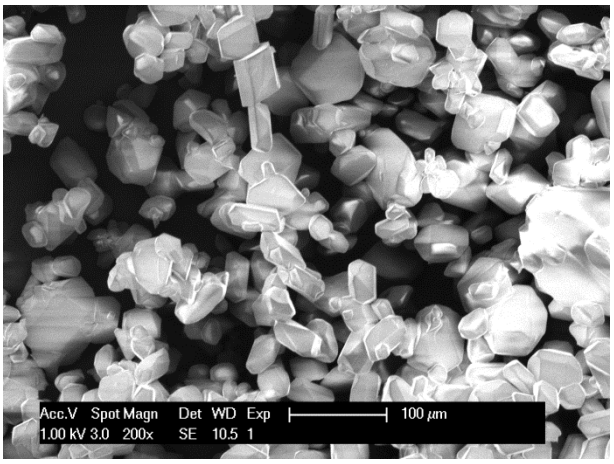

1140 kHz

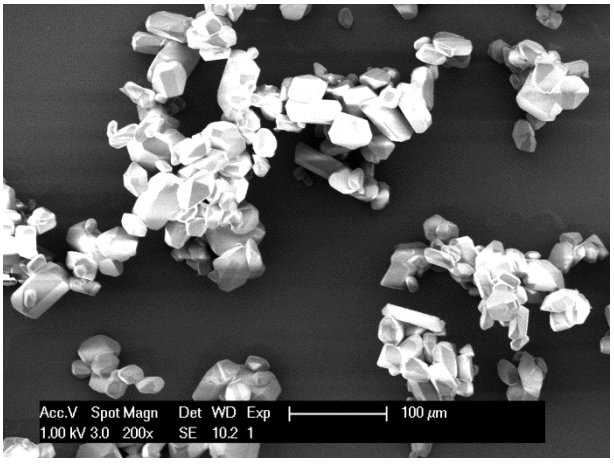

41 kHz

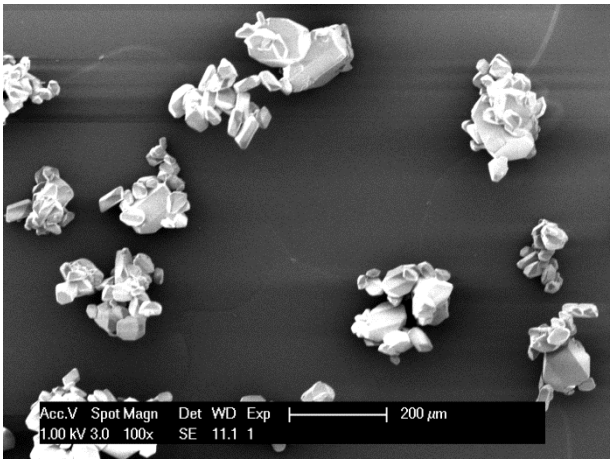

4.3. PUR

Blanco

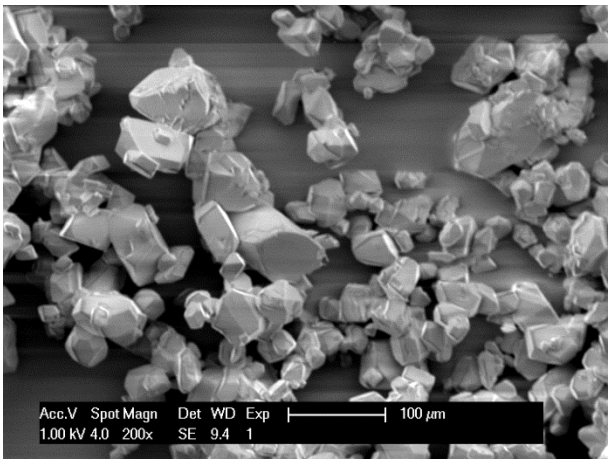

1140 kHz

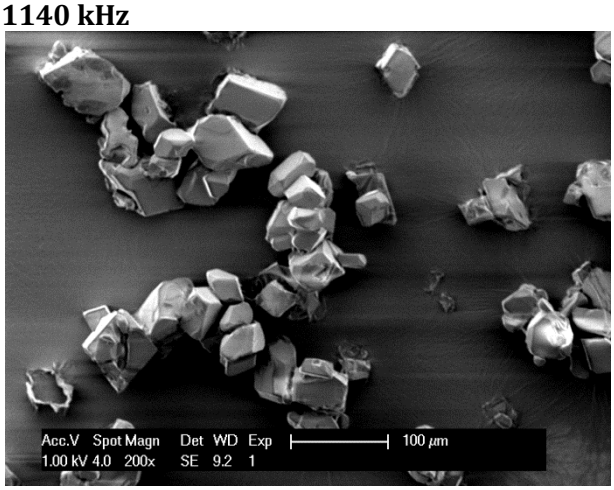

41 kHz

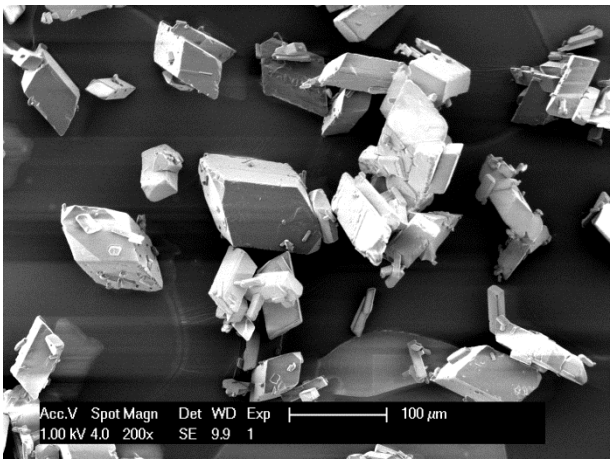

Annex 5. PARAMETERS OF THE EXECUTED SONOCHEMOLUMINISCENCE MEASUREMENTS

frequency (kHz)	material	pcal (W)	pin (W)	temp (°C)
41	Copper	8	9	28,0
41	Copper	4	5	28,0
41	Copper	15	17	28,0
41	Glass	8	14	28,0
41	Glass	4	8	28,0
41	Glass	15	23	28,0
41	PUR	8	13	26,0
41	PUR	4	6	26,0
41	PUR	15	26	26,0
98	Copper	8	9	28,0
98	Copper	4	5	28,0
98	Copper	15	17	28,0
98	Glass	8	14	28,0
98	Glass	4	5	28,0
98	Glass	15	26	28,0
98	PUR	8	13	26,0
98	PUR	4	24	26,0
98	PUR	15	7	26,0
570	Copper	8	13	27,2
570	Copper	4	5	27,2
570	Copper	15	27	27,2
570	Copper	27	50	27,2
570	Glass	8	14	25,5
570	Glass	4	5	25,5
570	Glass	15	26	25,5
570	Glass	22,5	40	25,5
570	PUR	8	13	25,5
570	PUR	4	6	25,5
570	PUR	15	26	25,5
570	PUR	38	55	25,5
1140	Copper	8	13	27,2
1140	Copper	4	6	27,2
1140	Copper	15	24	27,2
1140	Copper	35,5	60	27,2
1140	Glass	8	11	25,5
1140	Glass	4	5	25,5
1140	Glass	15	23	25,5
1140	Glass	29	45	25,5
1140	PUR	8	13	25,5
1140	PUR	4	6	25,5
1140	PUR	15	26	25,5
1140	PUR	44,5	65	25,5

Annex 6. WAVELENGTHS AT DIFFERENT FREQUENCIES

c (in water) = 1497 m/s at 25°C

λ (41 kHz) = 3,65 cm
λ (98 kHz) = 1,53 cm
λ (570 kHz) = 0,26 cm
λ (1140 kHz) = 0,131 cm

Annex 7. IMPACT OF FREQUENCY ON CAVITATIONS

7.1. PUR

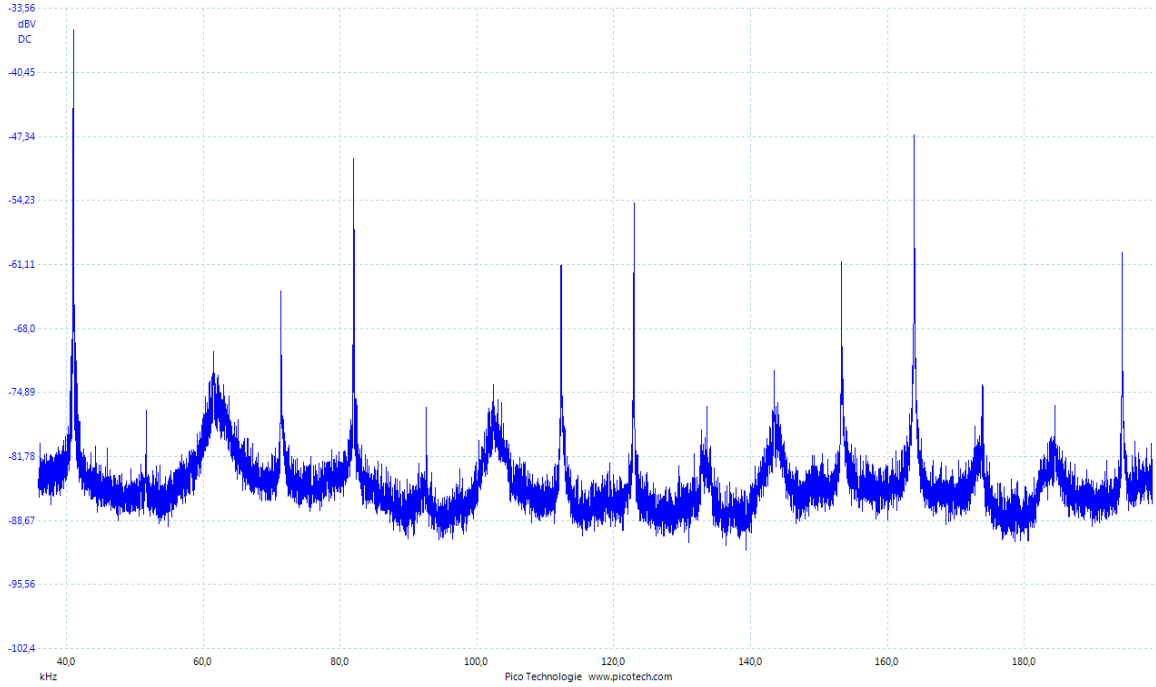

PUR - 8W - 41KHz

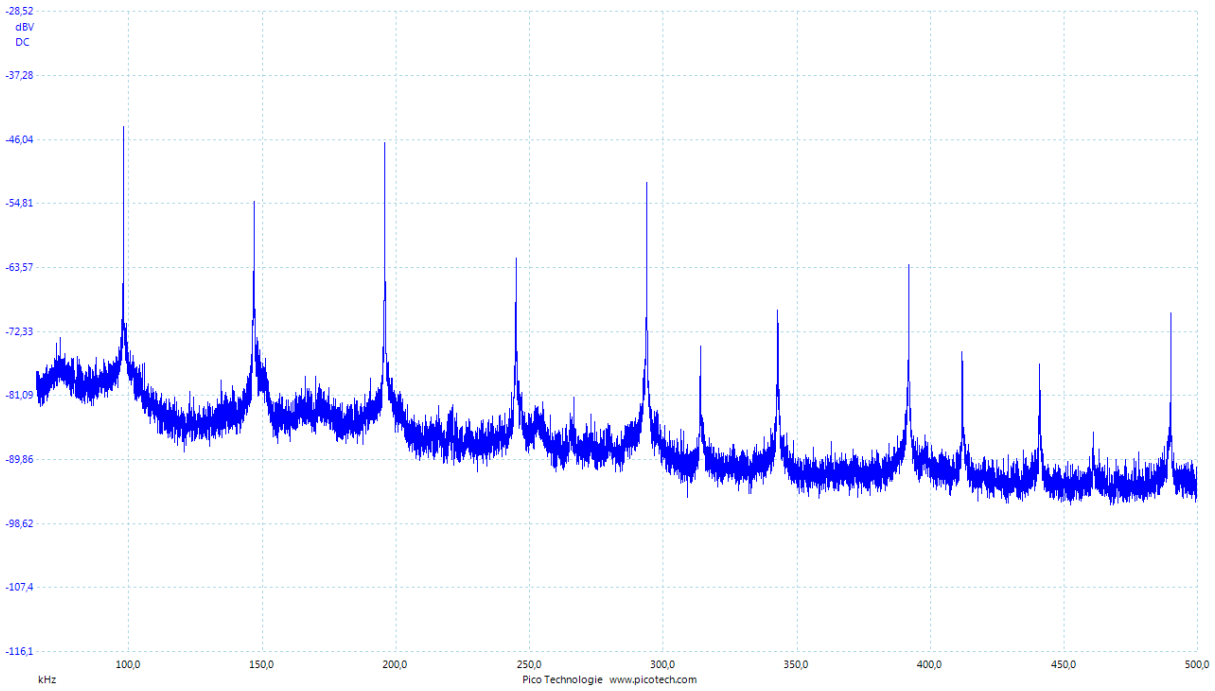

PUR -8W – 98 кHz

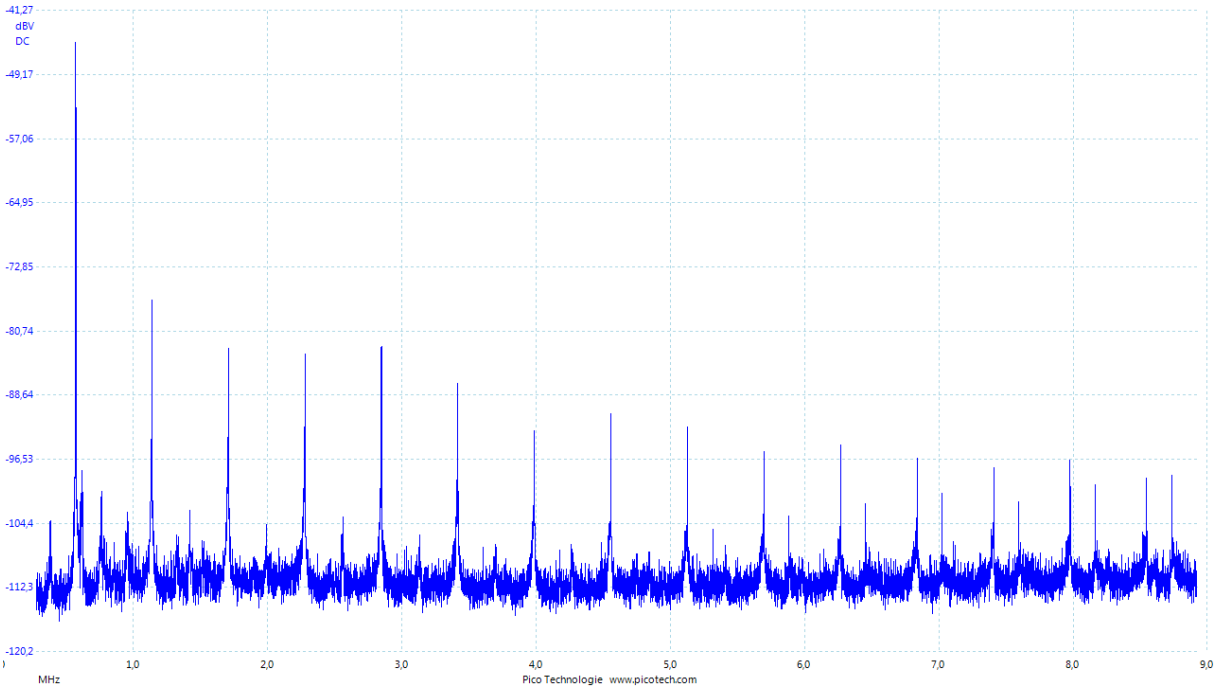

PUR - 8W - 570 кHz

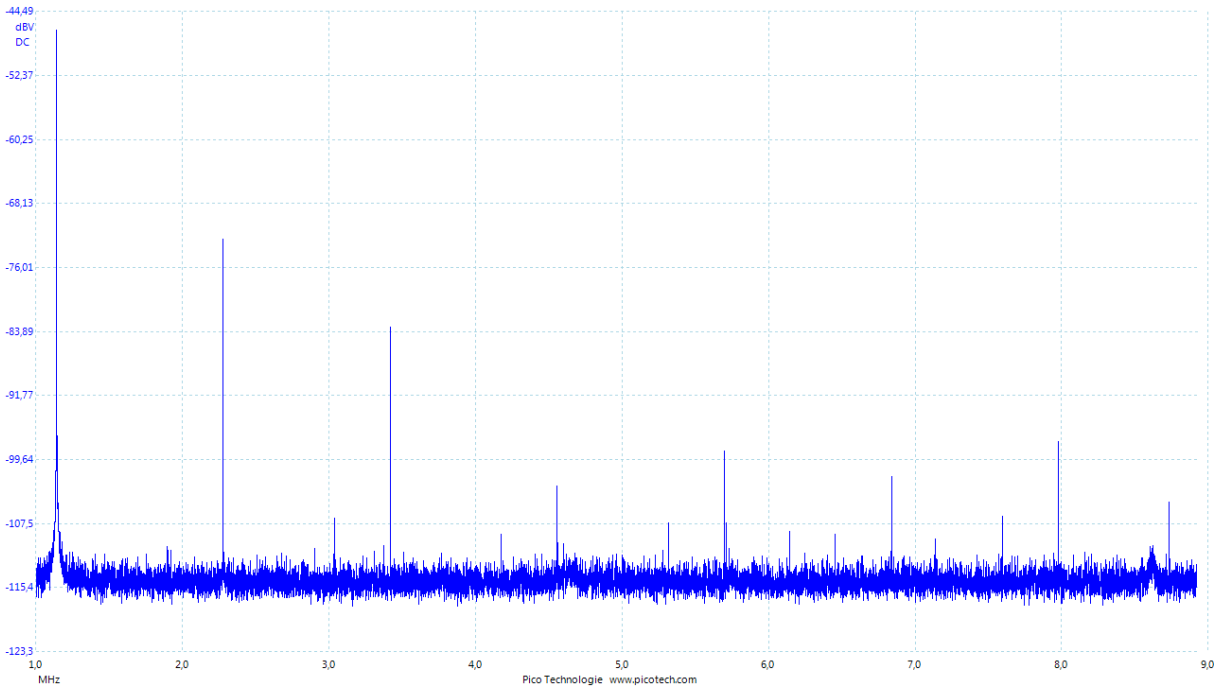

PUR - 8W - 1140 кHz

7.2. *AIR*

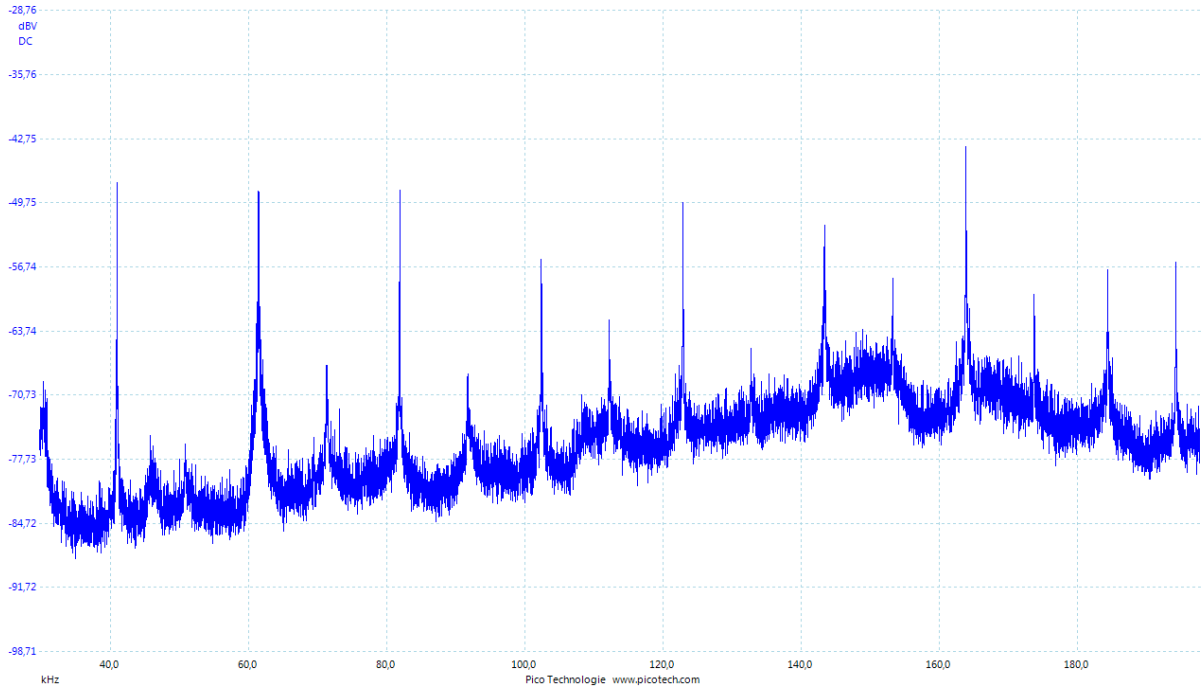

AIR - 8W -41 кHz

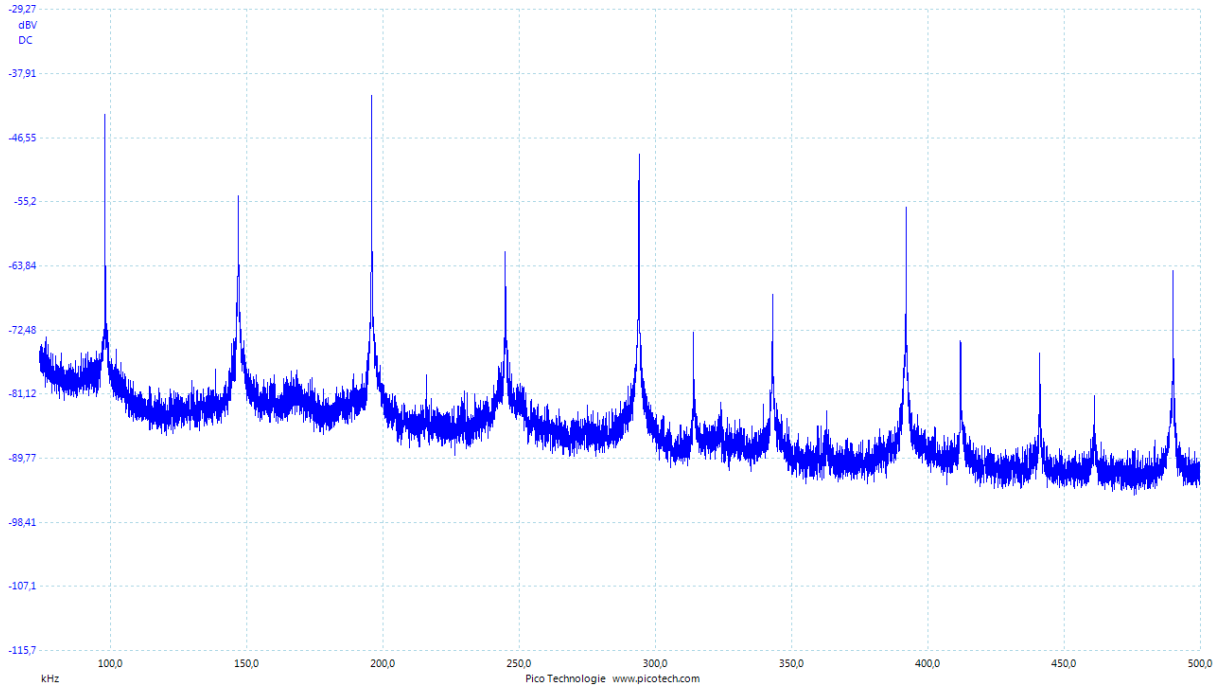

AIR - 8W - 98 кHz

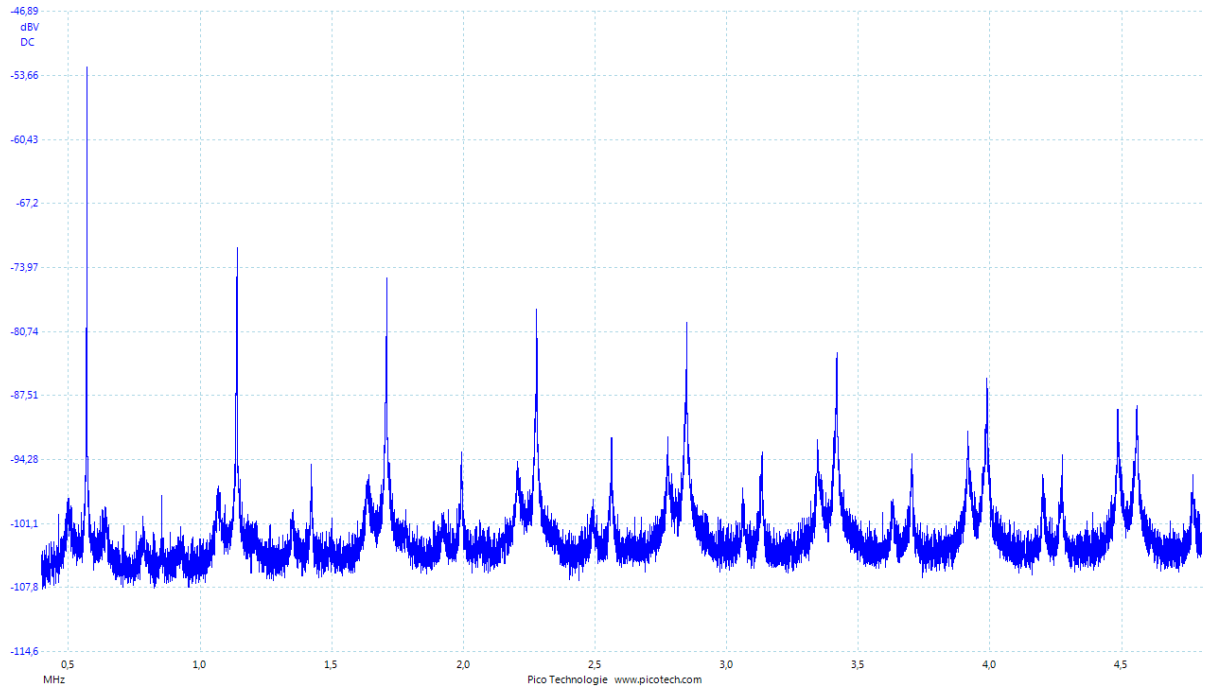

AIR - 8W - 570 кHz

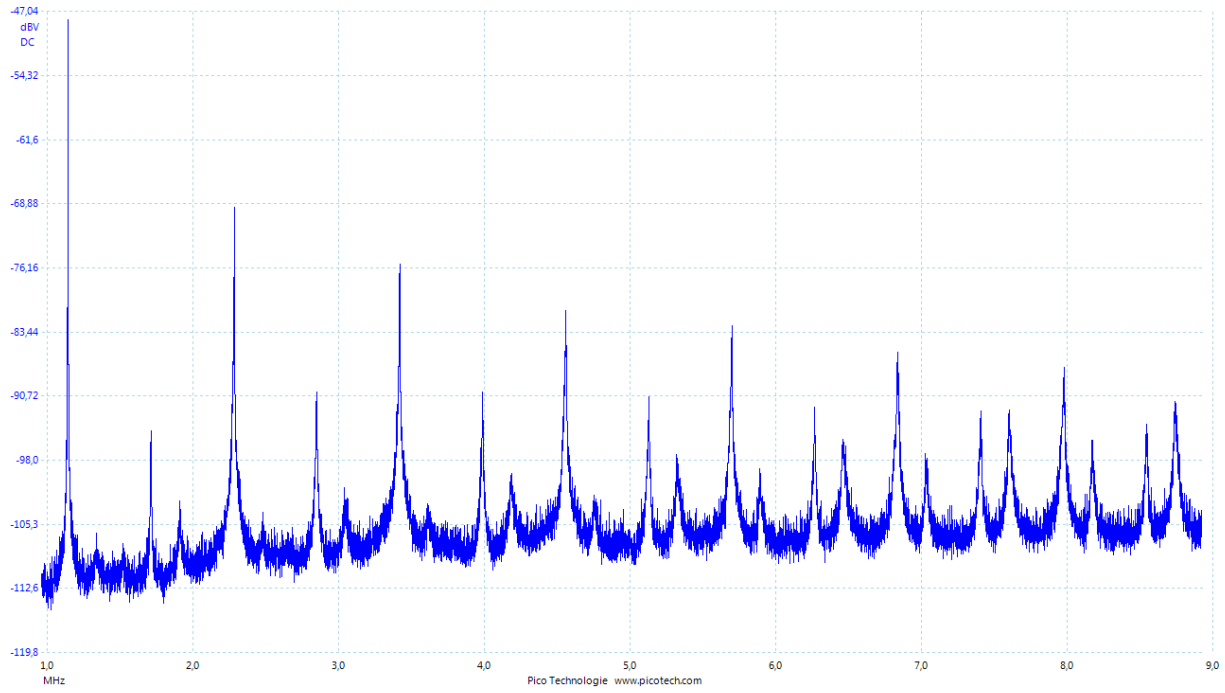

AIR - 8W - 1140 кHz

Annex 8. IMPACT OF SURFACE STABILIZERS ON CAVITATIONS

8.1. 1140 KHZ

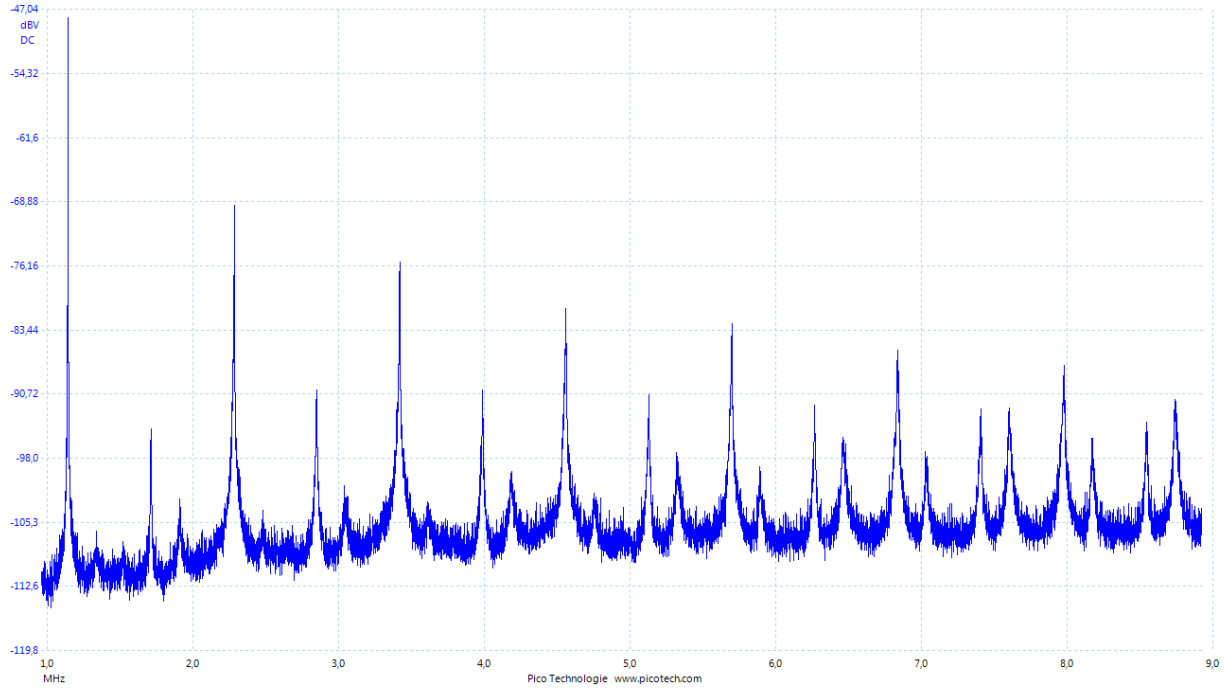

AIR - 8W - 1140 KHZ

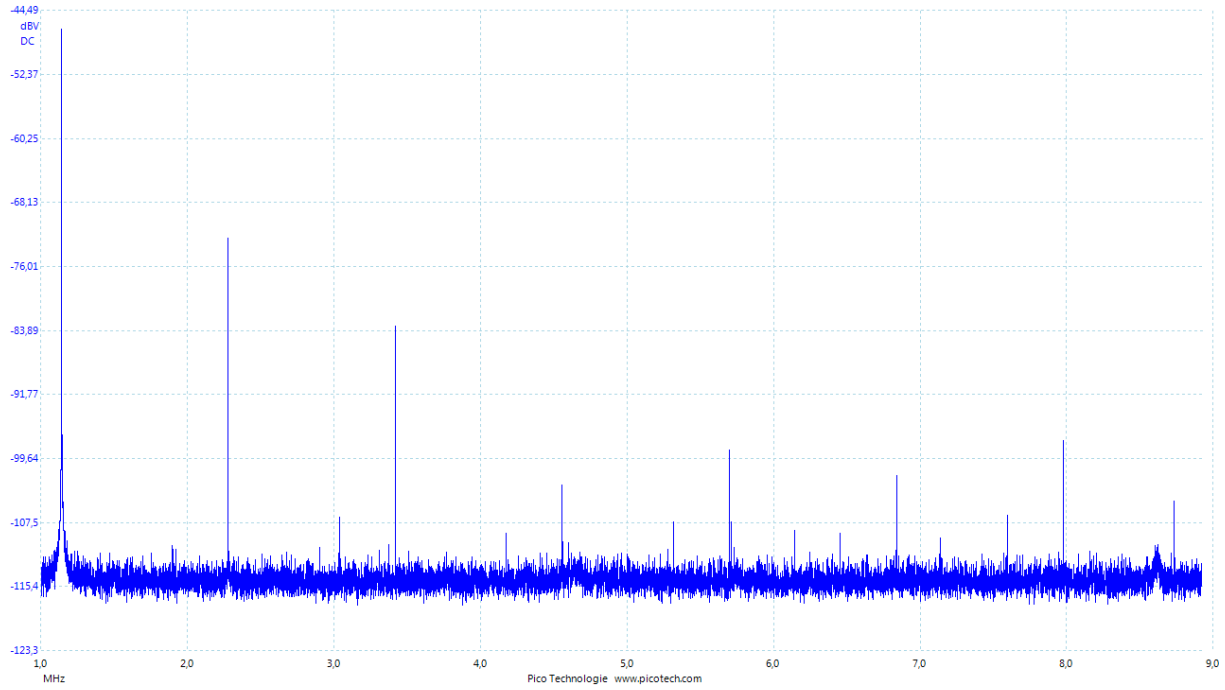

PUR - 8W - 1140 KHZ

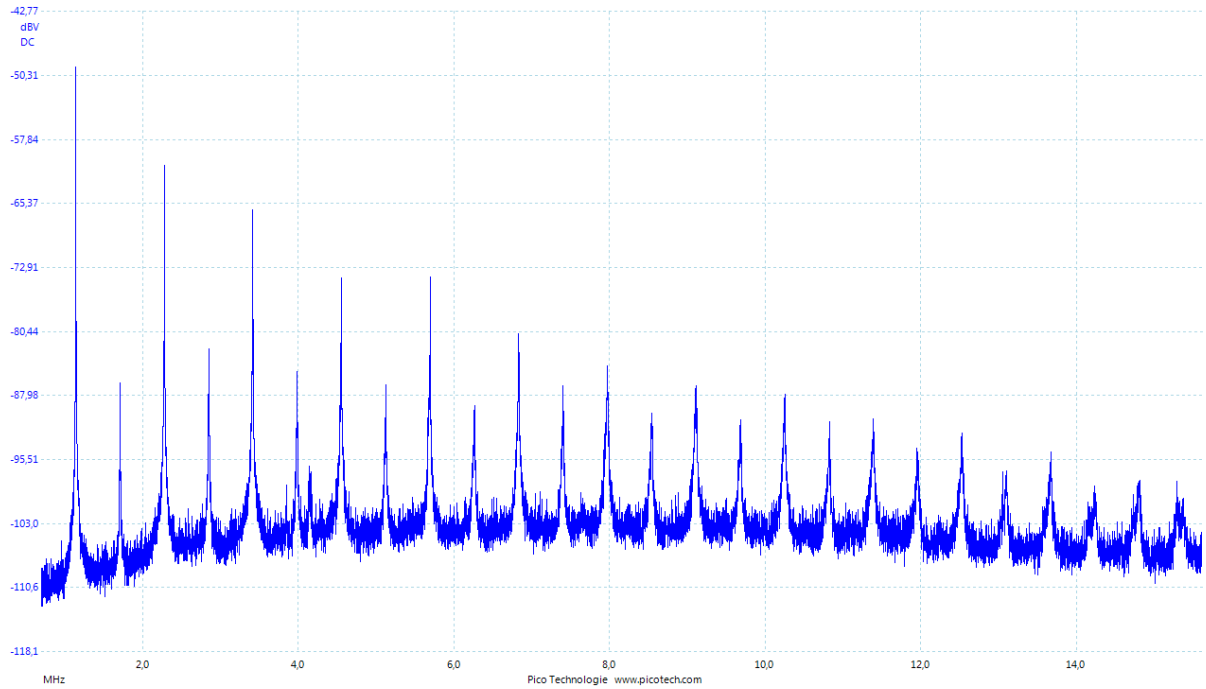

GLASS - 8W – 1140 кHz

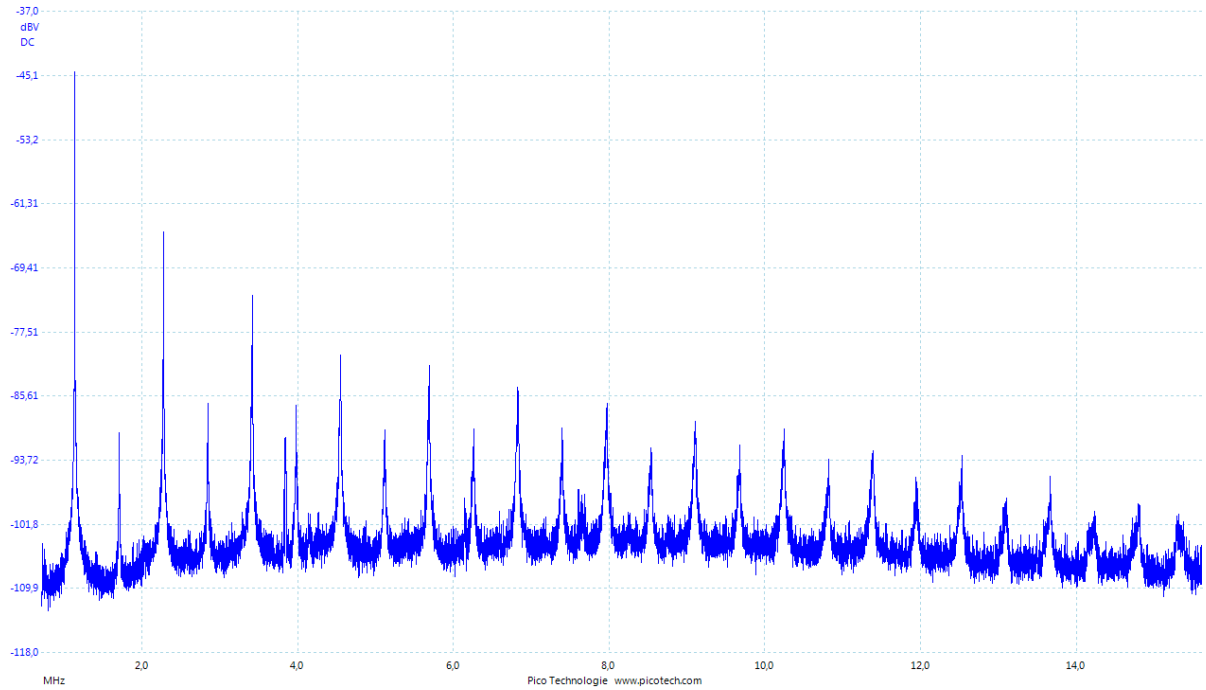

COPPER - 8W – 1140 кHz

8.2. 41 kHz

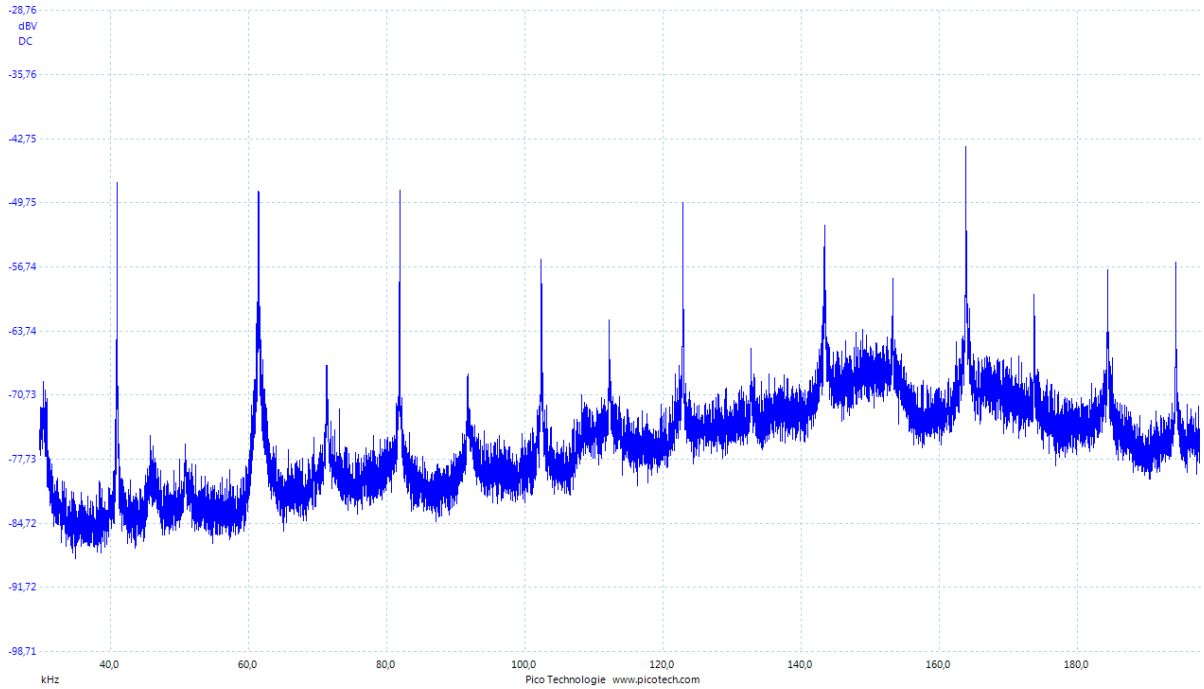

AIR - 8W - 41 kHz

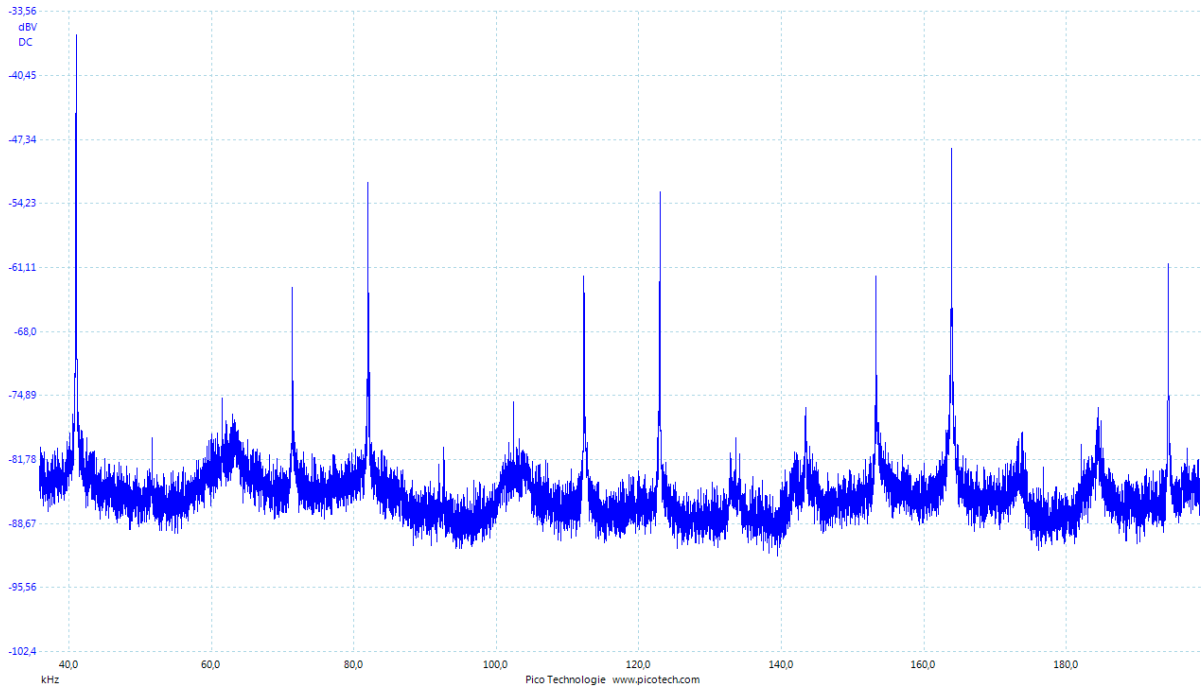

PUR - 8W - 41 kHz

Annex 9. IMPACT OF POWER ON THE US WAVES

9.1. IMPACT OF INPUT POWER USING COPPER

1140 kHz

4W 8W 15W 55W

570 kHz

4W 8W 15W 30W

98 kHz

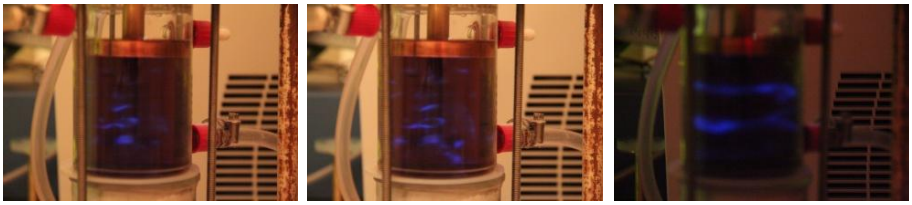

4W 8W 15W

41 kHz

4W 8W 15W

9.2. *Impact of input power using Glass*

1140 kHz

4W 8W 15W 60W

570 kHz

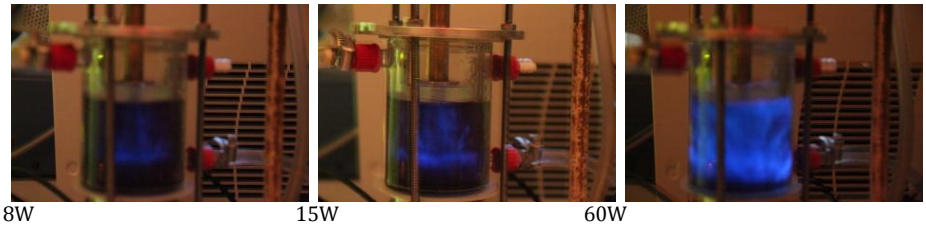

8W 15W 60W

98 kHz

4W 8W 15W

41 kHz

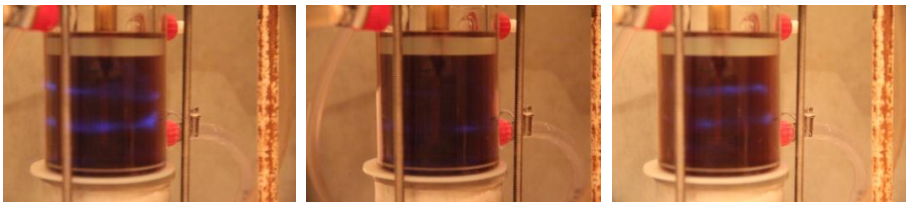

4W 8W 15W

9.3. *IMPACT OF INPUT POWER USING PUR*

1140 kHz

4W 8W 15W 65W

570 kHz

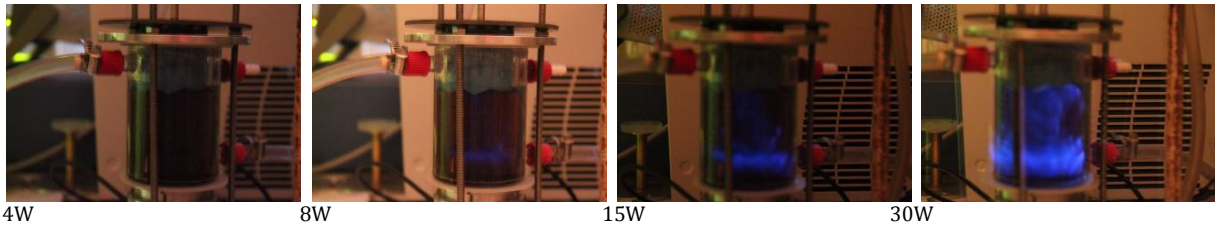

4W 8W 15W 30W

98 kHz

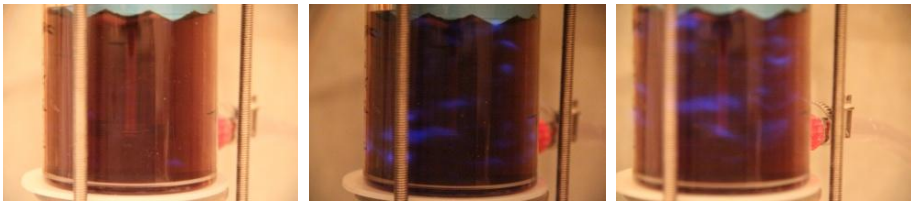

4W 8W 15W

41 kHz

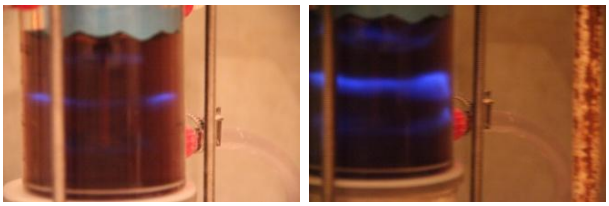

4W 8W

Annex 10. IMPACT OF POWER ON CAVITATIONS (NO SURFACE STABILIZER)

10.1. 41 KHZ

4 W calorimetric power

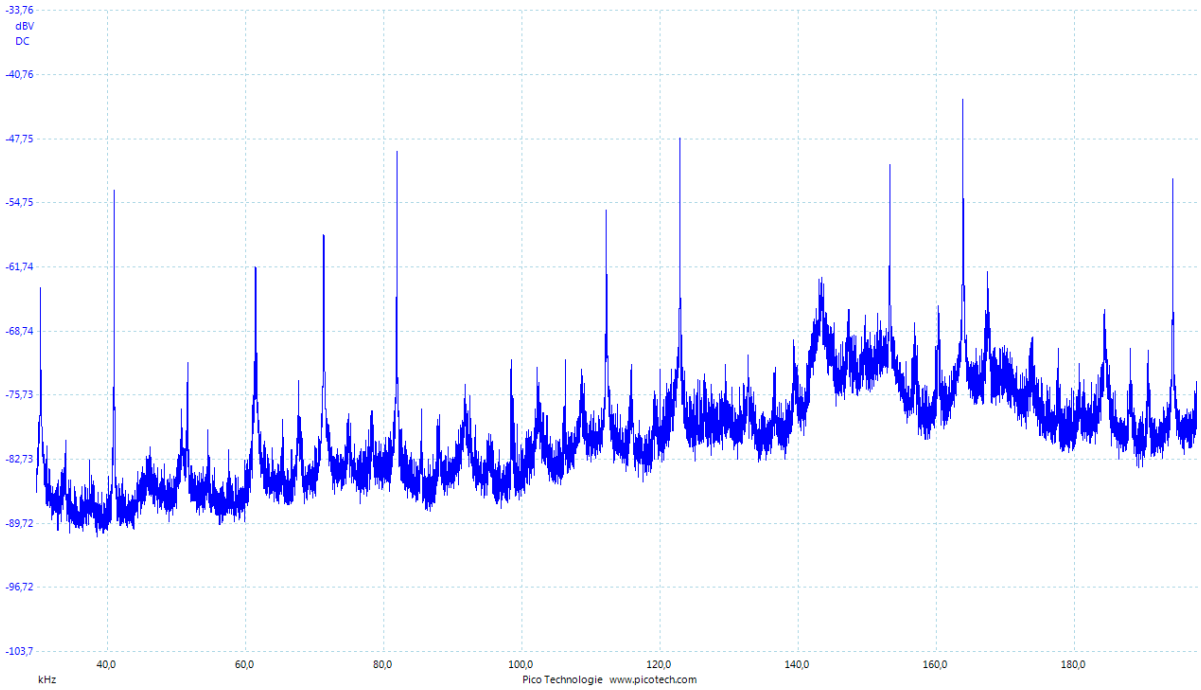

8 W calorimetric power

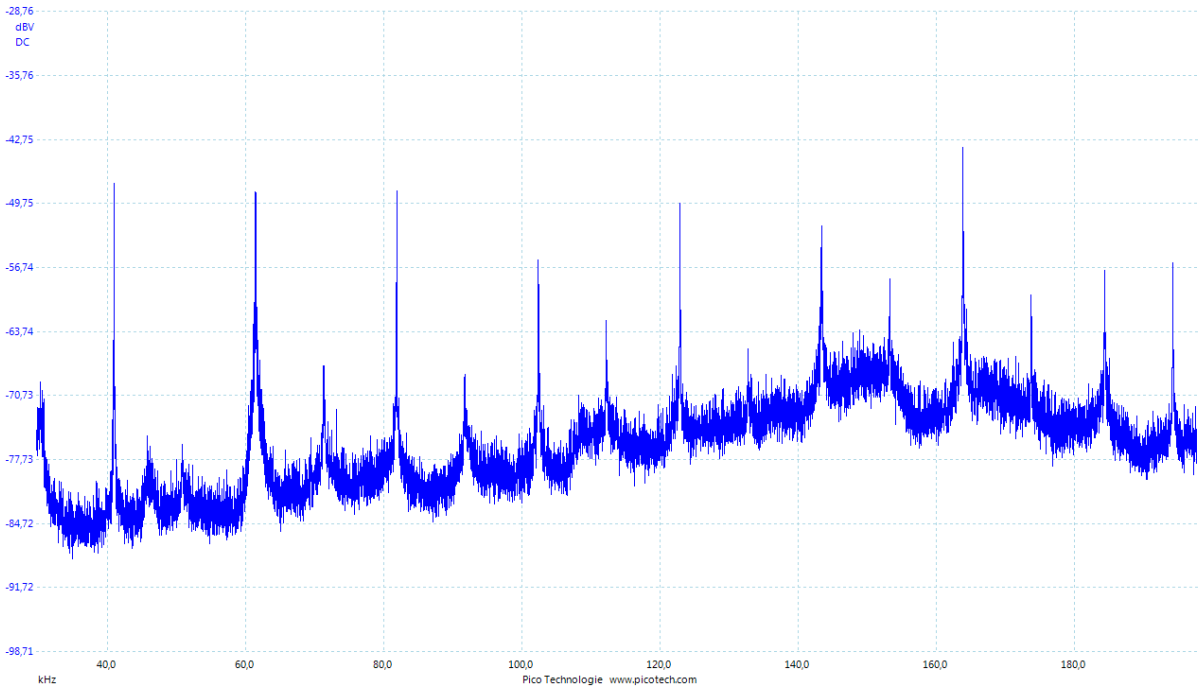

15 W calorimetric power

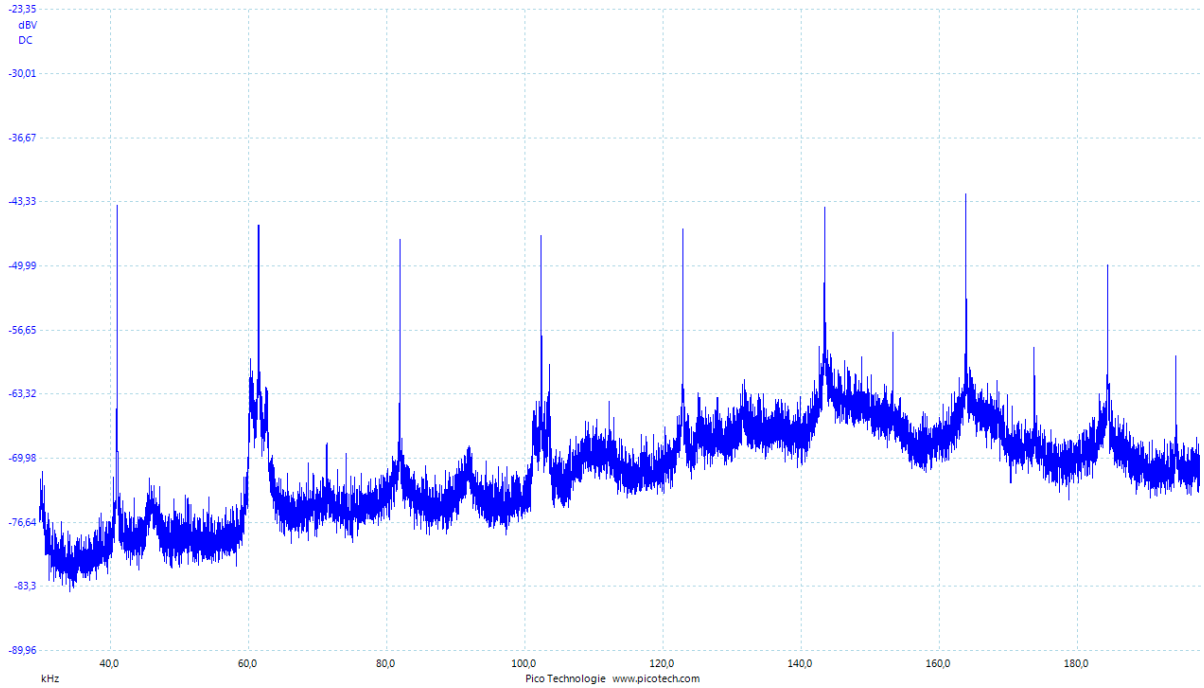

10.2. 1140 kHz

4W calorimetric power

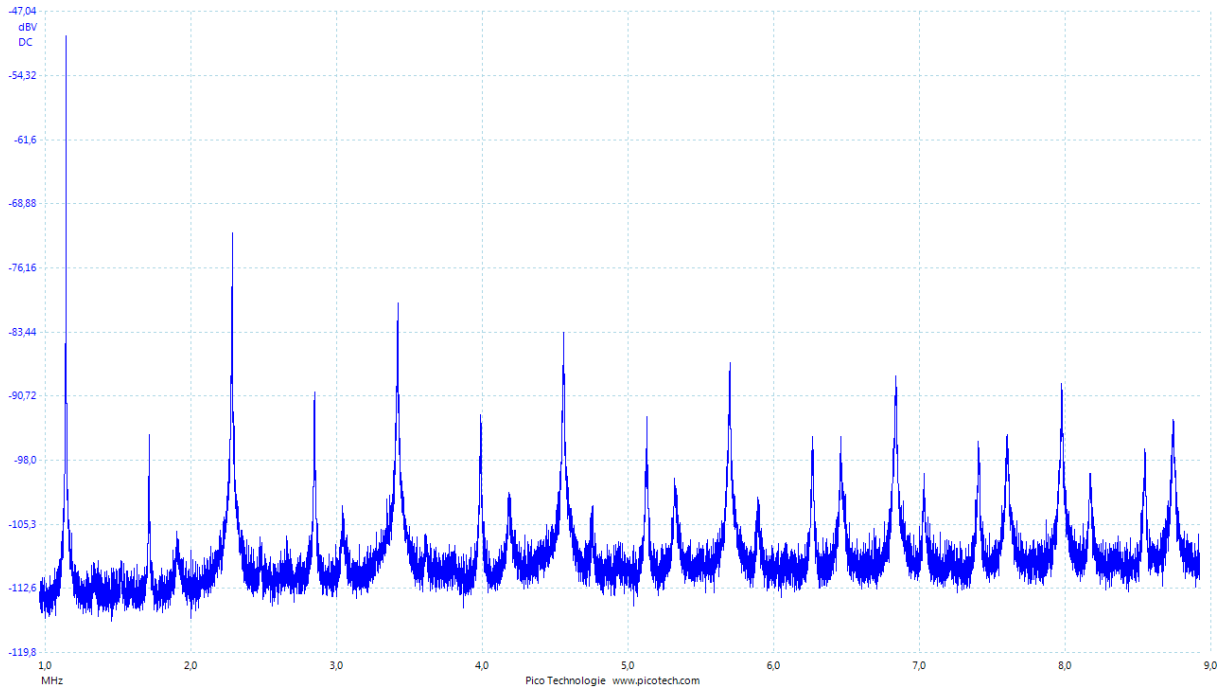

8W calorimetric power

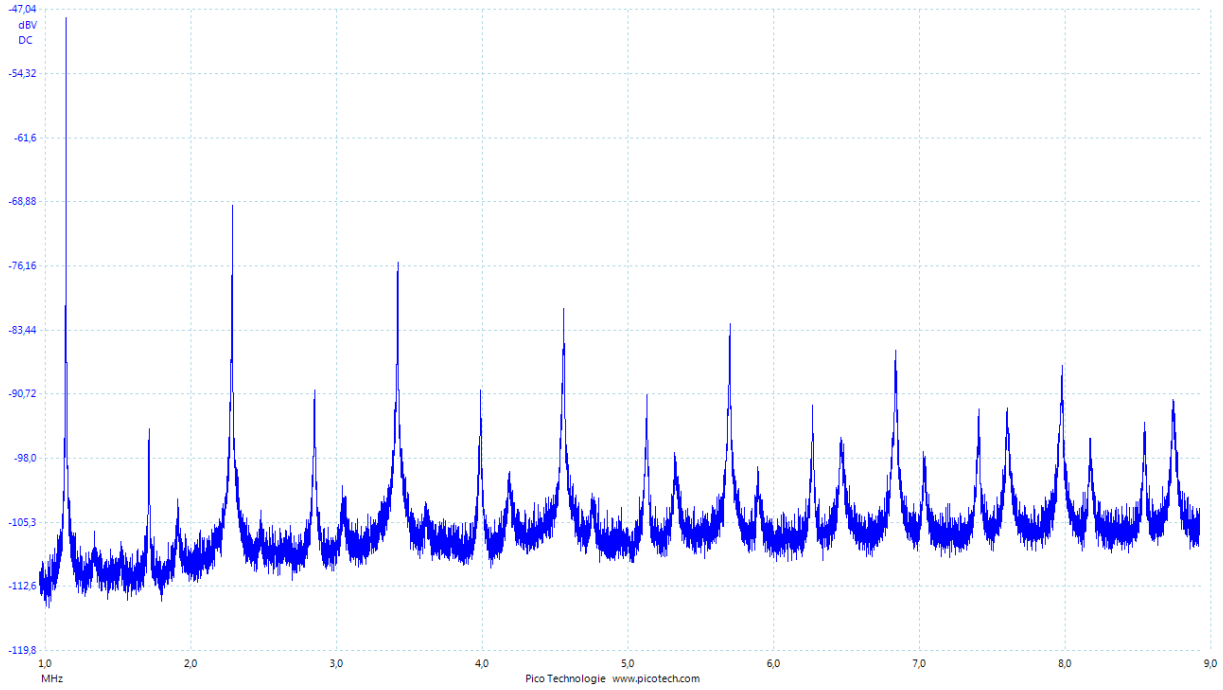

15W calorimetric power

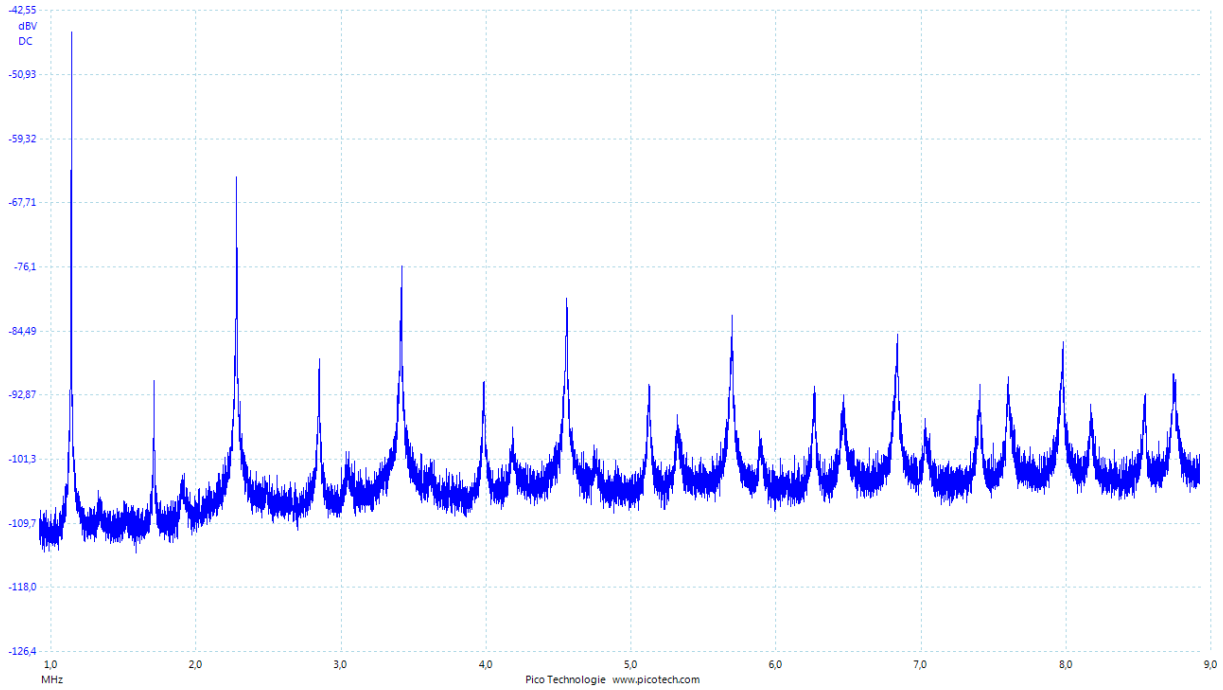

Annex 11. IMPACT OF STIRRER ON US WAVES AT 8W

11.1. LOW FREQUENCIES

Copper

With stirrer 400rpm

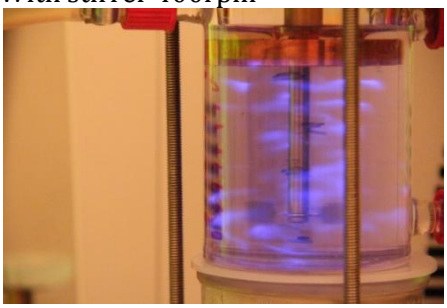

98kHz
7 bands

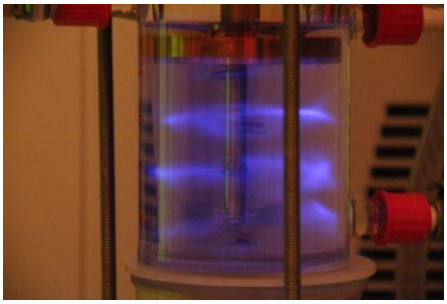

41kHz
3 bands

No stirrer

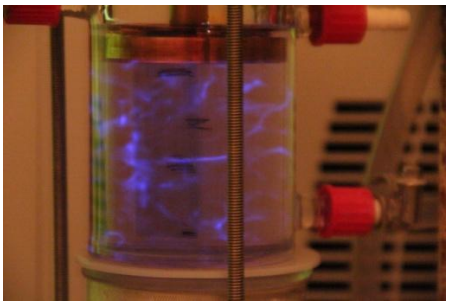

98kHz
Random spectrum, clearly visible

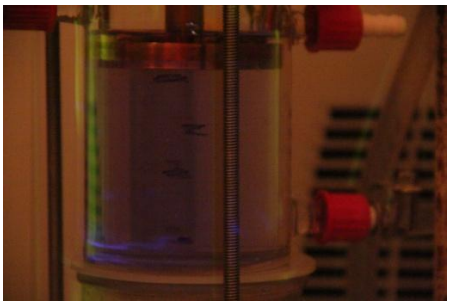

41kHz
Random spectrum, hardly visible

With stirrer 0rpm

98kHz
No image

41kHz
no image

Glass

With stirrer 400rpm

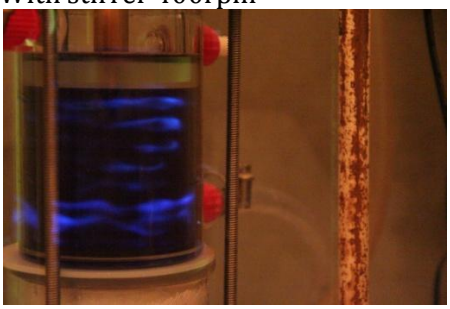

98kHz
7 bands

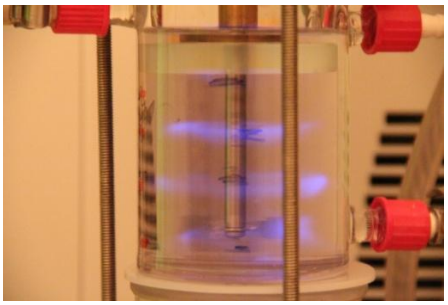

41kHz
3 bands

No stirrer

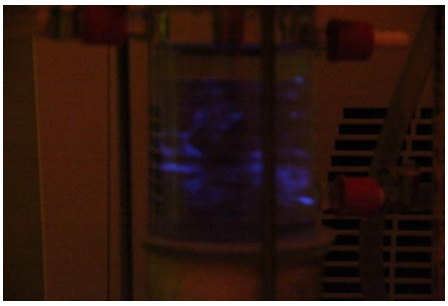

98kHz
Random spectrum, clearly visible

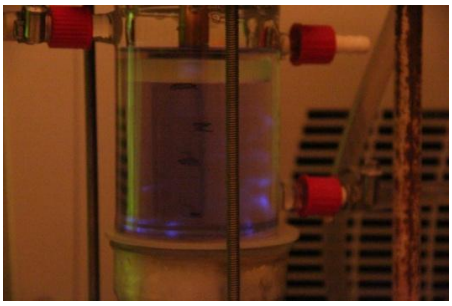

41kHz
Random spectrum, hardly visible

With stirrer 0rpm

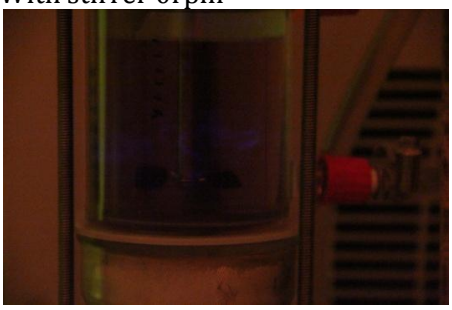

98kHz
Random illuminations, very hard visible

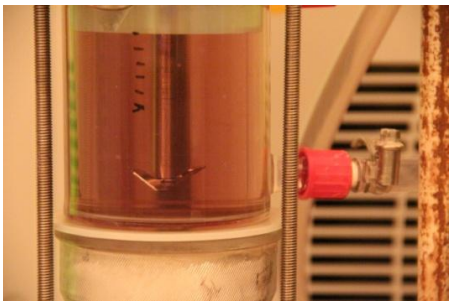

41kHz
no image

Air

With stirrer 400rpm

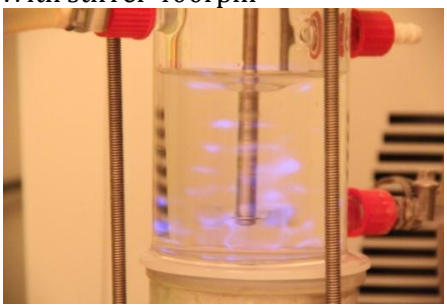

98 kHz
7 bands

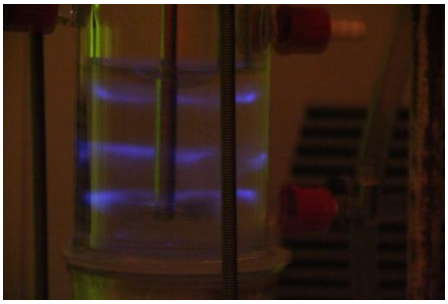

41kHz
3 bands

No stirrer

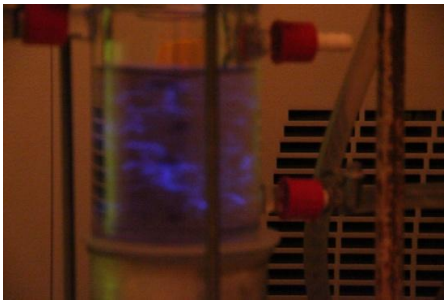

98kHz
Random spectrum, clearly visible

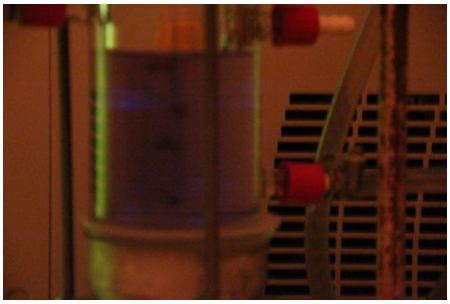

41kHz
Random spectrum, hardly visible

With stirrer 0rpm

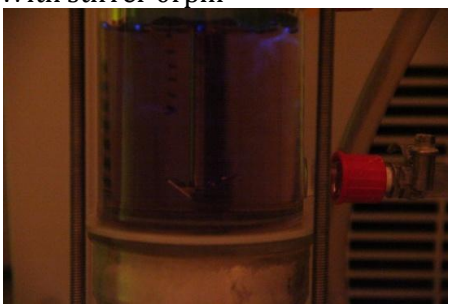

98kHz
Random spectrum, hardly visible

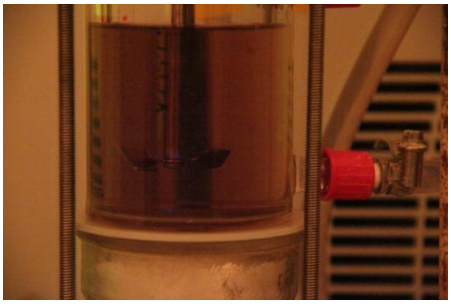

41kHz
no image

PUR

With stirrer 400rpm

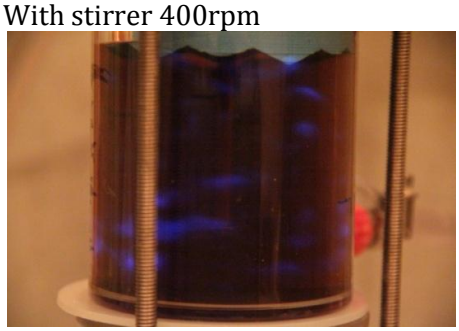

98kHz
7 bands

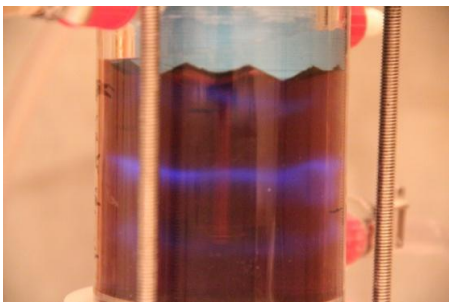

41kHz
3 bands

No stirrer

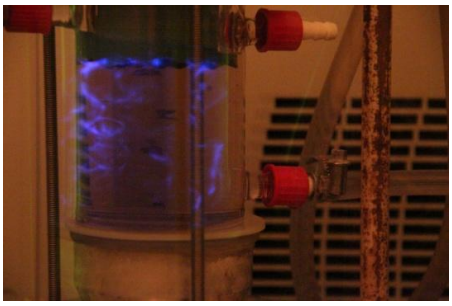

98kHz
Random spectrum, clearly visible

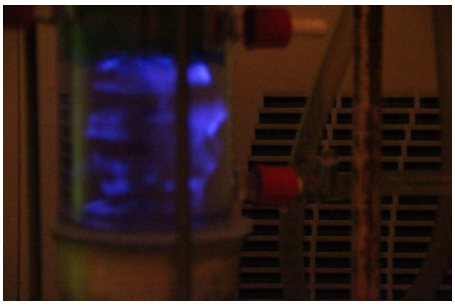

41kHz
Random spectrum, clearly visible

With stirrer 0rpm

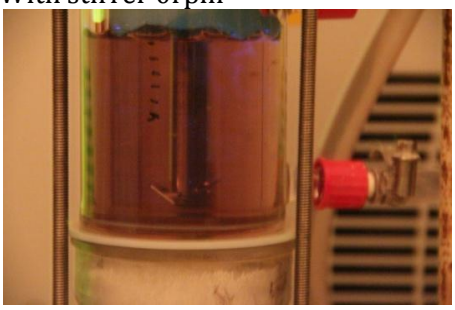

98kHz
Hardly visible spectrum

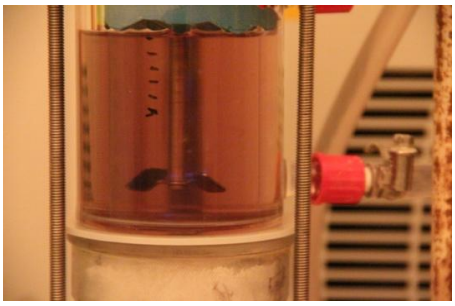

41kHz
no image

11.2. HIGH FREQUENCIES

Copper

With stirrer 400rpm

1140 kHz

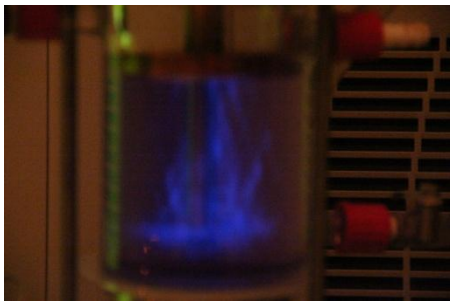

570 kHz

No stirrer

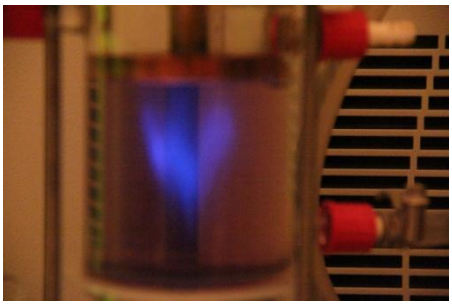

1140 kHz

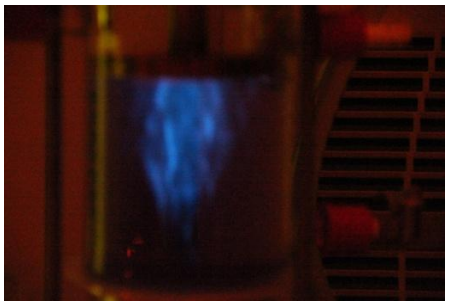

570 kHz

With stirrer 0rpm

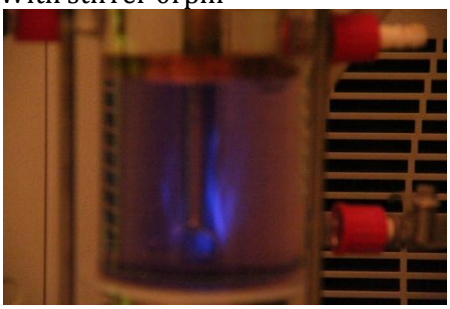

1140 kHz

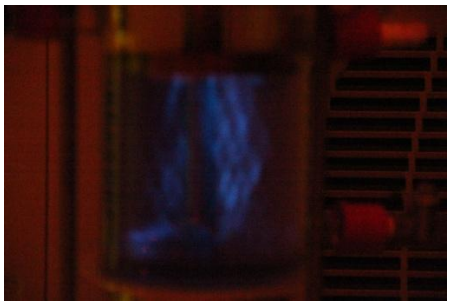

570 kHz

Glass

With stirrer 400rpm

1140 kHz

570 kHz

No stirrer

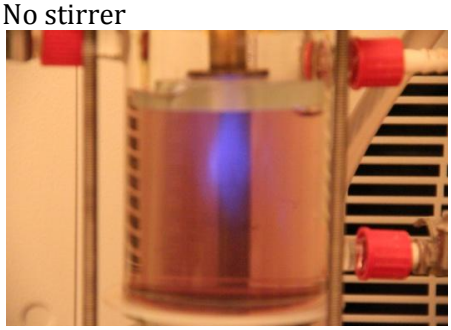

1140 kHz

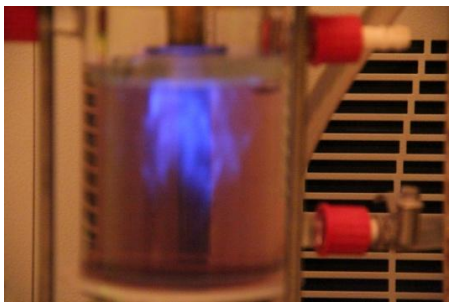

570 kHz

With stirrer 0rpm

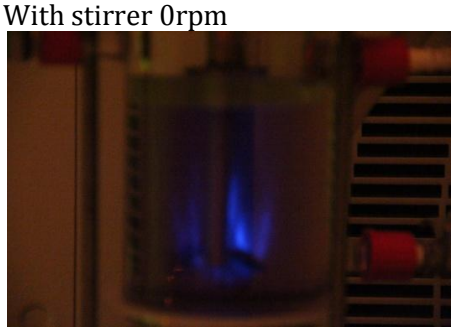

1140 kHz

570 kHz

Air

With stirrer 400rpm

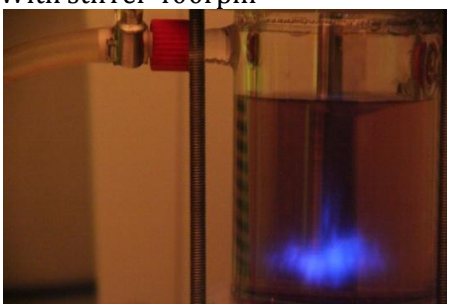

1140 kHz

570 kHz

No stirrer

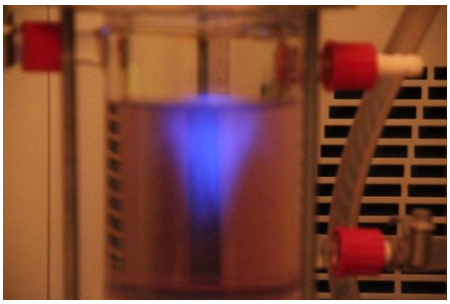

1140 kHz

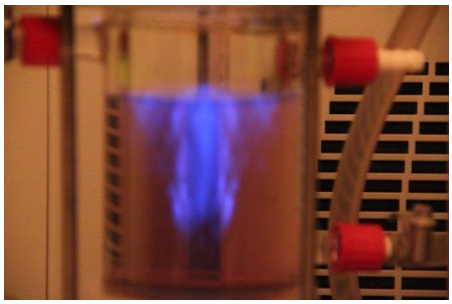

570 kHz

With stirrer 0rpm

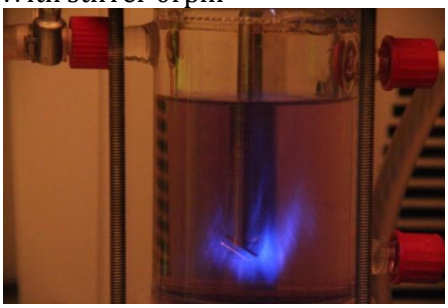

1140 kHz

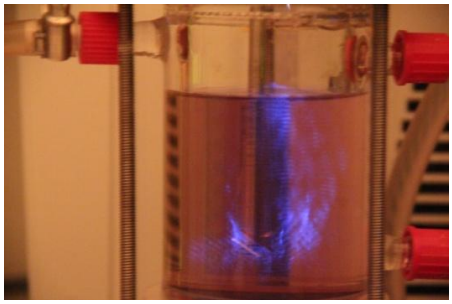

570 kHz

PUR

With stirrer 400rpm

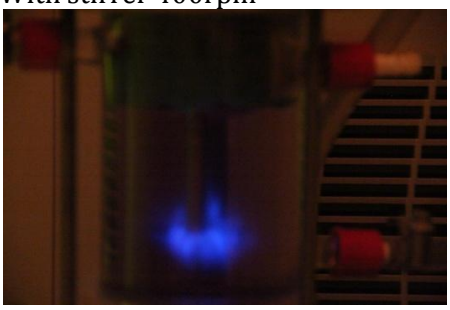

1140 kHz

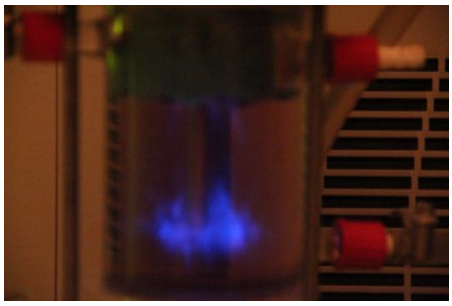

570 kHz

No stirrer

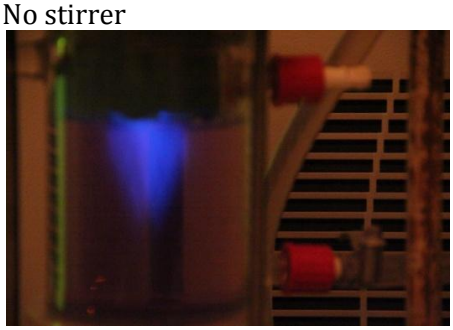

1140 kHz

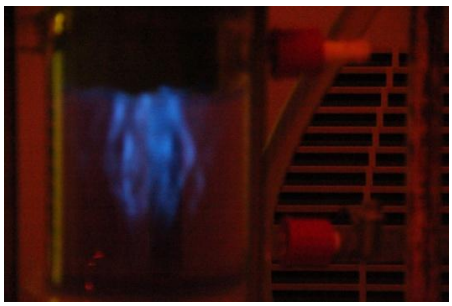

570 kHz

With stirrer 0rpm

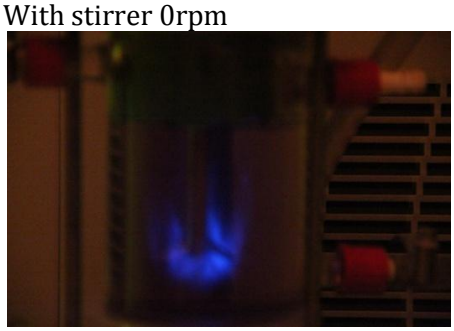

1140 kHz

570 kHz

Annex 12. IMPACT OF THE SURFACE STABILIZER HEIGHT ON THE WAVE PATTERN

41 kHz

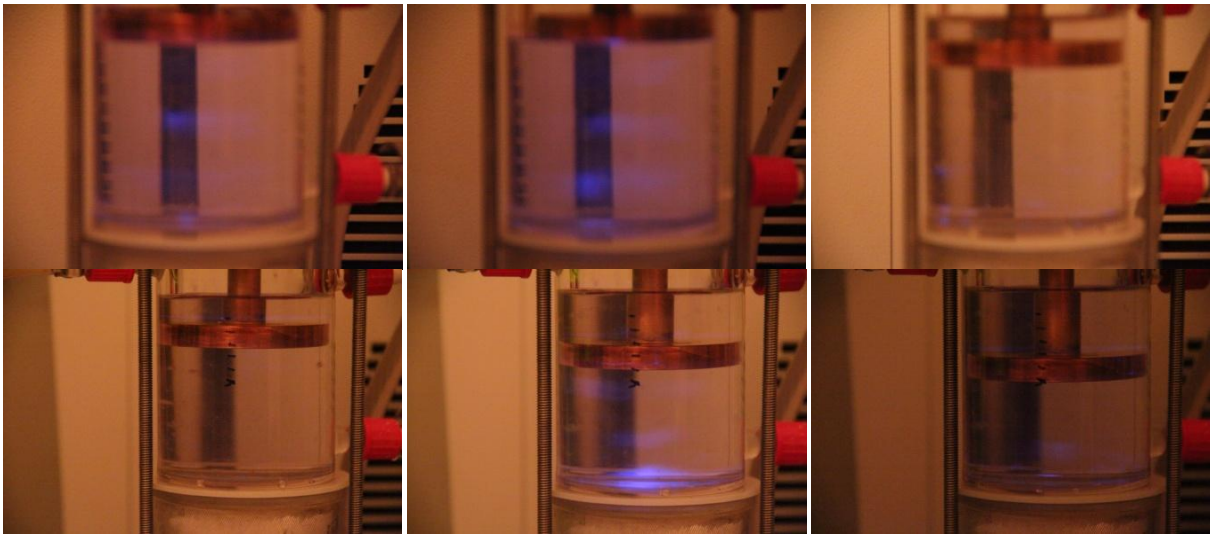

98 kHz

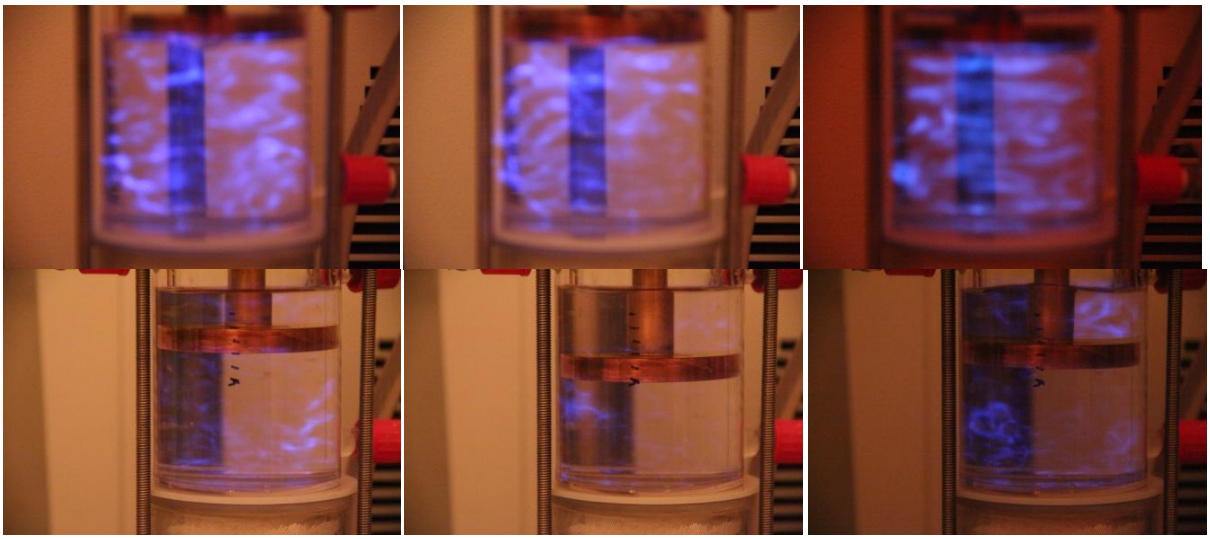

570 kHz

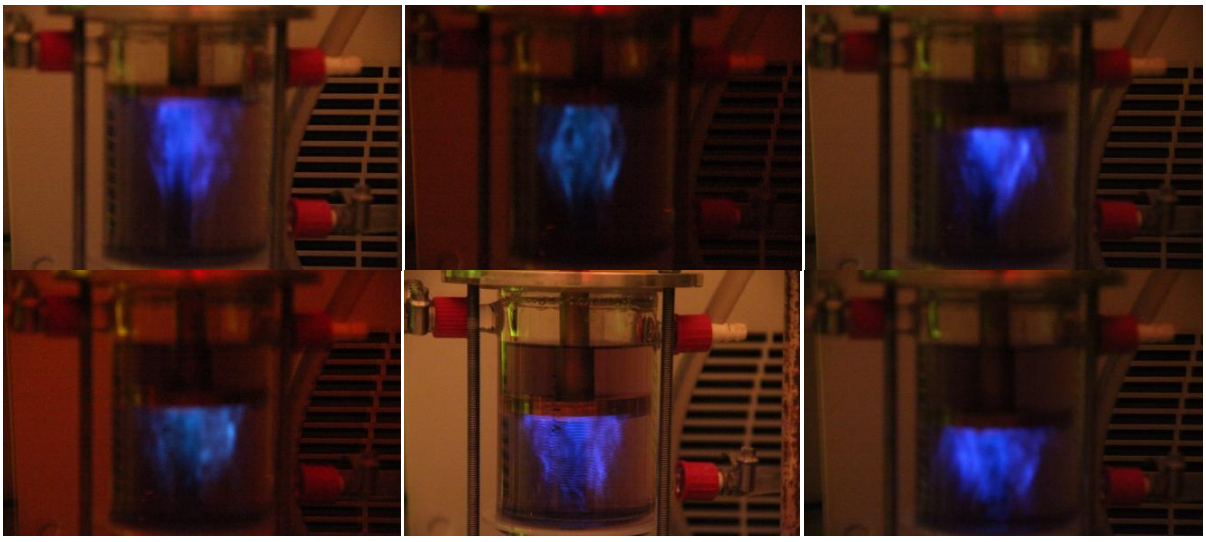

1140 kHz

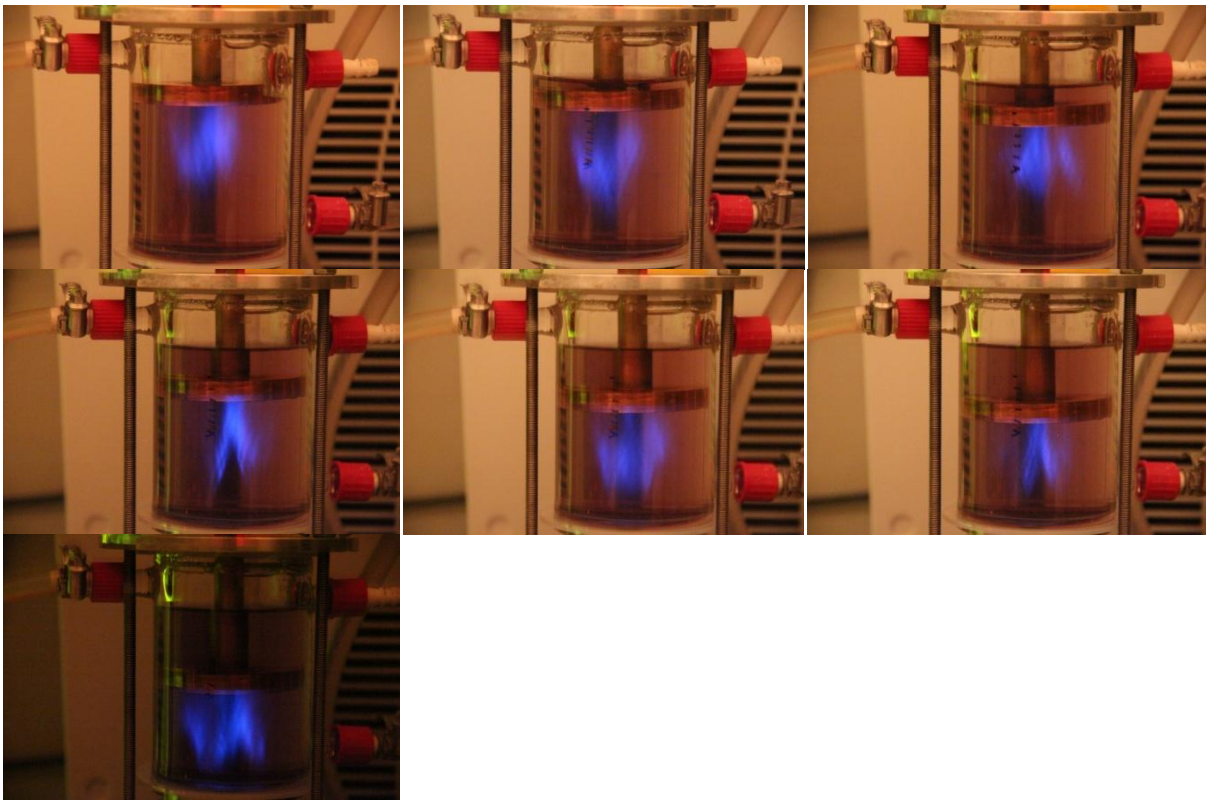

Annex 13. IMPACT OF STIRRER ON THE CAVITATIONS

With stirrer 400 rpm

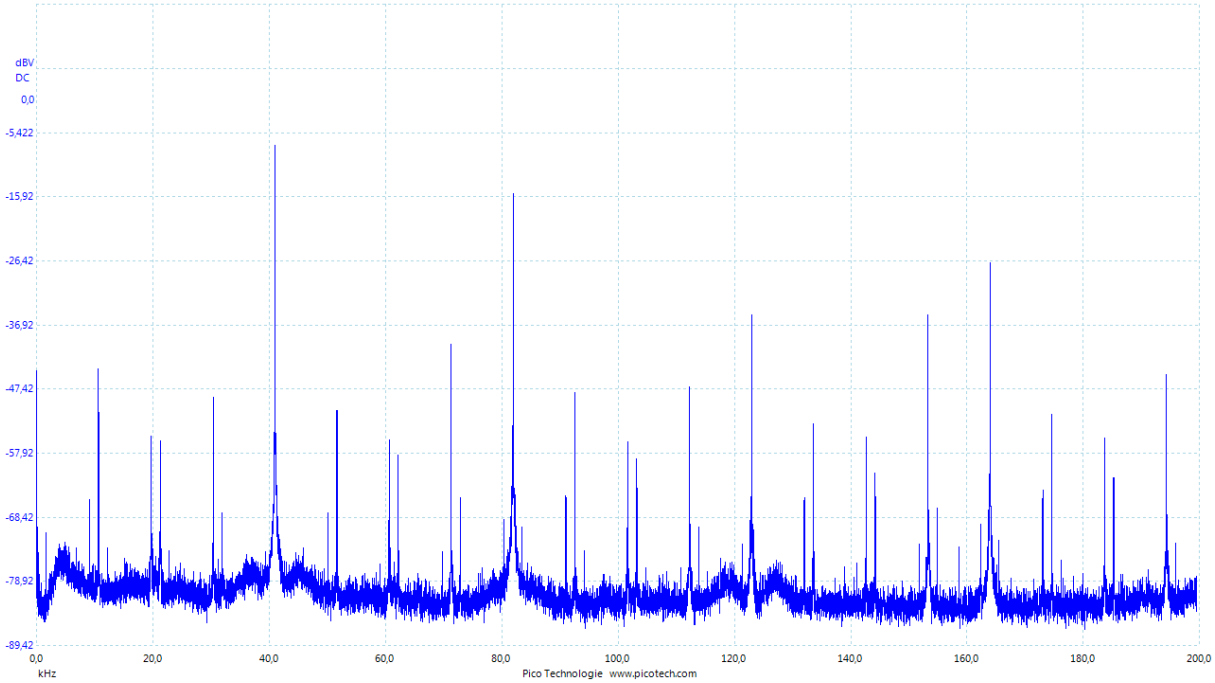

With stirrer 0 rpm

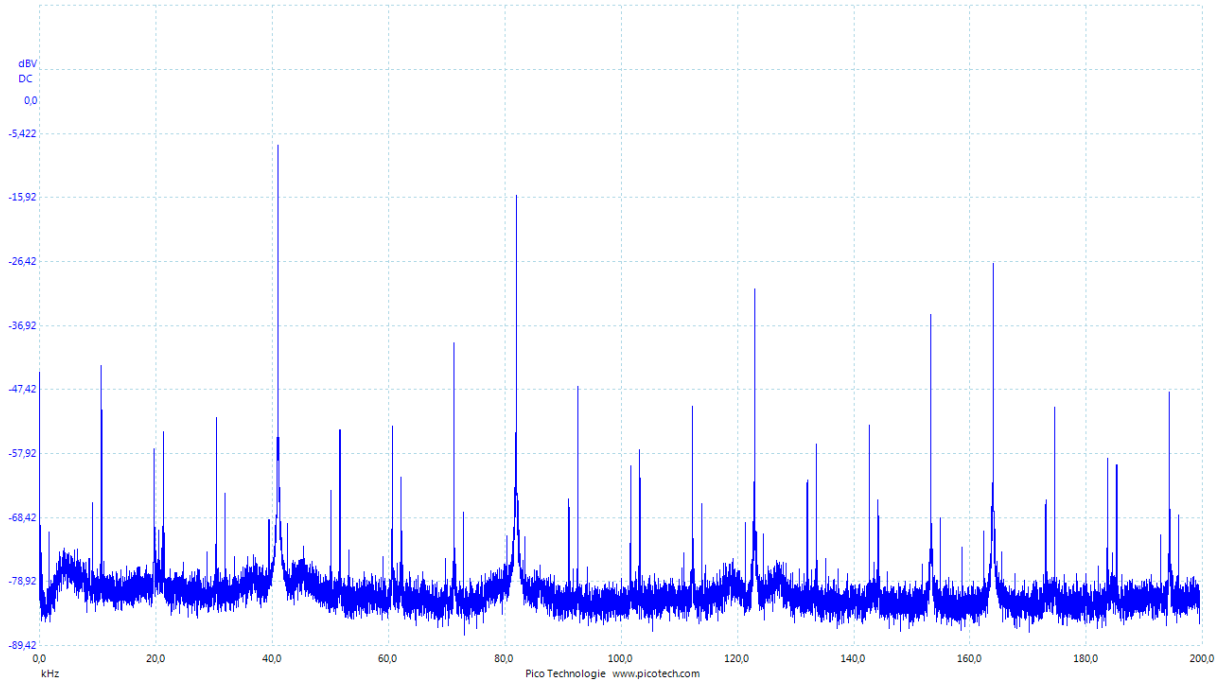

No stirrer

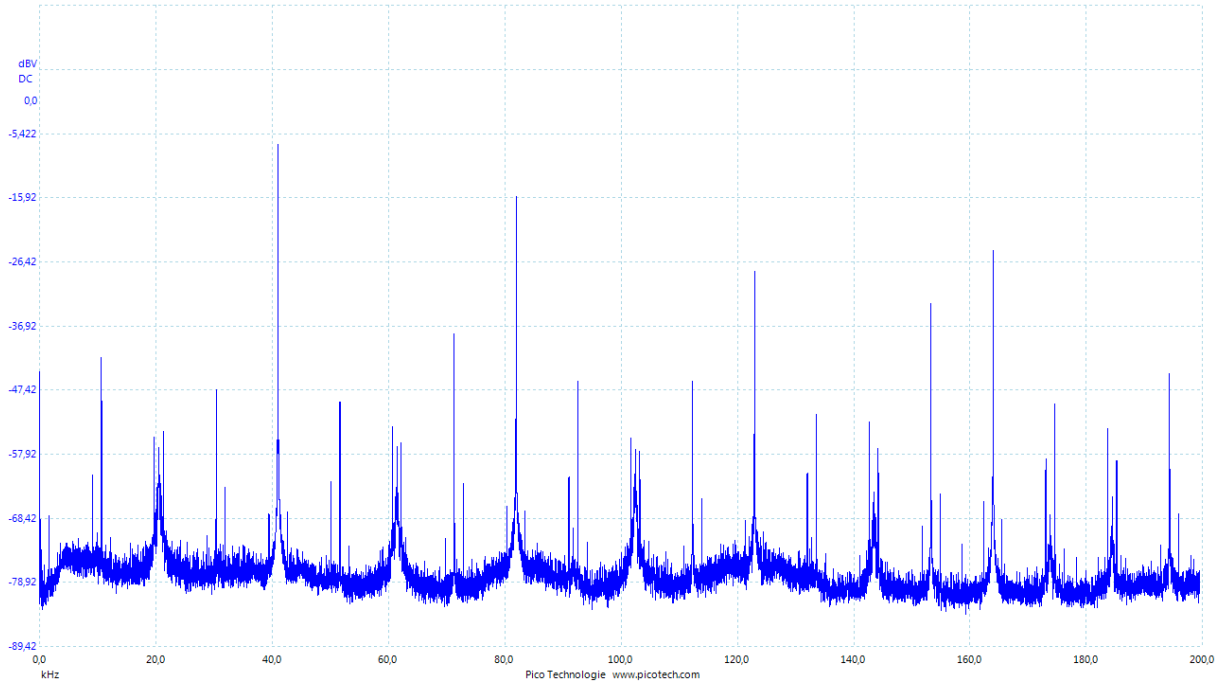

Annex 14. CAVITATION NOISE AT DIFFERENT DISTANCES FROM THE TRANSDUCER WITHOUT USING A STIRRER

14.1. 41 KHZ

1,0 cm above transducer

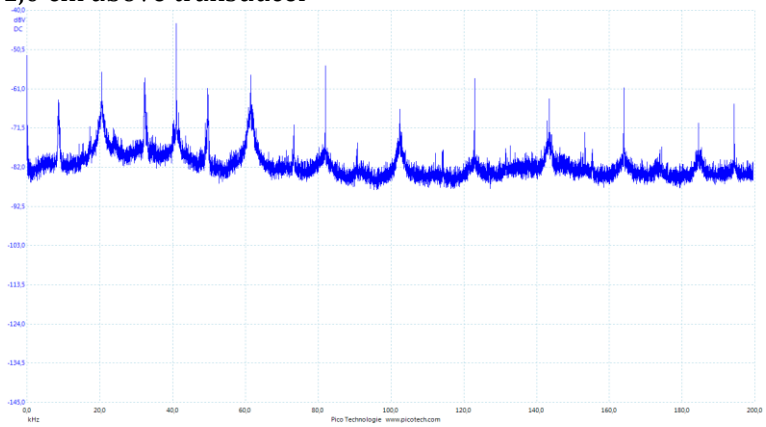

1,6 cm above transducer

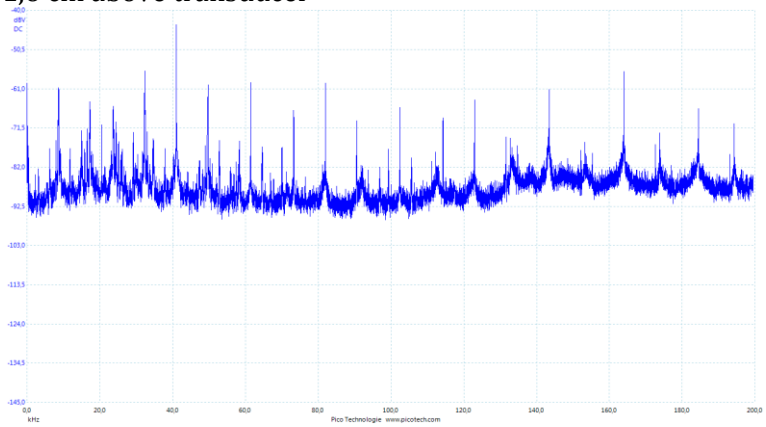

2,3 cm above transducer

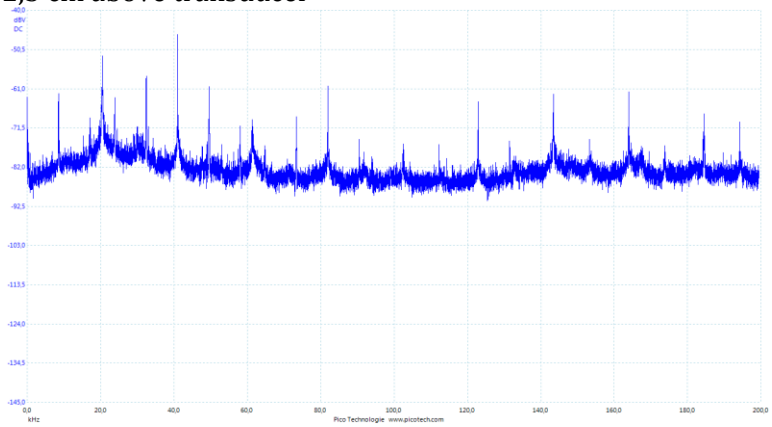

3,6 cm above transducer

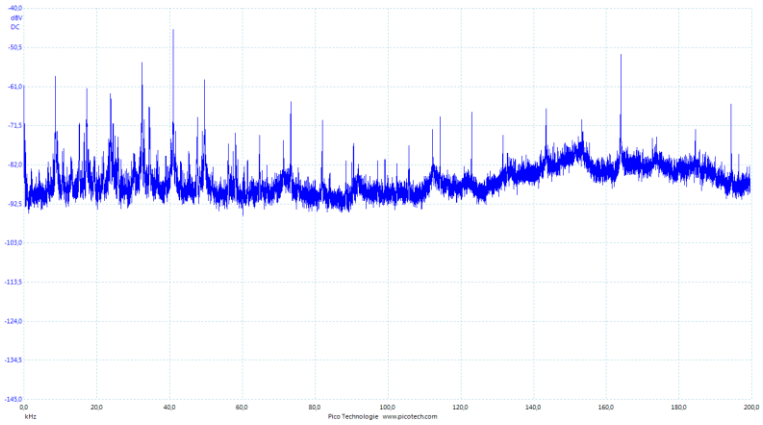

4,0 cm above transducer

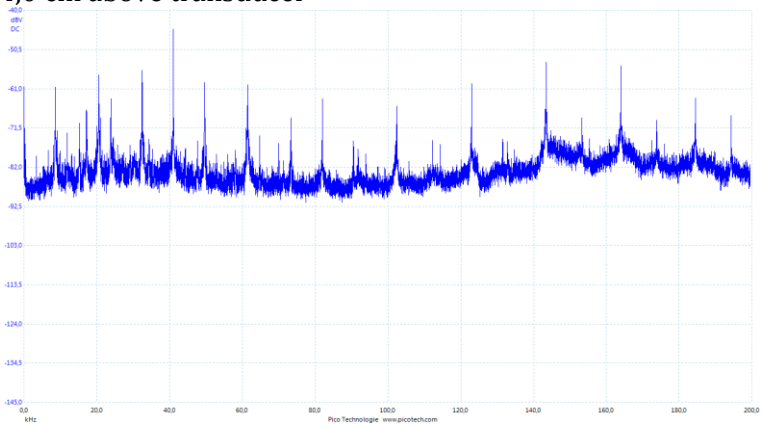

4,6 cm above transducer

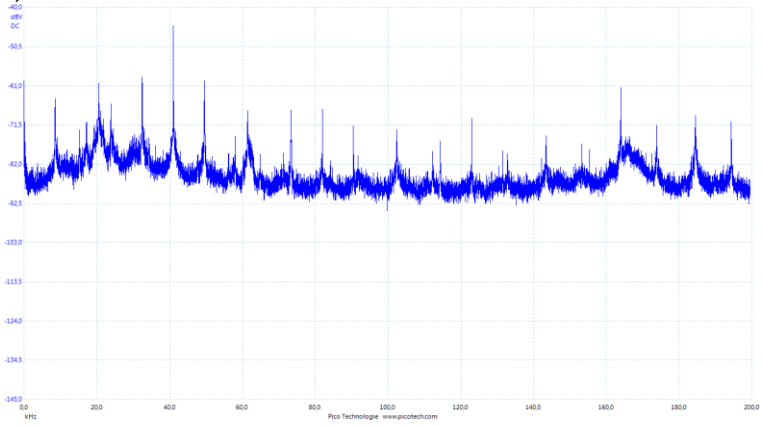

5cm above transducer

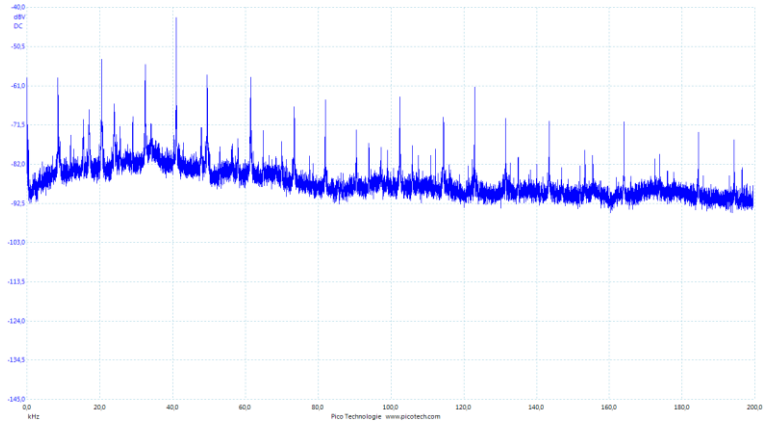

14.2. 98 kHz

0,5 cm above transducer

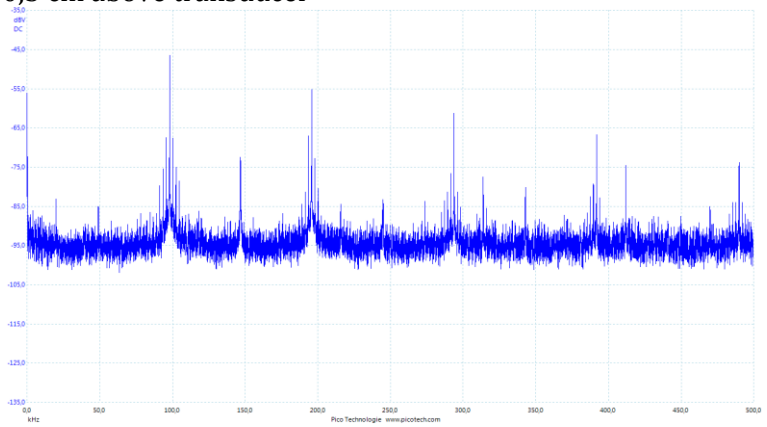

0,9 cm above transducer

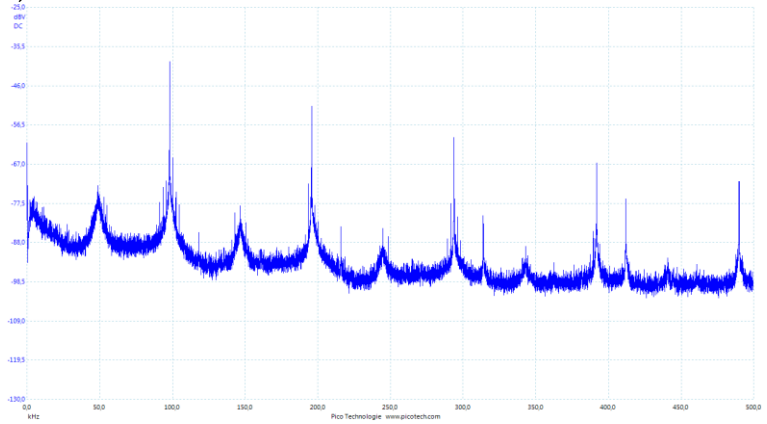

1,4 cm above transducer

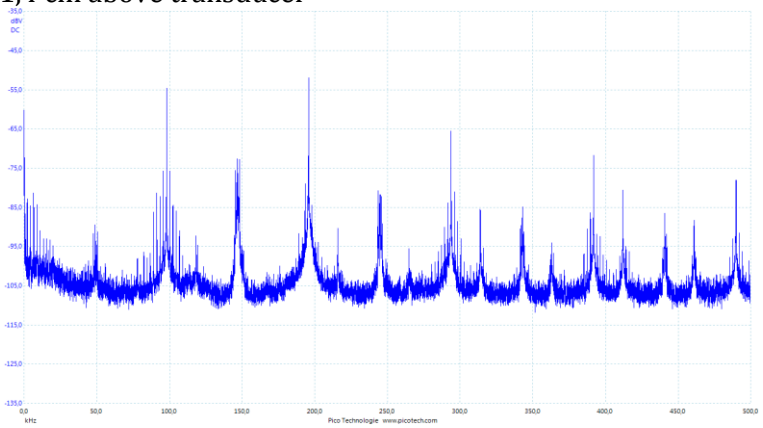

1,8 cm above transducer

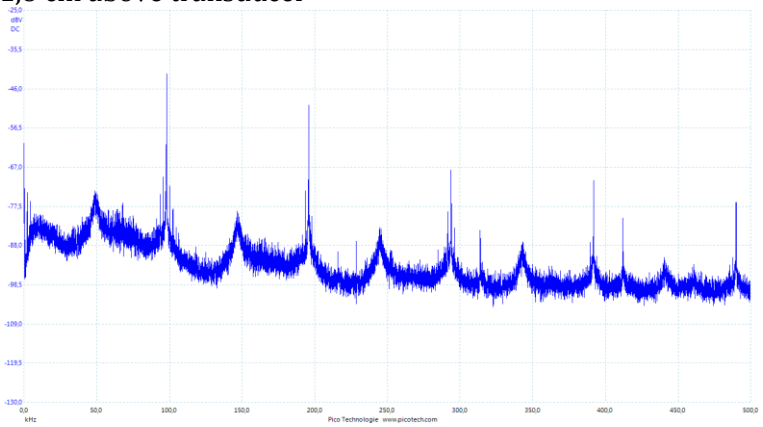

2,3 cm above transducer

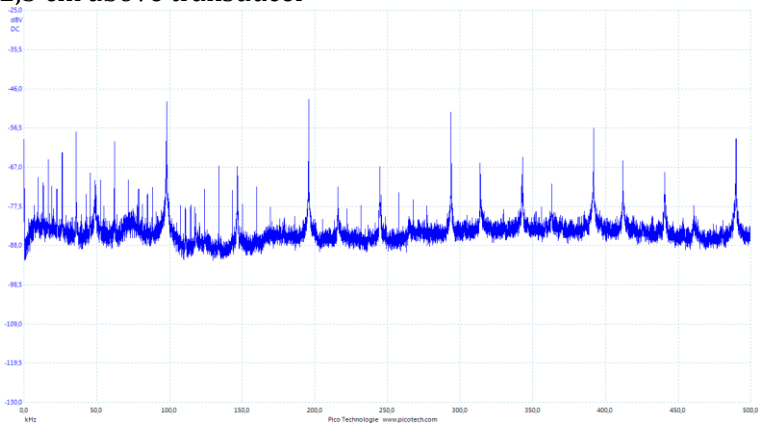

2,7cm above transducer

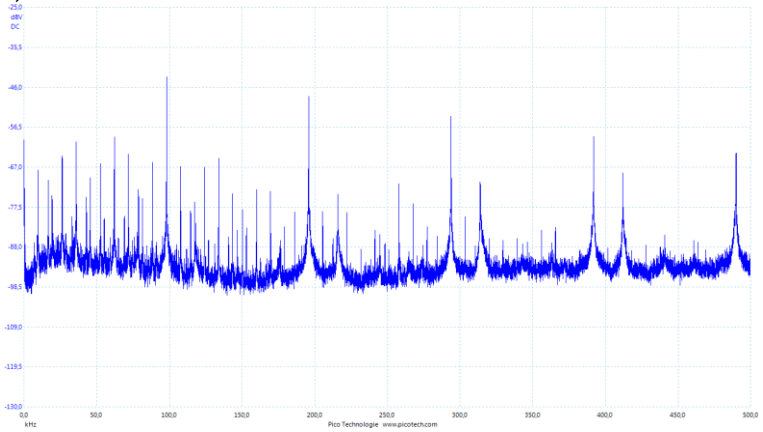

3,0 cm above transducer

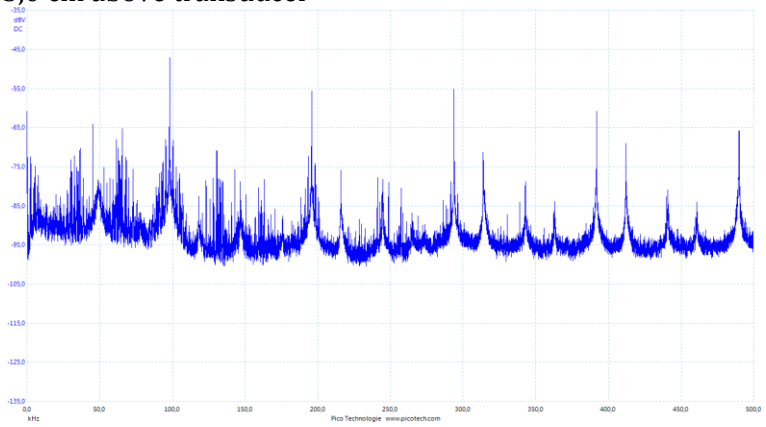

3,2 cm above transducer

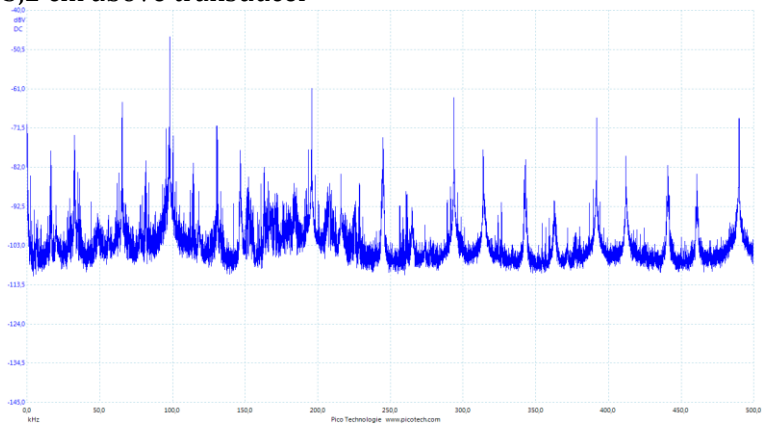

3,6 cm above transducer

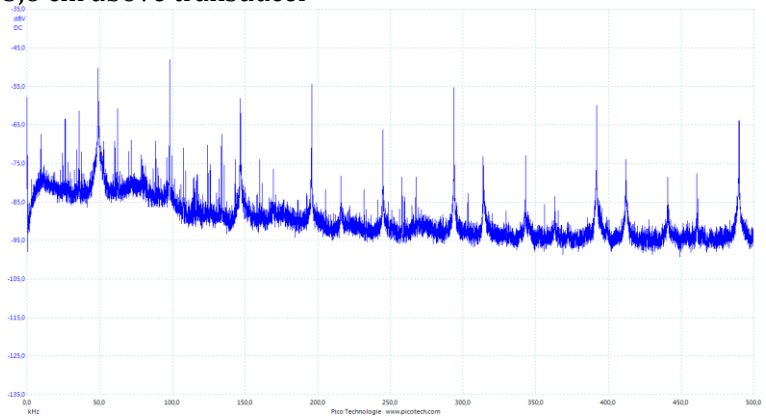

4,0 cm above transducer

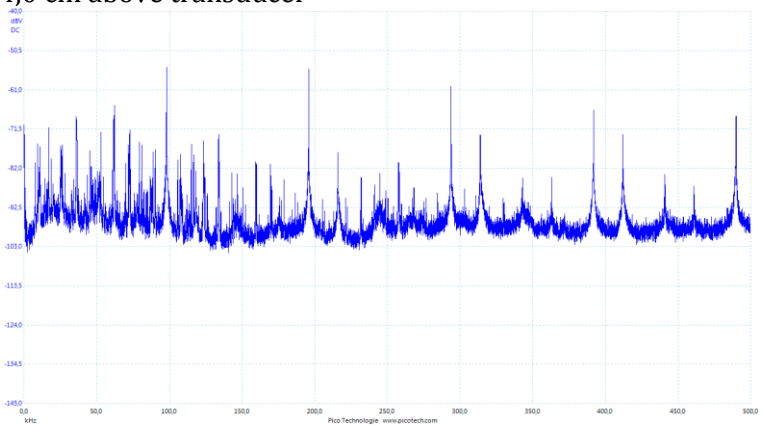

4,5 cm above transducer

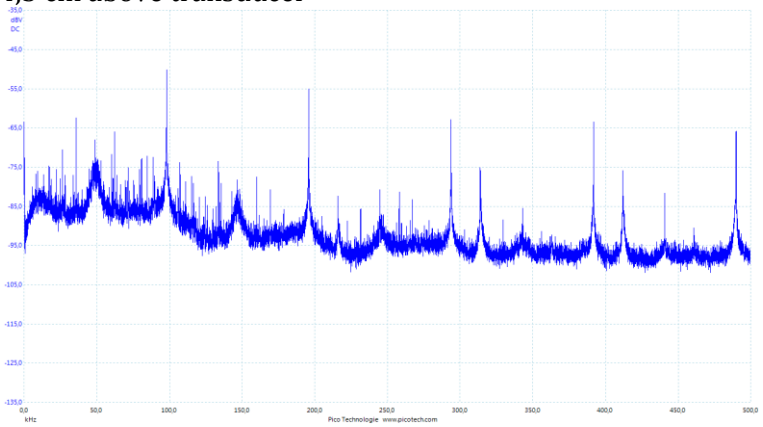

5,0 cm above transducer

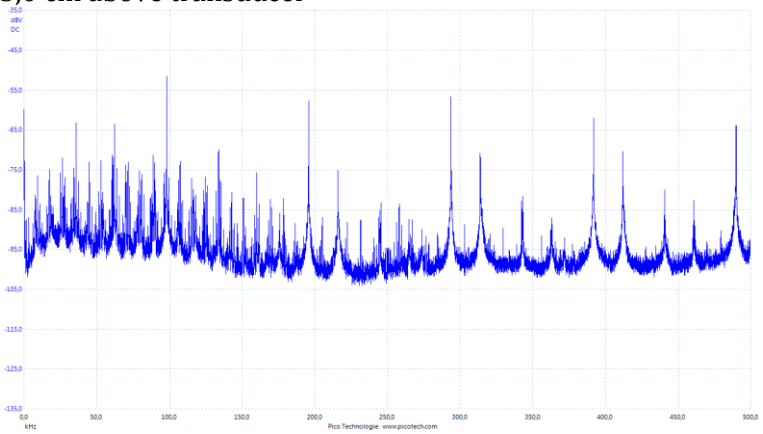

Annex 15. WAVE FORMS USING A HORN TRANSDUCER

15.1. 12,5W CALORIMETRIC POWER

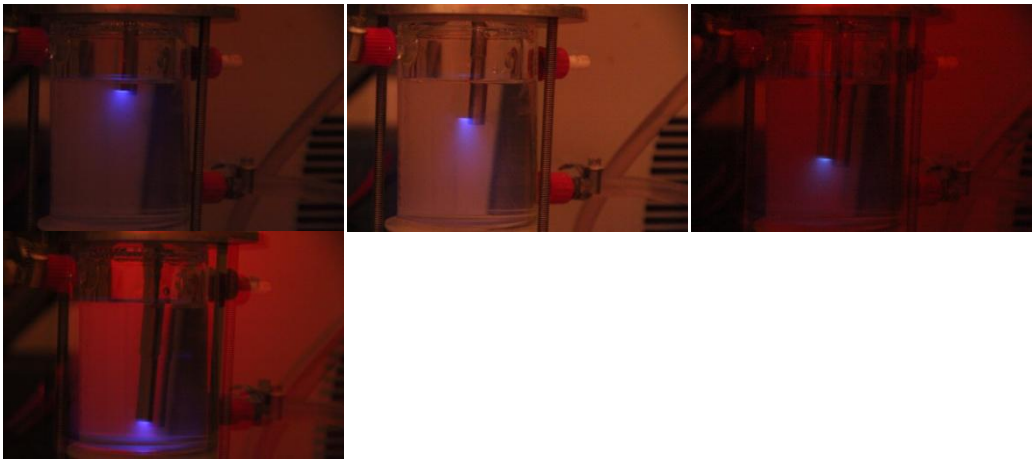

15.2. 50W CALORIMETRIC POWER

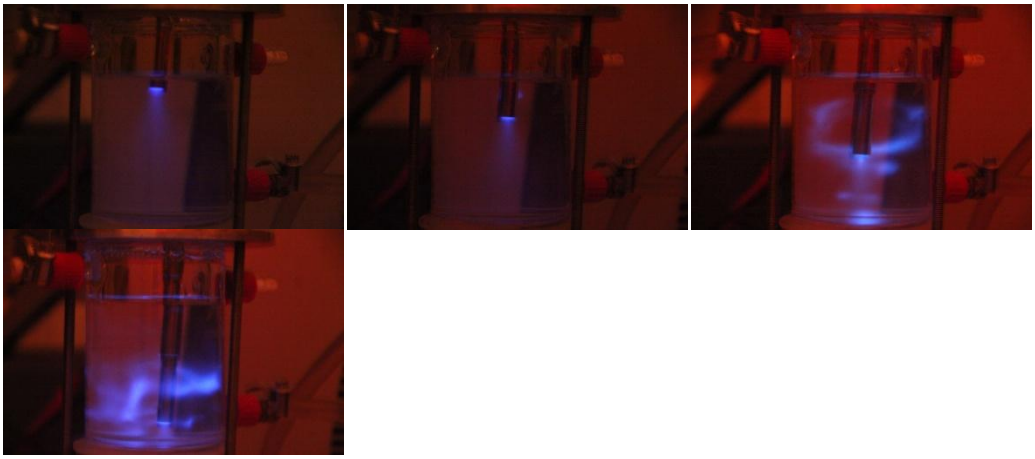

15.3. IMPACT OF STIRRER ON THE WAVES USING A HORN TRANSDUCER

12,5 W

50W

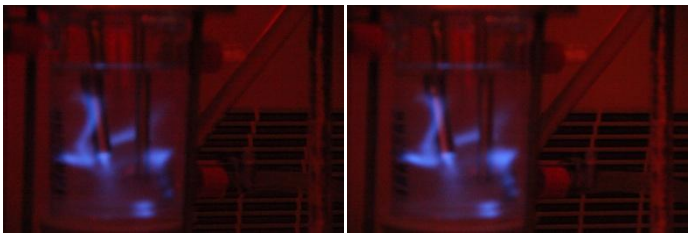

Auteursrechtelijke overeenkomst

Ik/wij verlenen het wereldwijde auteursrecht voor de ingediende eindverhandeling:
Characteristics and effect of US parameters and surface stabilizer on the sonocrystallization process of paracetamol

Richting: **master in de industriële wetenschappen: biochemie**
Jaar: **2014**

in alle mogelijke mediaformaten, - bestaande en in de toekomst te ontwikkelen - , aan de Universiteit Hasselt.

Niet tegenstaand deze toekenning van het auteursrecht aan de Universiteit Hasselt behoud ik als auteur het recht om de eindverhandeling, - in zijn geheel of gedeeltelijk -, vrij te reproduceren, (her)publiceren of distribueren zonder de toelating te moeten verkrijgen van de Universiteit Hasselt.

Ik bevestig dat de eindverhandeling mijn origineel werk is, en dat ik het recht heb om de rechten te verlenen die in deze overeenkomst worden beschreven. Ik verklaar tevens dat de eindverhandeling, naar mijn weten, het auteursrecht van anderen niet overtreedt.

Ik verklaar tevens dat ik voor het materiaal in de eindverhandeling dat beschermd wordt door het auteursrecht, de nodige toelatingen heb verkregen zodat ik deze ook aan de Universiteit Hasselt kan overdragen en dat dit duidelijk in de tekst en inhoud van de eindverhandeling werd genotificeerd.

Universiteit Hasselt zal mij als auteur(s) van de eindverhandeling identificeren en zal geen wijzigingen aanbrengen aan de eindverhandeling, uitgezonderd deze toegelaten door deze overeenkomst.

Voor akkoord,

Paredis, Mathijs

Datum: **12/06/2014**